CRC Report No. AV-20-20

DETERMINATION OF HEAT OF VAPORIZATION AND CREATING ENTHALPY DIAGRAMS FOR SEVERAL COMMON JET FUELS AND AVIATION GASOLINES

Final Report

August 2023

COORDINATING RESEARCH COUNCIL, INC.
5755 NORTH POINT PARKWAY • SUITE 265 • ALPHARETTA, GA 30022

The Coordinating Research Council, Inc. (CRC) is a non-profit corporation supported by the petroleum and automotive equipment industries. CRC operates through the committees made up of technical experts from industry and government who voluntarily participate. The four main areas of research within CRC are: air pollution (atmospheric and engineering studies); aviation fuels, lubricants, and equipment performance; heavy-duty vehicle fuels, lubricants, and equipment performance (e.g., diesel trucks); and light-duty vehicle fuels, lubricants, and equipment performance (e.g., passenger cars). CRC's function is to provide the mechanism for joint research conducted by the two industries that will help in determining the optimum combination of petroleum products and automotive equipment. CRC's work is limited to research that is mutually beneficial to the two industries involved. The final results of the research conducted by, or under the auspices of, CRC are available to the public.

The University of Delaware (UDEL) makes no representations extends no warranties, express or implied, concerning the data provided in this report and any resulting information thereof.

Further, UDEL makes no representations, extends no warranties, and assumes no responsibilities that the testing method or the use of data in whole or in part will not infringe the claims of any patents or other third party rights.

UDEL and CRC are separate and independent entities, and neither is the agent of the other. The users of these data agree to indemnify UDEL and their personnel free and harmless from any and all loss, cost, damage, claim, action, or liability on account of the death of or injury to any person or persons or damage to or destruction of any property resulting from or growing out of any alleged negligence on the part of the user of these data.

This page intentionally left blank
for back-to-back printing

Determination of Heat of Vaporization and Creating Enthalpy Diagrams for Several Common Jet Fuels and Aviation Gasolines (Avgas)

FINAL REPORT

Prepared for

Coordinating Research Council, Inc.
5755 North Point Parkway, Ste. 265
Alpharetta, GA 30022

Prepared by

Steve Sauerbrunn
Scientist
University of Delaware
Center for Composite Materials
Newark, Delaware

CRC Project No. AV-20-14 and AV-20-20

August 2023

This page intentionally left blank
for back-to-back printing

Executive Summary

This is the Final Report for Project CRC-AV-20-14 and CRC-AV-20-20 "Determination of Heat of Vaporization and Creating Enthalpy Diagrams for Several Common Jet Fuels and Aviation Gasolines". Heat of vaporization (HOV) is not provided for Jet A or Jet A-1 in Figure 2-19 in the current CRC Aviation Fuel Properties Handbook (the Handbook) [1]. There are no Enthalpy Diagrams for these two commercial fuels which are the main-stay of Civil Aviation. This is because the original data were generated in an era when military fuels were the focus of the Council. Enthalpy diagrams are used for determining the state of the fuel in the design of fuel systems for, and performance of, gas turbine augmenter or afterburner designs and their operability calculations, and in design and performance considerations of fuel systems where fuel will be used as a heat transfer medium. Different types of fuel injectors in engine main combustors and auxiliary power units generate many different spray droplet sizes, in several different environments, and these design curves help to determine vapor generation for ignition analysis. These curves provide a source of information when trying to understand what has happened in an aircraft accident and its aftermath or a fuel spill and fire investigation. HOV is also used in the study of events where fuel vapor production is an important part of an analysis preceding fire initiation, such as in an observed tailpipe fire. For Aviation Gasolines (Avgas) HOV is important to ensure correct formation and distribution of the fuel: air vapor necessary for combustion in a spark ignition piston engine. HOV influences the heat extracted from the engine intake system, which, under certain conditions, can induce ice formation requiring careful management and possibly application of exhaust manifold heat.

The high-pressure differential scanning calorimeter (HPDSC) is very well suited to the measurement of HOV of these fuels at atmospheric pressure and also the production of enthalpy curves, at various pressures, used for the construction of master enthalpy diagrams. This report includes the HOV values for: Jet A, Jet A-1, JP-4, JP-5, JP-8, JP-TS, FT-SPK, TS-1, Avgas (low and high aromatic formulations), as well as several synthetic jet fuels and blends. This report also includes the Enthalpy Diagrams for: Jet A-1, JP-8, JP-5, Jet A, JP-8, TS-1, JP-4, Avgas (low and high aromatic formulations).

The HOV of the two Avgas samples are very similar, 256.3 and 287.2 J/g. Also, the first endothermic peaks in the HOV curves, Figures 72 and 73, are very close to each other, 84.1 and 79.8 °C. This indicates that either Avgas sample will perform about the same with regards to the carburetor and/or venturi icing. This report only covers the HOV for the samples provided, these conforming to the volatility criteria set in ASTM D910 and D7547. Different grades of Avgas are available within these specifications that have different engine performance for other reasons such as: preignition (knocking), spark plug fouling (loss of spark), etc.

This page intentionally left blank
for back-to-back printing

Table of Contents

Table of Contents (cont'd)

List of Figures

List of Tables

This page intentionally left blank
for back-to-back printing

1. List of Acronyms and Abbreviations

HPDSC is a high-pressure differential scanning calorimeter. This instrument measures heat flow during evaporation of a sample at different pressures.

HOV or ΔH_{vap} is the heat of vaporization. It is the same as the heat of evaporation. This is the heat (energy) associated with the transition from a liquid to a gas, at a fixed temperature. The Heat of Vaporization is also called the Latent Heat of Vaporization or the Enthalpy of Vaporization. HOV can be expressed in units of J/mol or J/g.

J/mol is Joules per mole, the units typically reported for the HOV of a pure substance.

J/g is Joules per gram, the units typically reported for the HOV of a mixture.

PSI is pressure in pounds per square inch and is relative to absolute vacuum.

PSIG is pressure in "pounds per square inch gauge" and is relative to atmospheric pressure.

T/C is a thermocouple.

Quasi-Isothermal (QI) DSC is a DSC test where the sample is not exactly isothermal and the sample temperature will be changing by a small heating rate, typically less than 0.1 °C/min.

Critical Point is the temperature and pressure, above which, the sample is a critical fluid, which has the properties of a gas and a liquid, with no distinction between the two. A sample that is above the critical point in both temperature and pressure does not have a heat of vaporization.

Critical Temperature (T_c or $T_{critical}$) is the temperature where the sample is a critical fluid, which has the properties of a gas and a liquid, with no distinction between the two.

Critical Pressure (P_c) is the pressure where the sample is a critical fluid, which has the properties of a gas and a liquid, with no distinction between the two.

2. Background

The Coordinating Research Council (CRC) has sponsored this testing for the "Determination of Heat of Vaporization and Creating Enthalpy Diagram for Several Common Jet Fuels" (CRC Project No. AV-20-14). Enthalpy charts are used for determining the state of the fuel in the design of fuel systems for, and performance of, gas turbine augmenter or afterburner designs and their operability calculations, and in design and performance considerations of fuel systems where fuel will be used as a heat transfer medium. Different types of fuel injectors in engine main combustors and auxiliary power units generate many different spray droplet sizes,

in several different environments, and these design curves help to determine vapor generation for ignition analysis. These curves provide a source of information when trying to understand what has happened in an aircraft accident and its aftermath or a fuel spill and fire investigation. Heat of Vaporization is also used in the study of events where fuel vapor production is an important part of an analysis preceding fire initiation, such as in an observed tailpipe fire.

Heat of Vaporization

The heat of vaporization (HOV, also symbolized as ΔH_{vap}) is the energy that is needed to completely convert a given quantity of a substance from a liquid to a gaseous state at a given temperature and pressure, usually measured at atmospheric pressure. For simple substances (pure chemicals), the HOV can be calculated from the Clausius-Clapeyron equation [2, 3] by measuring the boiling point of a pure substance at several different pressures, or the vapor pressure at several different temperatures. The approach (e.g., used in ASTM E2071 [4]) gives the HOV for the substance in J/mol. Heat of vaporization is the amount of heat required to make a physical change from the liquid phase to the gas phase, shown in the equation below, with n-hexane being shown as an example.

$$C_6H_{14_{Liquid}} \xrightarrow{\Delta H_{Vaporization}} C_6H_{14_{Gas}}$$

Heat of vaporization of pure liquid compounds can be achieved using several estimation techniques, most notable being the Clausius-Clapeyron equation,

$$\ln\left(\frac{P}{P_0}\right) = -\frac{\Delta H_{Vap}}{RT} + C$$

Where R = gas constant
T = temperature (K)
C = a constant
P = measured pressure
P_0 = reference pressure

The ASTM standard E2071 [4] uses this technique with a high-pressure DSC. The technique is limited to liquids that boil within a narrow temperature range, usually pure compounds. This technique is an estimation of the heat of vaporization because ideal gas behavior is assumed, which is the basic premise of the Clausius-Clapeyron equation.

Engineers who design turbine engines need the HOV in units of energy per mass, such as J/g, to improve the fuel efficiency of new engine designs. The HOV of multicomponent, volatile blends, such as jet fuels, must be measured directly and cannot be estimated using the Clausius-Clapeyron equation.

The HOV, in J/g, is easily measured with a DSC using aluminum crucibles with a laser drilled 50 µm orifice. This technique has been used for many years [5, 6 and 7] to determine the boiling point and HOV of pure liquids. It may also be used to measure these properties for organic mixtures, such as jet fuels.

The heat flow (W/g) measured through the vaporization process can also be integrated to give a single average HOV value for the entire jet fuel blend.

3. Scope

The scope of the project is to provide HOV for Jet A and Jet A-1 for the requisite curve, and replicate Figure 2-18 of the Handbook for Jet A and Jet A-1 fuel (see Figure 1 below) [1]. This effort is to provide HOV data for several jet and Avgas fuels and the enthalpy diagram (and data) for a subset of synthetic jet fuels.

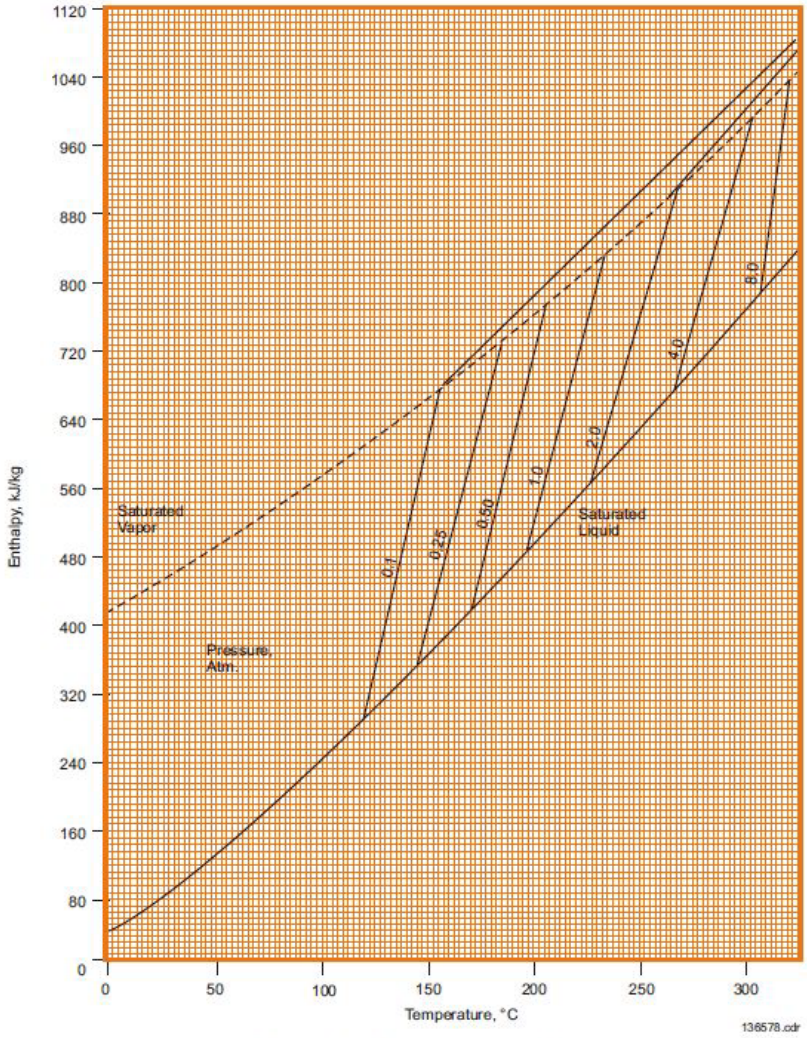

Figure 2-18. Enthalpy Diagram – JP-5

Figure 1: Enthalpy Diagram for JP-5

4. Experimental

4.1. Materials

Jet fuels and Aviation gasolines were provided by a variety of sources; details are given in Table 1.

Table 1: Sources of Jet Fuels and Aviation Gasolines

JF#	Type	Marking on container	Company	Country	State	City	Manufacturer
1	Jet A	Jet A	Shell	USA	CA	Martinez	Shell
2	Jet A-1	Jet A-1	Shell	Netherlands		Rotterdam	Shell
3	Jet A-1	Jet A-1	A/S Dansk Shell	Denmark		Fredericia	A/S Dansk Shell
4	Jet A-1	T309 Jel Fuel Nord	Shell	Germany		Koln	Shell
5	Jet A-1	Q92283 Jet Fuel S^2d	Shell	Germany		Koln	Shell
6	GEVO ATJ	11498 Biojet fuel	WPAFB	USA	OH	WPAFB	Gevo
7	Test Fld.	12345 Biojet Fuel, Component Derived, Flat distillation	WPAFB	USA	OH	WPAFB	AFRL/RQTF
8	Jet A	10325 Jet Fuel A	WPAFB	USA	OH	WPAFB	Shell
9	JP-5	10289 Fuel, JP-5	WPAFB	USA	OH	WPAFB	Valero
10	JP-8	10264 Fuel, JP-8	WPAFB	USA	OH	WPAFB	NuStar
11	JP-TS	4527 Fuel, JPTS	WPAFB	USA	OH	WPAFB	Ashland
12	Test Fld.	12223 Fuel, 84/16C14 blend, (C9 + C14 blend), Asymmetric	WPAFB	USA	OH	WPAFB	AFRL/RQTF
13	HEFA/JP-8	12711 HRJ Blend, (50/50 Blend)	WPAFB	USA	OH	WPAFB	AFRL/RQTF
14	Jet A-1	F-T Fully Synthetic	Sasol	S Africa		Sasolburg	Sasol
15	Jet A-1	Semi-Synthetic 48%FT-SPK + 52% Jet A-1	Sasol	S Africa		Sasolburg	Sasol
16	FT-SPK	FT-SPK, Neat Blend Mat'l.	Sasol	S Africa		Sasolburg	Sasol
17	TS-1	IE.Rax, GOST 10227-86 Grade TS-1	Air BP	UK		Kent	Air BP
18	**JP-4 (W)**	NRL, Patuxent, no Liner in Cap	Nova Research	USA	VA	Alexandria	Chevron USA
19	Jet A-1	Jet A-1 "408-6595 JET straight run"	Total	France		Harfleur	Total
20	Jet A-1	Hydro-treated Jet A-1 "408-65 86"	Total	France		Harfleur	Total
21	Jet A-1	Meroxed Jet A-1 "D111-U32"	Total	France		Harfleur	Total
22	**JP-4**	JP-4, NRL Patuxent, DLA Alaska	Nova Research	USA	VA	Alexandria	Chevron USA
23	JP-5	AVCAT F-44, MoD Sample	RNAS Culdrose	UK		Helston	
24	Jet A-1 (JF-8)	with MIL additives	Emo-Trans GmbH	Germany		Moerfelden-Walld	BP Australia
AG-LA	AG100LL	Pascagoula Refinery, TEL, <3% aromatics	Chevron	USA	MS	Pascagoula	Chevron USA
AG-HA	LBP Naphtha	TEL, >16% aromatics	Exxon Mobil	USA	TX	Spring	Exxon Mobil

Note: The jet fuels were given a unique number "JF#NN", where NN is the sequence of the arrival of the jet fuel to the testing lab.

4.2. Instrumental

A NETZSCH HPDSC (model DSC 204 HP) was used for this testing. The HPDSC was also connected to a refrigerated water recirculating temperature controller (Julabo F25) and controlled at 1 °C. The HPDSC was operated under vacuum (Welch model 2014B-01 PTFE diaphragm vacuum pump) for some experiments. The vacuum was measured using a gauge (WIKA PN 20/2556722/1/2) with a range from 0 to -30 inHg with 0.5 inHg divisions. The high-pressure was measured with a 0 to 200 psig pressure gauge (Cecomp Electronics PN F16B200psig-NC). The pressure of the 68 atm (1000 psig) tests for the enthalpy diagrams was measured using the gauge built into the HPDSC. Pictures of the entire HPDSC setup are shown in Figures C15 and C16 in Appendix C. Aluminum crucibles, 25 µL, (NETZSCH PN 6.239.2-64.5.01) were used for all experiments. Solid aluminum lids (NETZSCH PN 66.239.2-64.5.02) were used for the 68 atm test for the enthalpy diagrams. Otherwise, laser drilled (50 µm) aluminum lids (NETZSCH PN 6.239.2-54.801) were used. The jet fuel samples received were pipetted into a glass vials with PTFE lined caps (supplier: Discount Vials, PN: CT151760144-C-TEF-N) for more convenient storage. Positive displacement 5 to 10 µL capillary pipets (supplier: Drummond Scientific Company, PN: 5-000-2010) were used to pipet the jet fuel from the storage vial into the DSC crucibles.

4.3. Temperature Calibration

The HPDSC calibration materials were supplied by NETZSCH (PN 6.239.2-91.3). All five standards were used to calibrate temperature, per ASTM E967, at each pressure used in this testing. The calibration correction was derived from a straight-line best fit to the corrections for each of the standards. The pressure changes the thermal conductivity between the sample and the DSC sensor. Lower pressure decreases the thermal conductivity and moves the onset of melting to higher temperatures.

Table 2: Temperature Standards

Sample	Mass, mg	Melting point, °C
Indium	11.97	156.6
Tin	15.43	231.9
Bismuth	14.94	271.4
Zinc	12.76	419.5
Cesium Chloride	12.31	476.6

4.4. Enthalpy Calibration

The DSC was calibrated to generate accurate enthalpy results. The DSC enthalpy is calibrated, per ASTM E968, using the known melting point enthalpy of several standards. The HPDSC calibration materials were supplied by NETZSCH (PN 6.239.2-91.3). All five standards were used to calibrate each pressure used in this testing. The enthalpy correction was derived from a straight-line best fit to the corrections for each of the standards. The pressure changes the thermal conductivity between the sample and the DSC sensor. Lower pressures decrease thermal conductivity and the observed enthalpy of melting and vaporization.

Table 3: Enthalpy Standards

Sample	Mass, mg	Enthalpy, J/g
Indium	11.97	28.6
Tin	15.43	60.5
Bismuth	14.94	53.1
Zinc	12.76	107.5
Cesium Chloride	12.31	47.91

5. HOV Testing

5.1. Sample Preparation for HOV Testing

The crucible and lid were tared on the five-place balance (METTLER TOLEDO model XP205DR). The liquid sample (about 7 to 10 µL) was pipetted into the aluminum crucible with a 5 to 10 µL capillary pipet. Laser drilled (50 µm) aluminum lids (NETZSCH PN 6.239.2-54.801) were used and cold welded to the crucible using the NETZSCH crimping press. The sample in the sealed crucible was weighed again until constant mass was achieved. This mass was recorded as the sample mass for the test. Photographs of the sample preparation are in Appendix C.

5.2. HOV Testing Method

The HPDSC was cooled using tap water running through the lid of the high-pressure chamber. The sample was placed in the HPDSC as quickly as possible after weighing. The pressure lid was fastened down. The HPDSC cell was filled with nitrogen gas to 50 psi and emptied three times. There was no gas flow through the HPDSC, so the sample was run in static nitrogen. The HPDSC cell was stabilized at 35 °C then heated at 5 °C/min to 400 °C, except for JP-4 (JF #22) and Avgas samples, which were too volatile to begin the test at 35 °C. In these cases, the water chiller was used and set to 1 °C. The HPDSC was allowed to stabilize at 15 °C +/- 1 °C before the sample was prepared. This reduces the amount of sample evaporation that might happen in the HPDSC while waiting for the temperature to come back to 15 °C. The test was started when the HPDSC cell stabilized at 15 +/- 1 °C.

5.3. HOV Data Evaluation Procedure

Region A in Figure 2 shows the endothermic shift in the baseline away from 0 mW/mg. This is due to the heat capacity of the liquid fuel. The region C is after all of the fuel has vaporized, so the baseline is close to 0 mW/mg. Since the fuel has completely vaporized in region C, there is no sample mass and therefore no heat capacity and the heat flow returns to zero. When integrating the area of the HOV peak, one needs to select a baseline type that will simulate the heat capacity of the sample as it is evaporating. The DSC does not measure the mass of the fuel during the experiment, so the baseline is simulated using a mathematically generated sigmoidal curve that follows the integral of the endotherm. This baseline technique is commonly used by all DSC manufacturers.

The vaporization (HOV) endotherm, negative peak shown in Figure 2, was integrated from about 60 °C to about 280 °C using a horizontal sigmoidal baseline. This baseline starts, region A, and stops, region C, with a horizontal slope. The sigmoid baseline, region B, follows the shape of an integral of the heat flow curve. The start and stop region of the baseline were chosen to be flat and nearly zero slope. The peak was analyzed as the lowest point on the heat flow scale. If there were two peaks, then the larger peak was analyzed. The shoulder peak was also analyzed and reported.

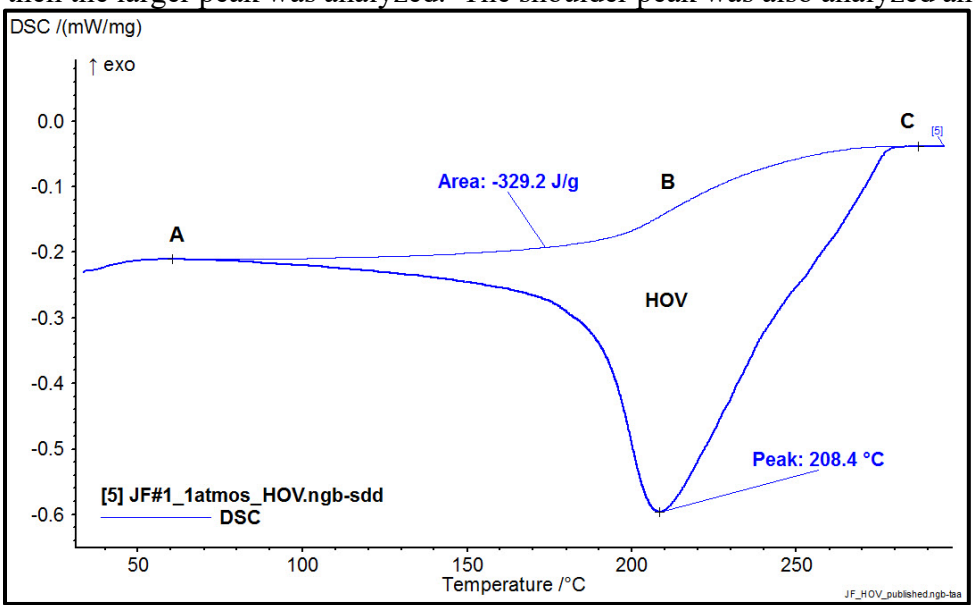

Figure 2: Example of HOV analysis

5.4. Summary of HOV Results

Table 4 is a summary of the HOV and the peak temperature for all the samples tested for HOV. JF#12, JP-4 (JF#18) and the Avgas samples each had two HOV peaks. The HOV for GEVO ATJ (JF#6) was too small for a proper fit of the sigmoidal baseline so the curve was analyzed using the tangential baseline. The tangential baseline will give the same results as the sigmoidal baseline provided the start and stop regions have a zero slope. This was the case for GEVO ATJ (JF#6). The raw DSC curves for the HOV of Jet Fuels are shown in Figures 3 to 26 below.

Table 4: HOV and Peak Temperature at One (1) Atm

JF #	Type	HOV	Peak	Comments
		(J/g)	(°C)	
1	Jet A	329.2	208.4	
2	Jet A-1	302.3	182.7	
3	Jet A-1	314.5	190.1	
4	Jet A-1	313.8	184.2	
5	Jet A-1	311.8	185.7	
6	GEVO ATJ	179.4	192.2	Tangential base
7	Test Fld.	393.6	171.1	
8	Jet A	301.2	202.1	
9	JP-5	294.5	218.6	
10	JP-8	266.9	185.7	
11	JP-TS	302.2	185.6	
12	Test Fld.	288.1	239.5	2 peaks, 209.6 °C
13	HEFA/JP-8	292.8	203.8	
14	Jet A-1	302.3	194.9	
15	Jet A-1	298.1	190.2	
16	FT-SPK	264.9	185.1	
17	TS-1	268.2	181.6	
18	JP-4 (W)	315.0	159.1	2 peaks, 201.5 °C
19	Jet A-1	294.8	190.2	
20	Jet A-1	310.6	193.6	
21	Jet A-1	302.6	192.3	
22	JP-4	309.7	118.6	
23	JP-5	291.3	216.9	
24	Jet A-1 (JF-8)	291.2	193.1	
AG-LA	Low aromatic	256.3	118.6	2 peaks, 79.8 °C
AG-HA	High aromatic	287.2	116.8	2 peaks, 84.1 °C

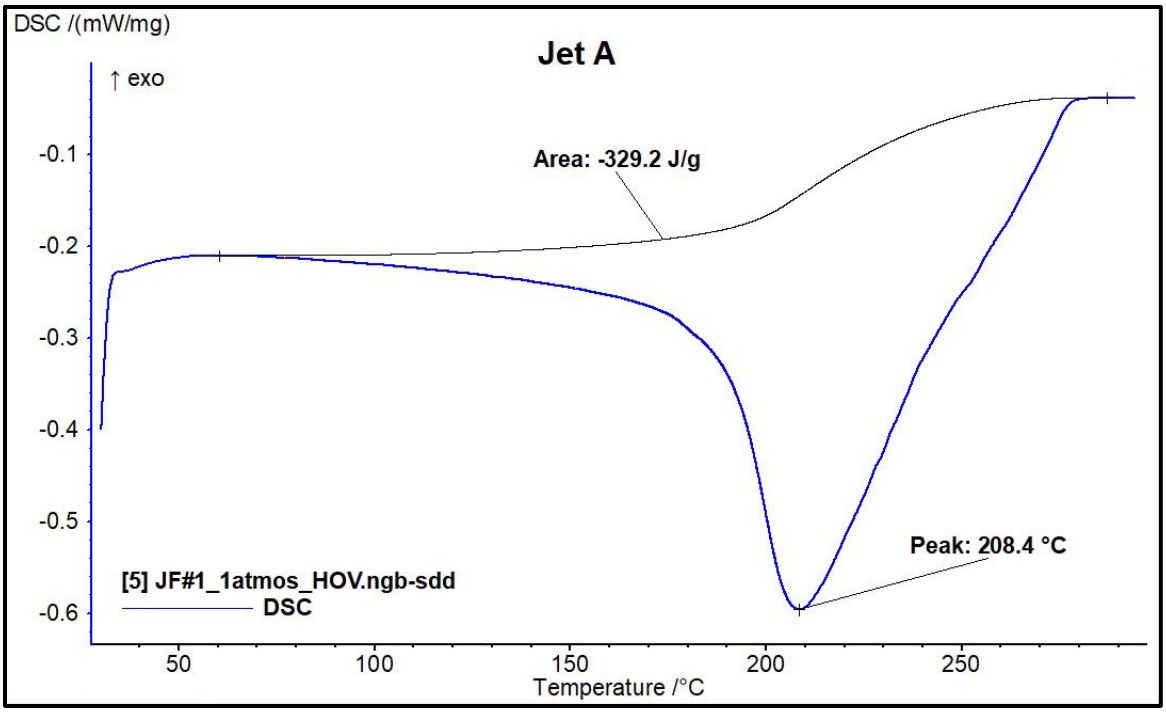

Figure 3: HOV analysis of Jet A, Shell, USA (JF#1).

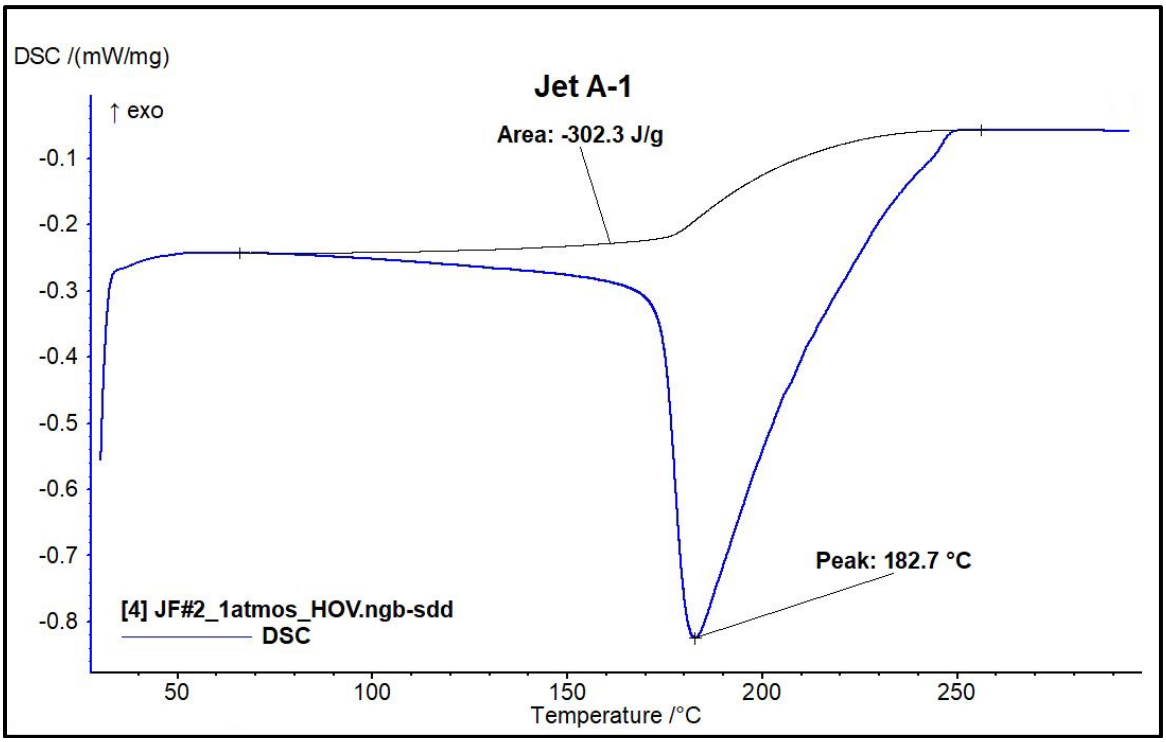

Figure 4: HOV analysis of Jet A-1, Shell Netherlands (JF#2).

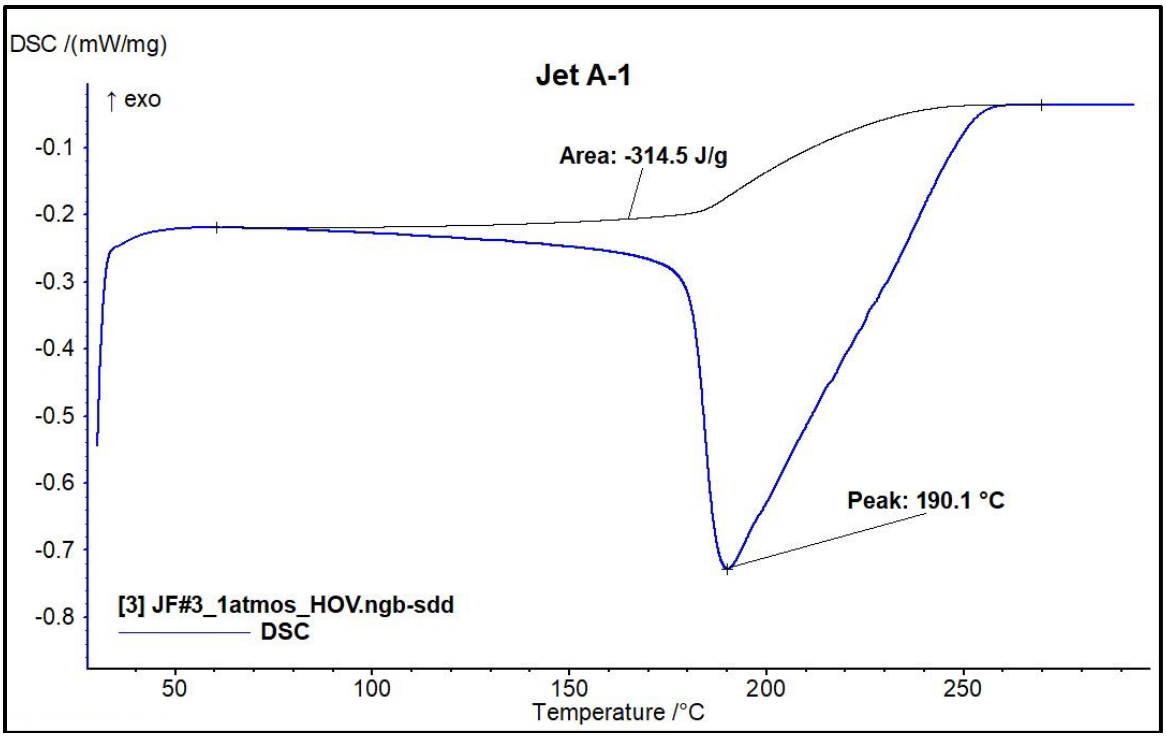

Figure 5: HOV analysis of Jet A-1, Dansk Shell, Denmark (JF#3).

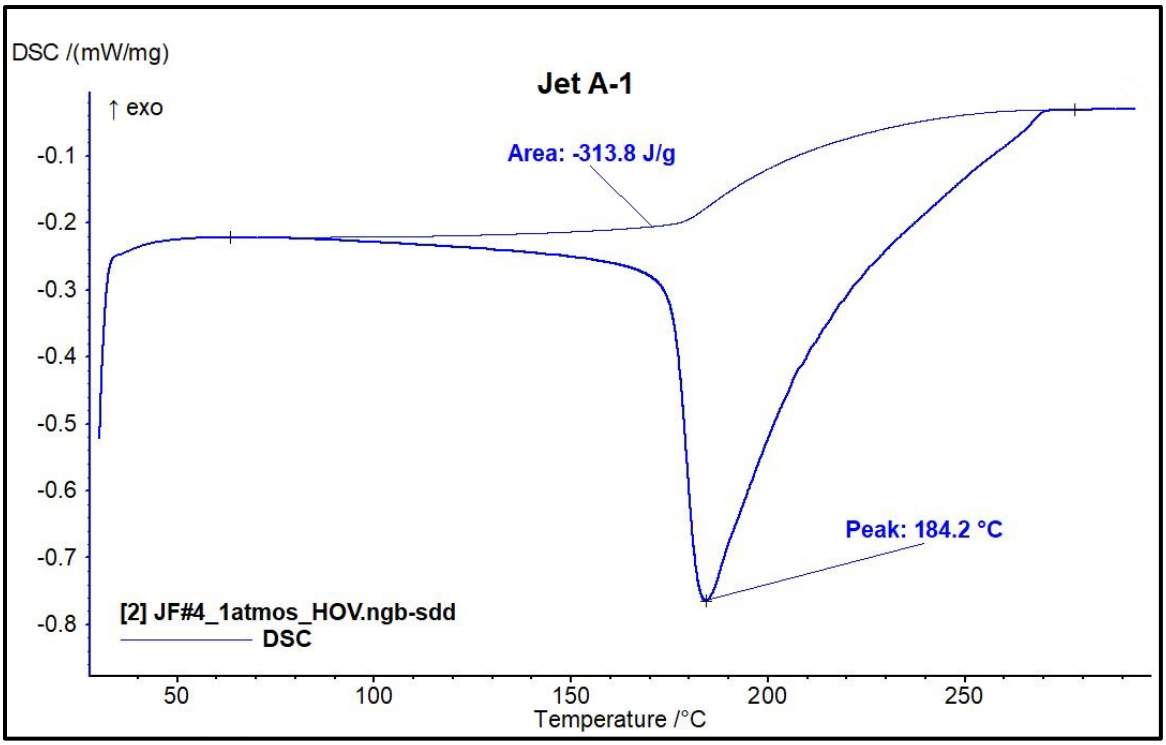

Figure 6: HOV analysis of Jet A-1, T309, Shell, Germany (JF#4).

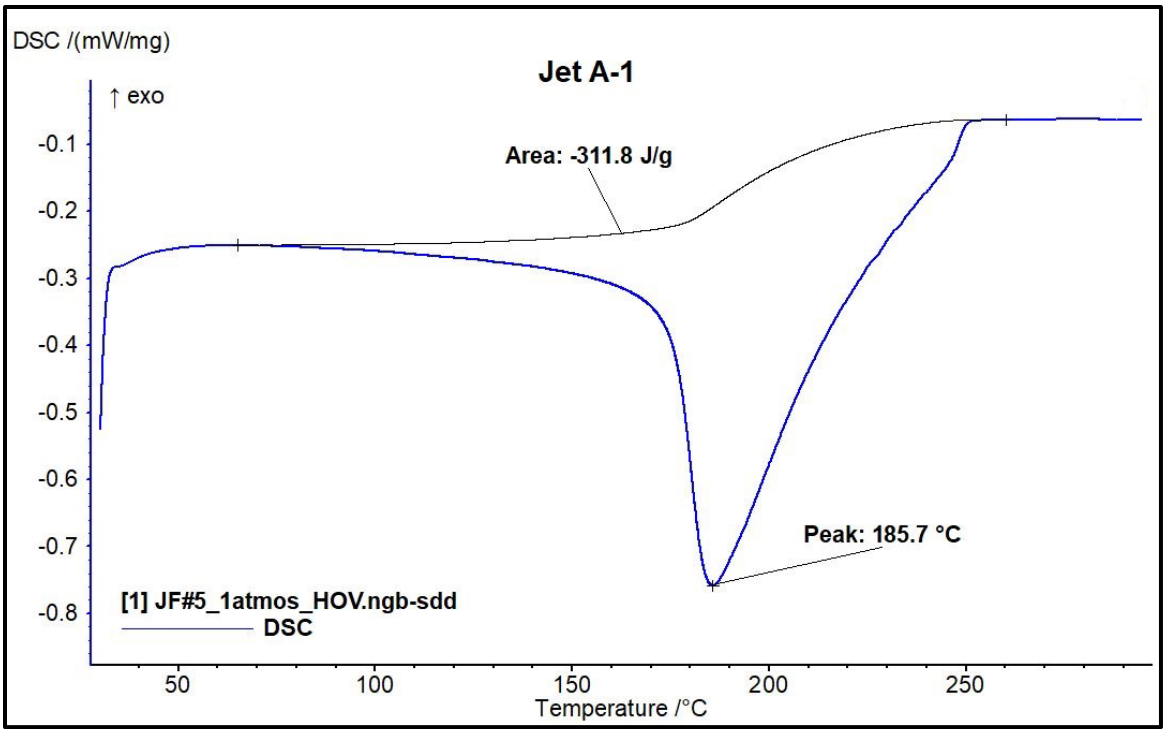

Figure 7: HOV analysis of Jet A-1, Q92283, Shell, Germany (JF#5).

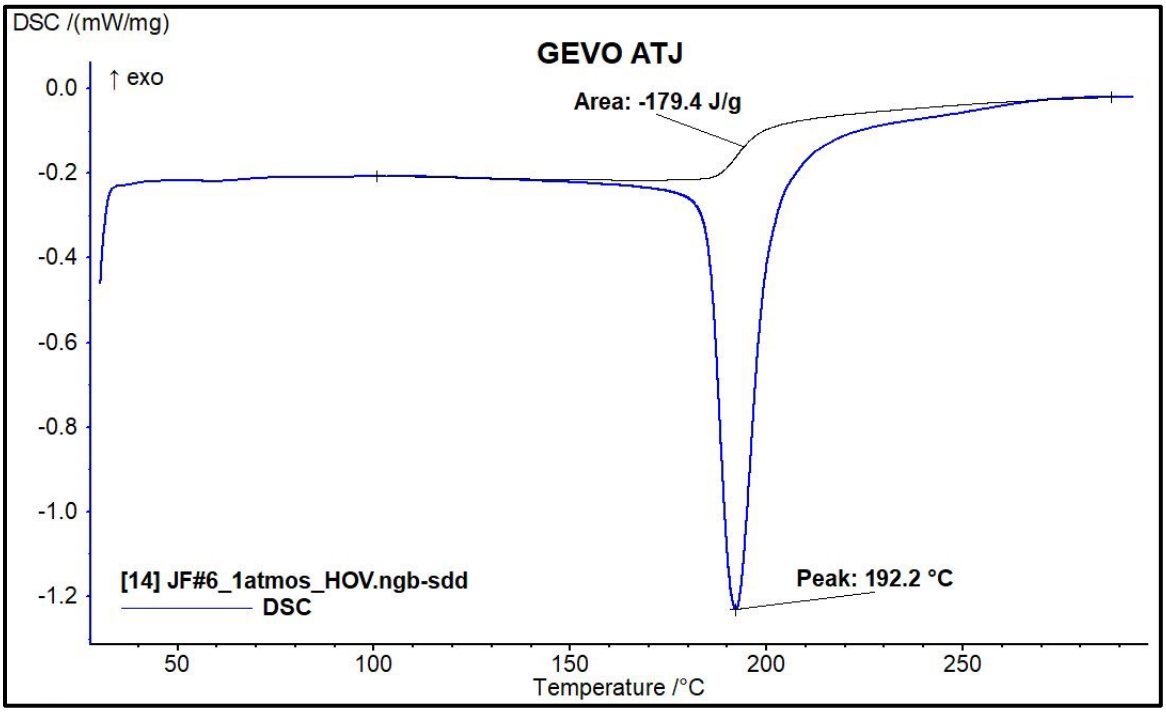

Figure 8: HOV analysis of Biojet, GEVO ATJ, WPAFB, USA (JF#6).

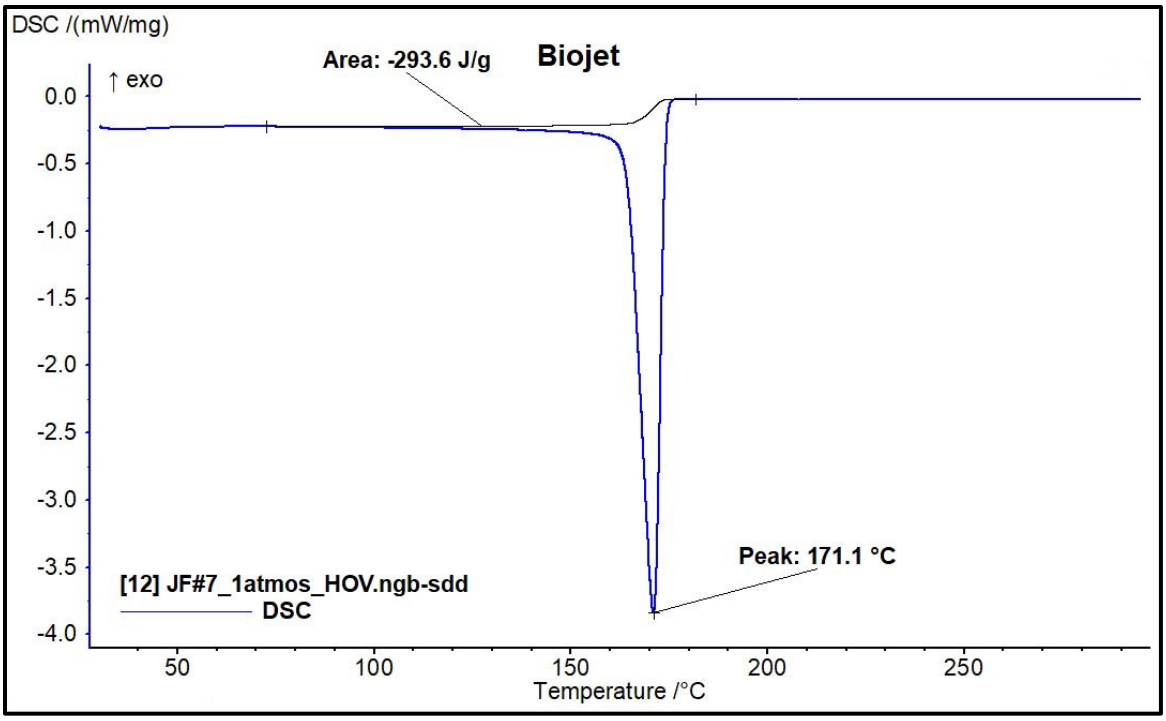

Figure 9: HOV analysis of Biojet, Test Fld, WPAFB, USA (JF#7).

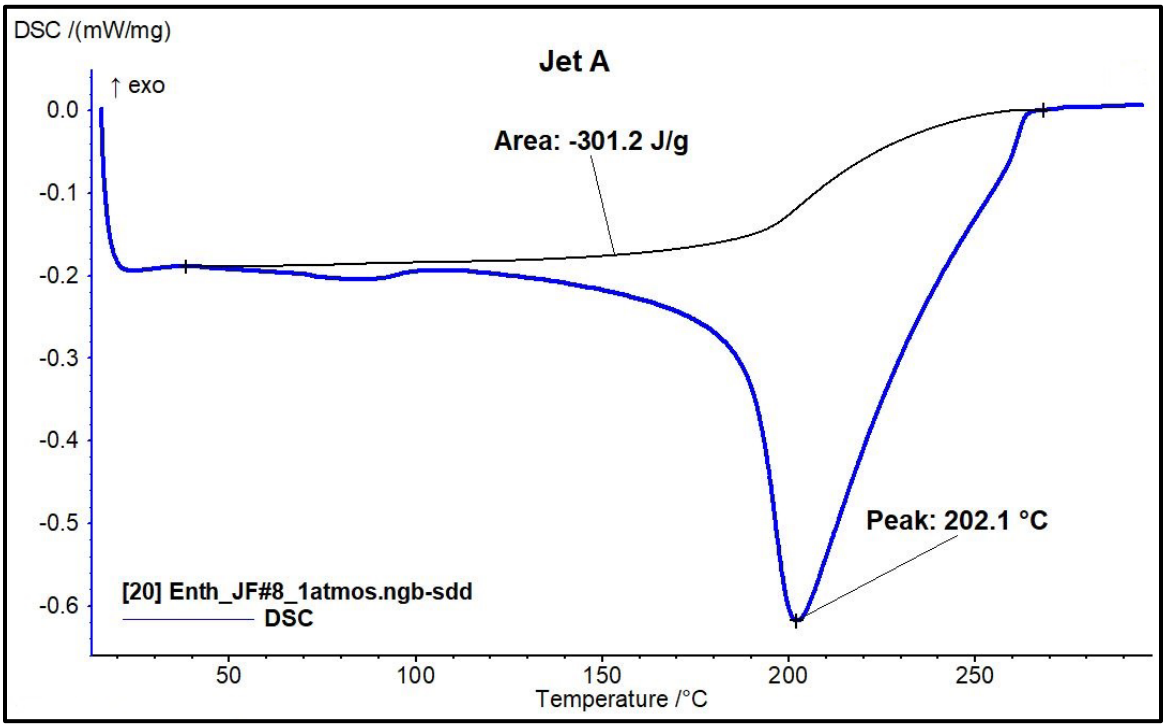

Figure 10: HOV analysis of Jet A, WPAFB, USA (JF#8).

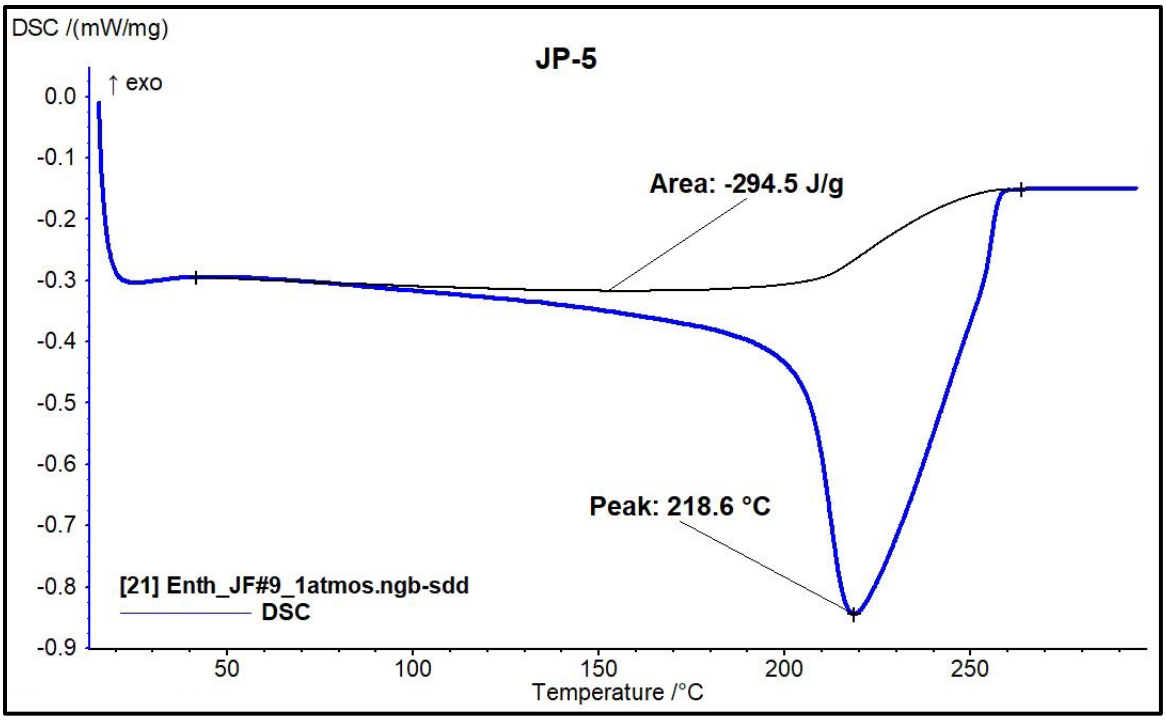

Figure 11: HOV analysis of JP-5, WPAFB, USA (JF#9).

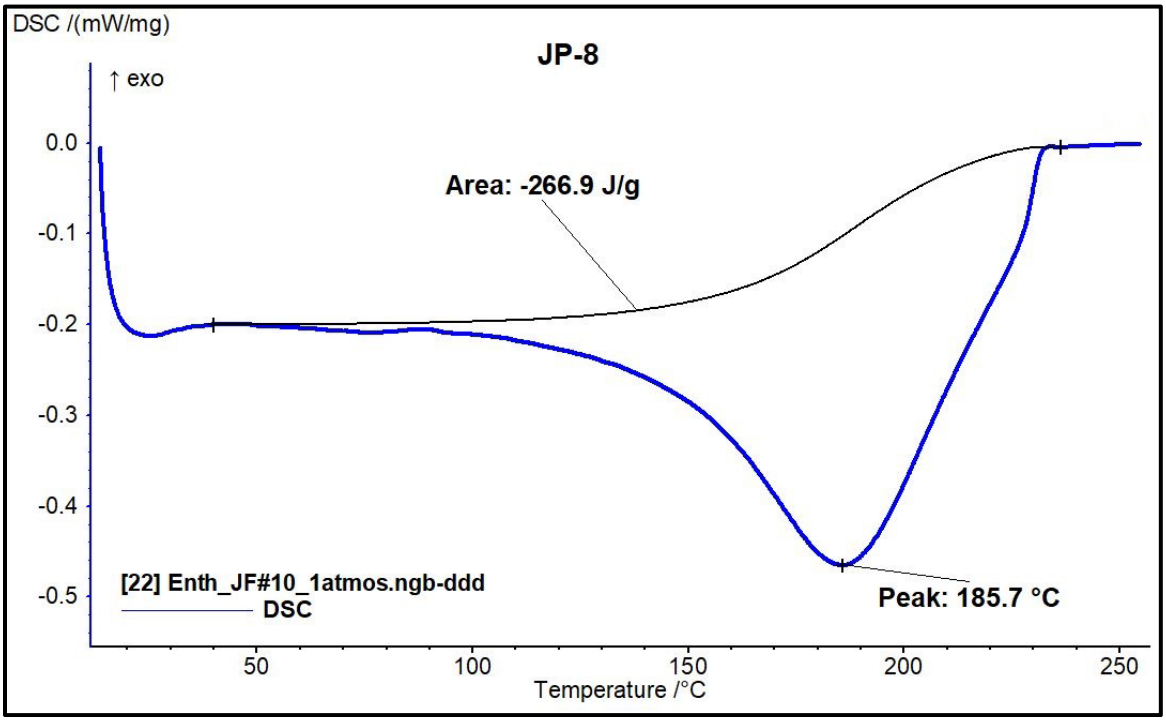

Figure 12: HOV analysis of JP-8, WPAFB, USA (JF#10).

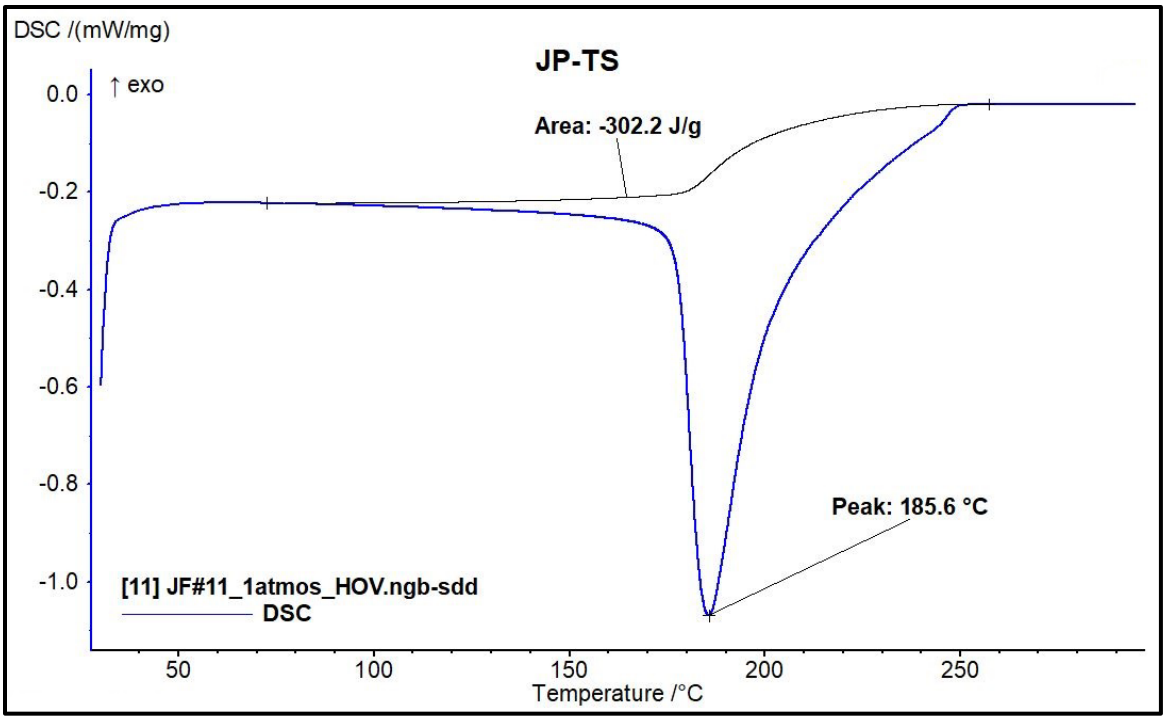

Figure 13: HOV analysis of JP-TS, Blend, WPAFB, USA (JF#11).

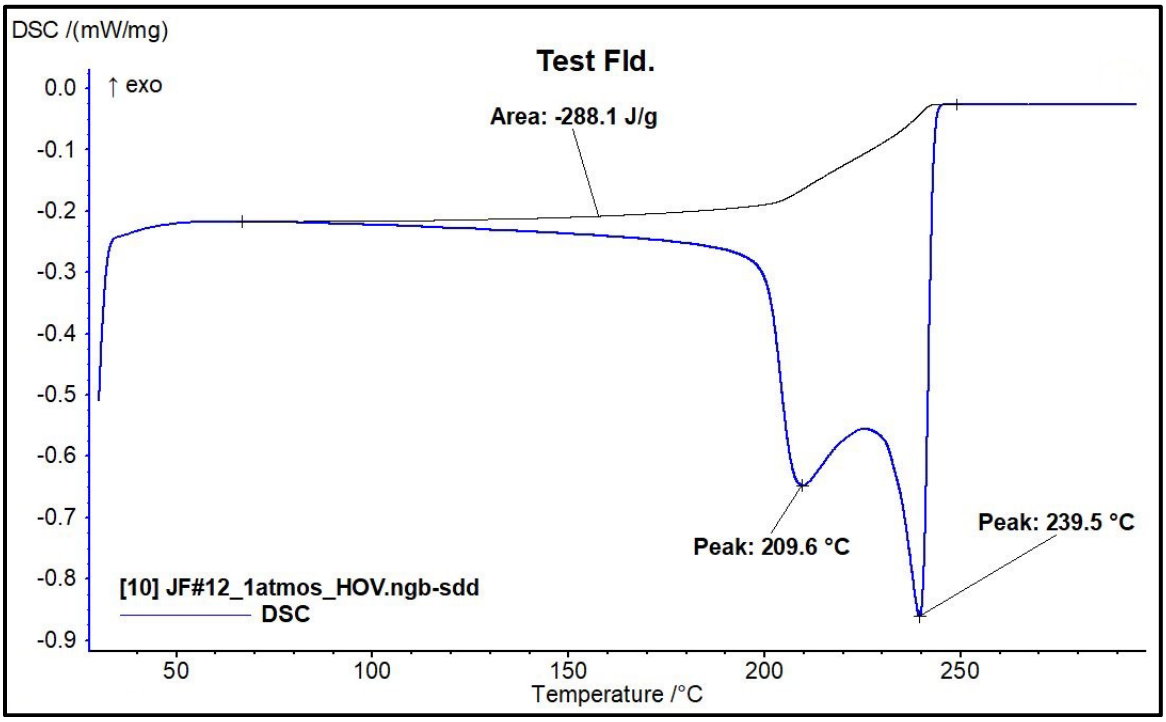

Figure 14: HOV analysis of Test Fld, 12223, WPAFB, USA (JF#12).

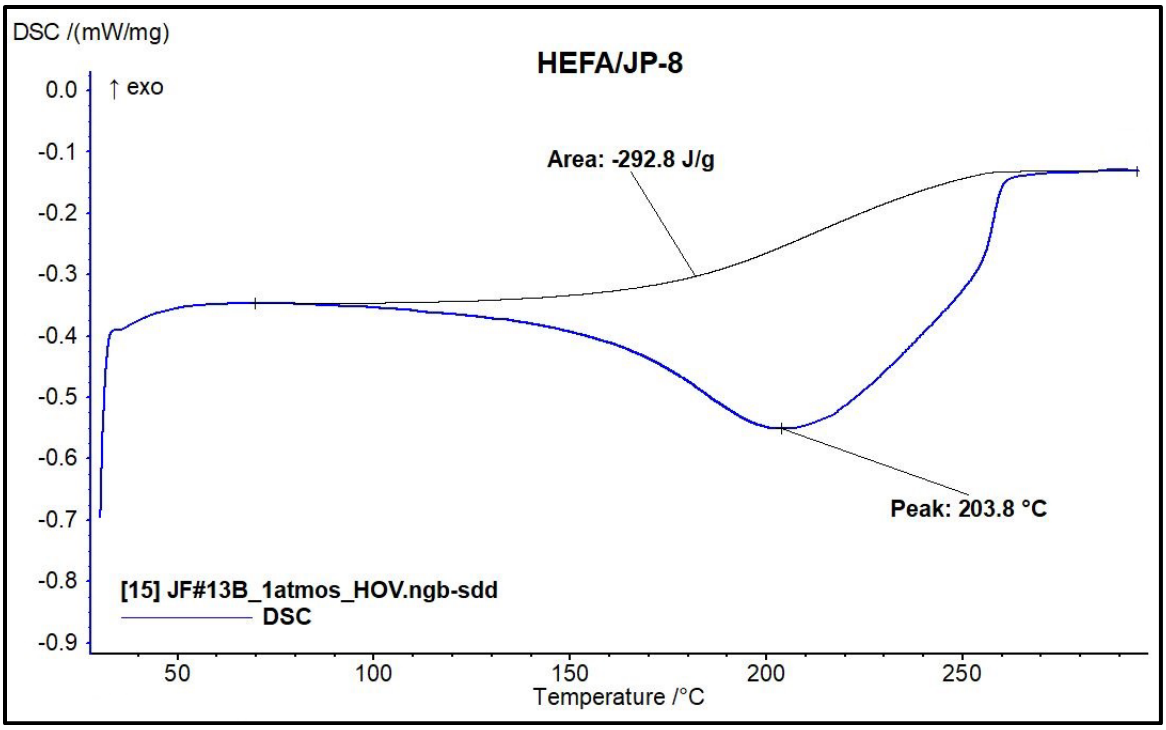

Figure 15: HOV analysis of HEFA/JP-8, Blend, WPAFB, USA (JF#13).

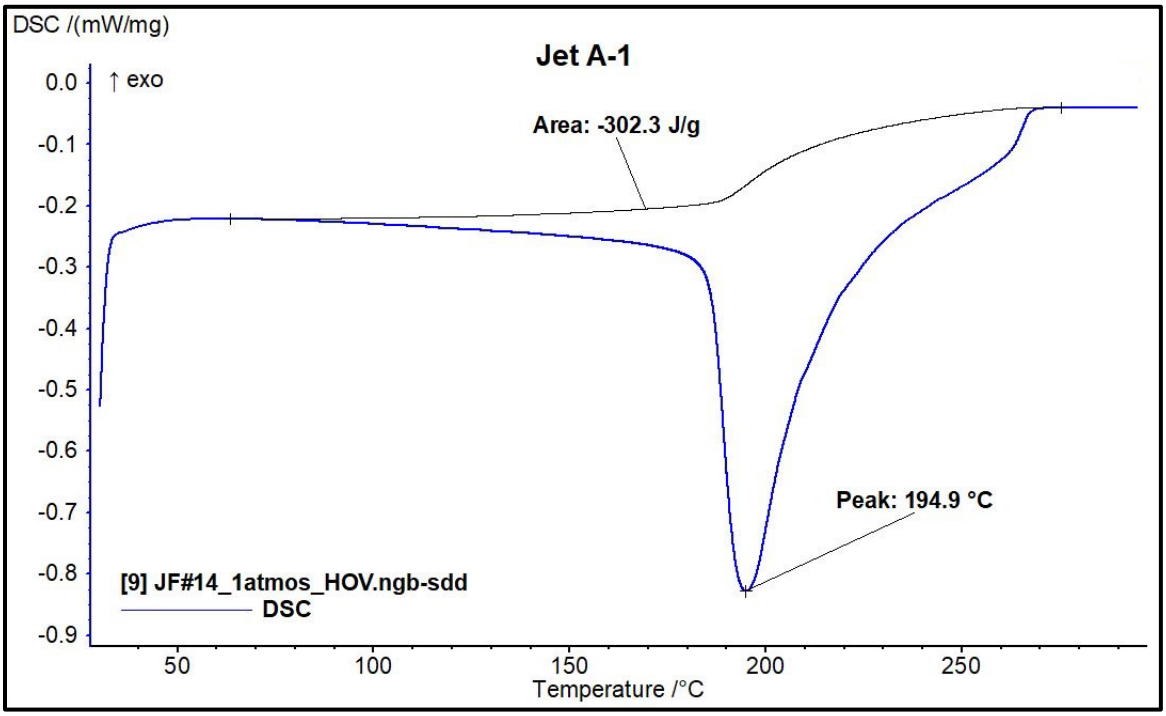

Figure 16: HOV analysis of Jet A-1, synthetic, Sasol, S Africa (JF#14).

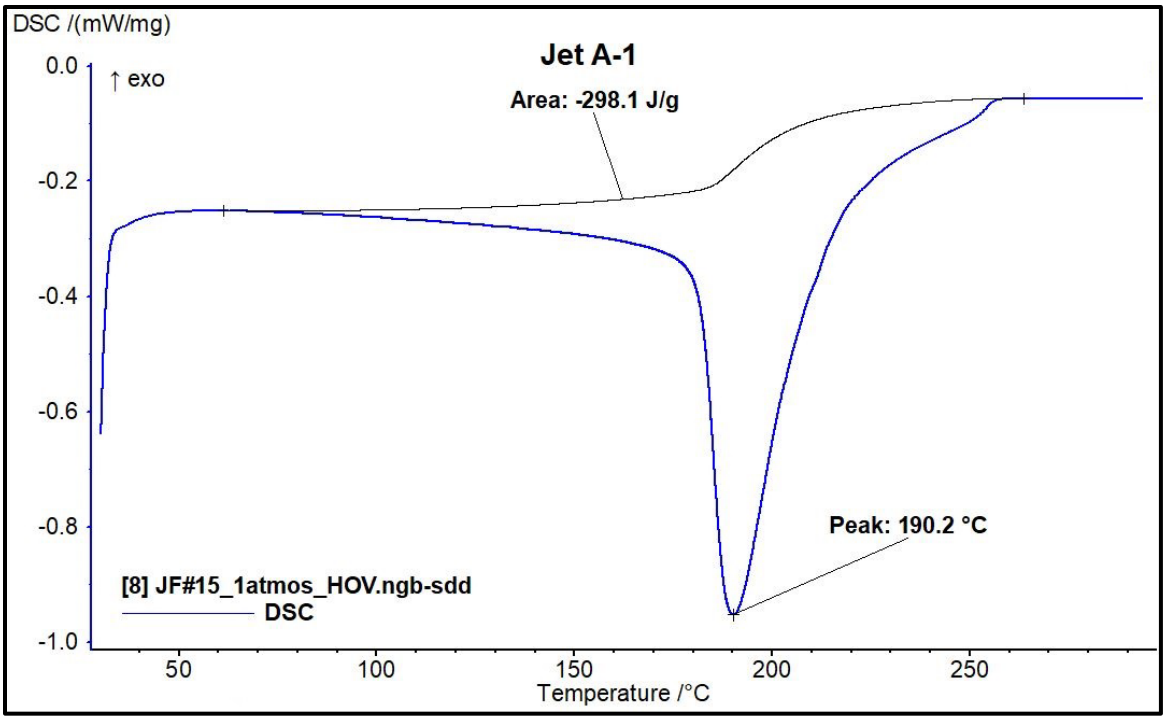

Figure 17: HOV analysis of Jet A-1, semi-synthetic, Sasol, S Africa (JF#15).

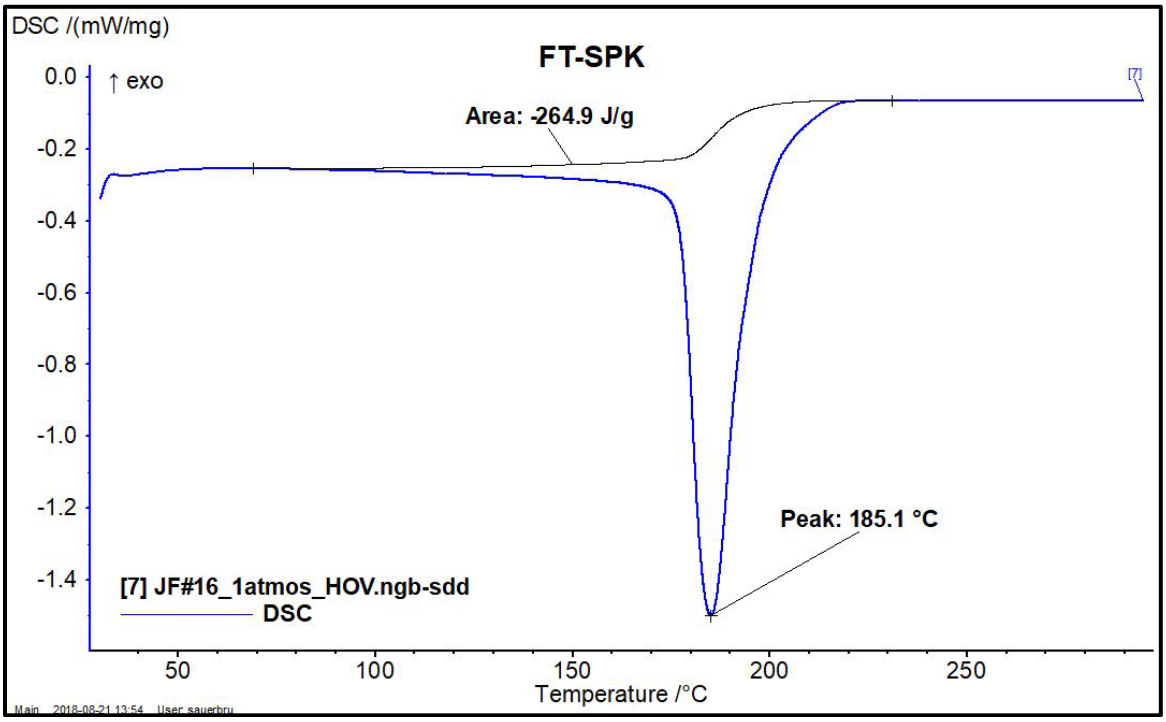

Figure 18: HOV analysis of FT-SPK, Sasol, S Africa (JF#16).

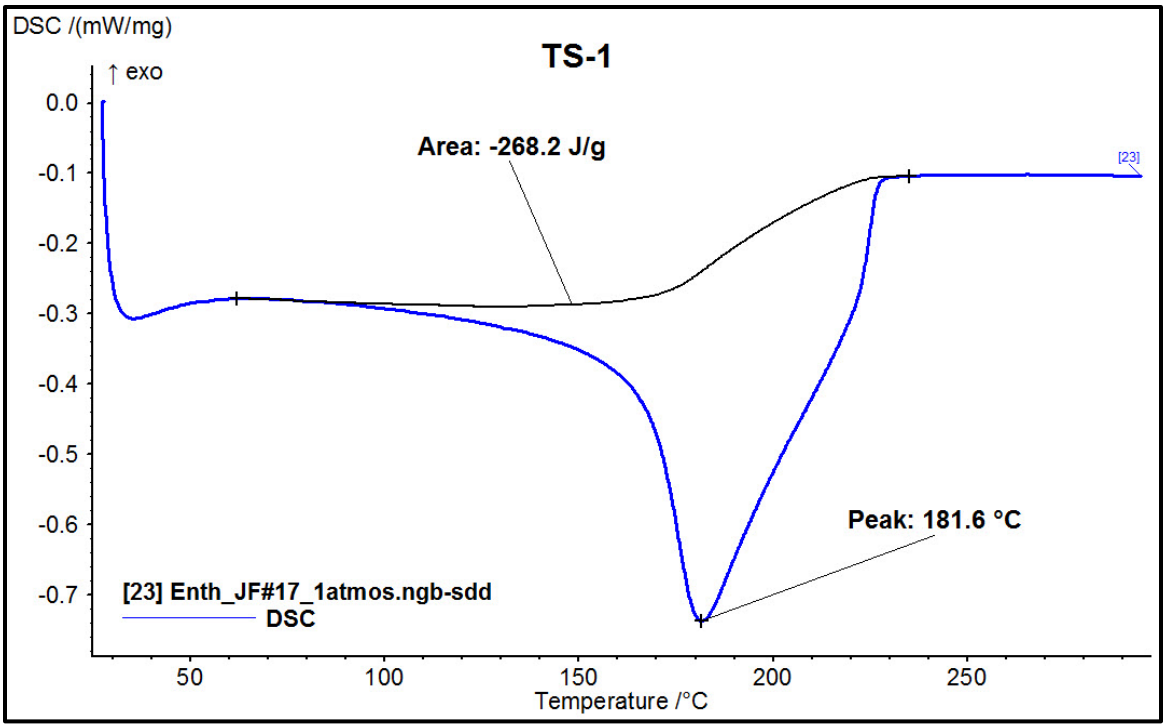

Figure 19: HOV analysis of TS-1, Air BP, UK (JF#17).

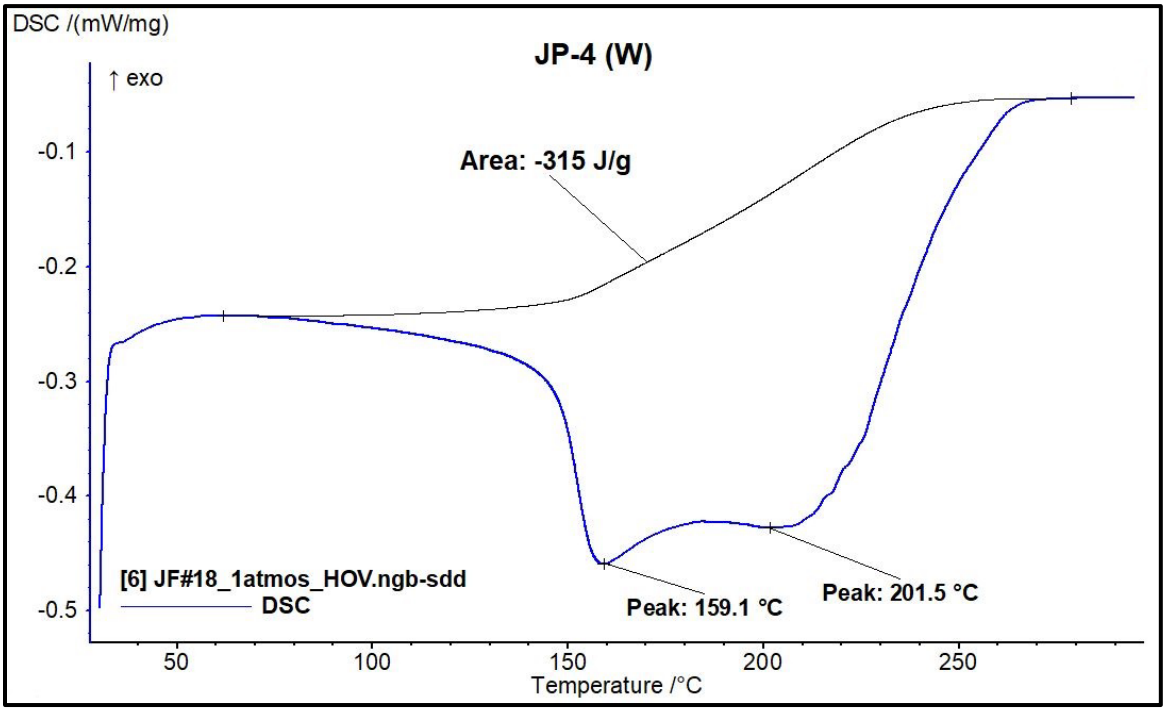

Figure 20: HOV analysis of JP-4 (W), Nova Research, USA, VA (JF#18).

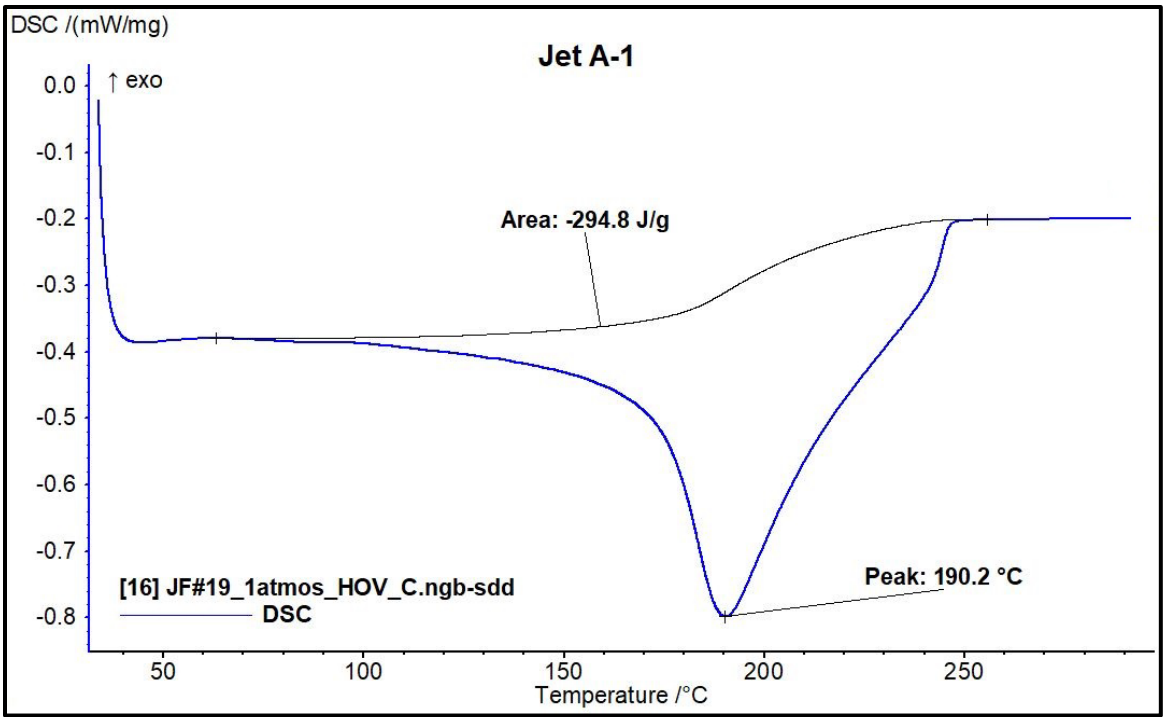

Figure 21: HOV analysis of Jet A-1, Total, France (JF#19).

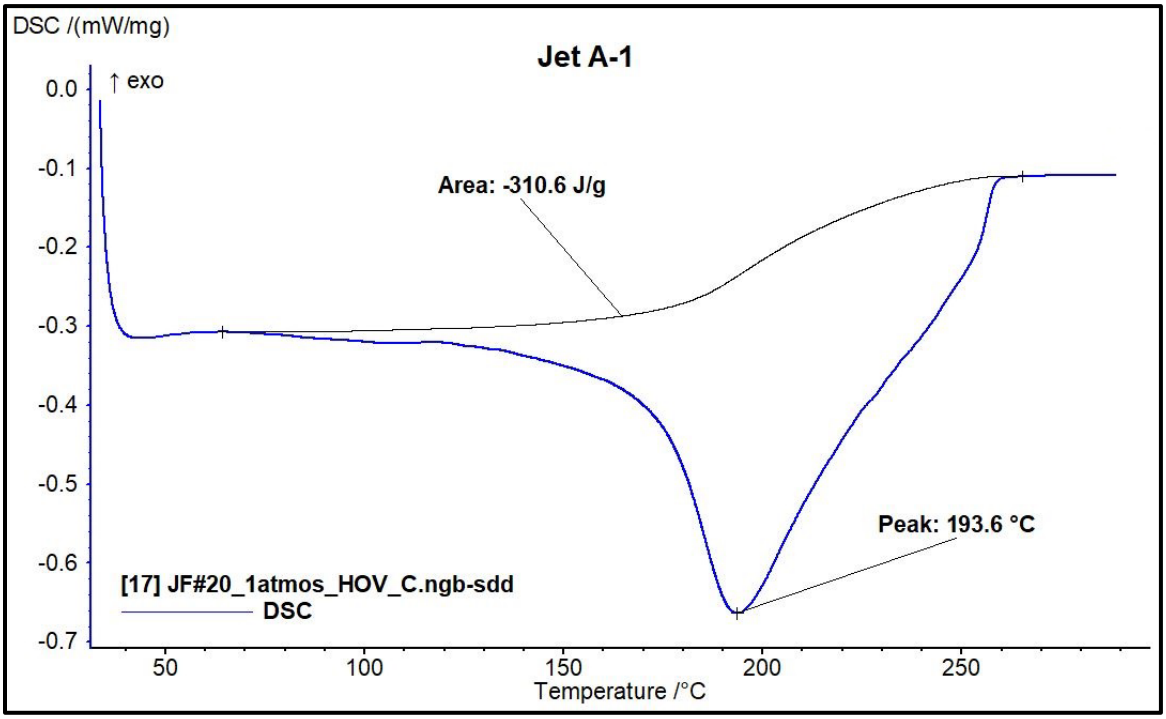

Figure 22: HOV analysis of Jet A-1, hydro-treated, Total, France (JF#20).

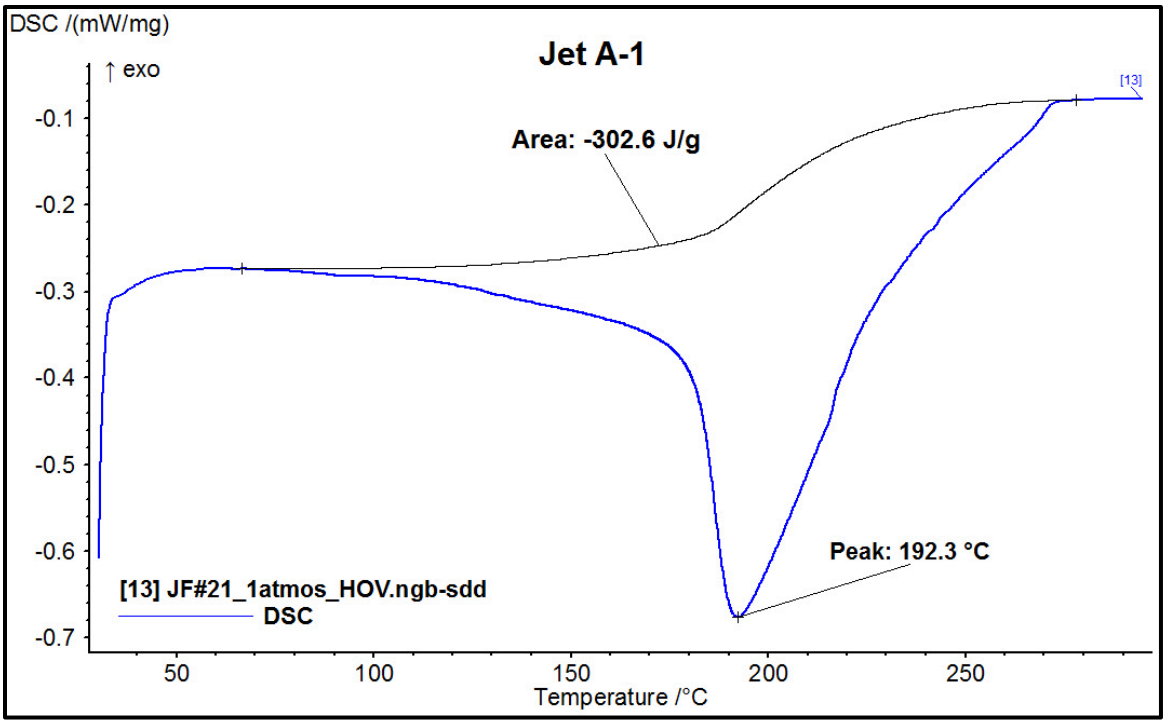

Figure 23: HOV analysis of Jet A-1, Merox™ treated, Total, France (JF#21).

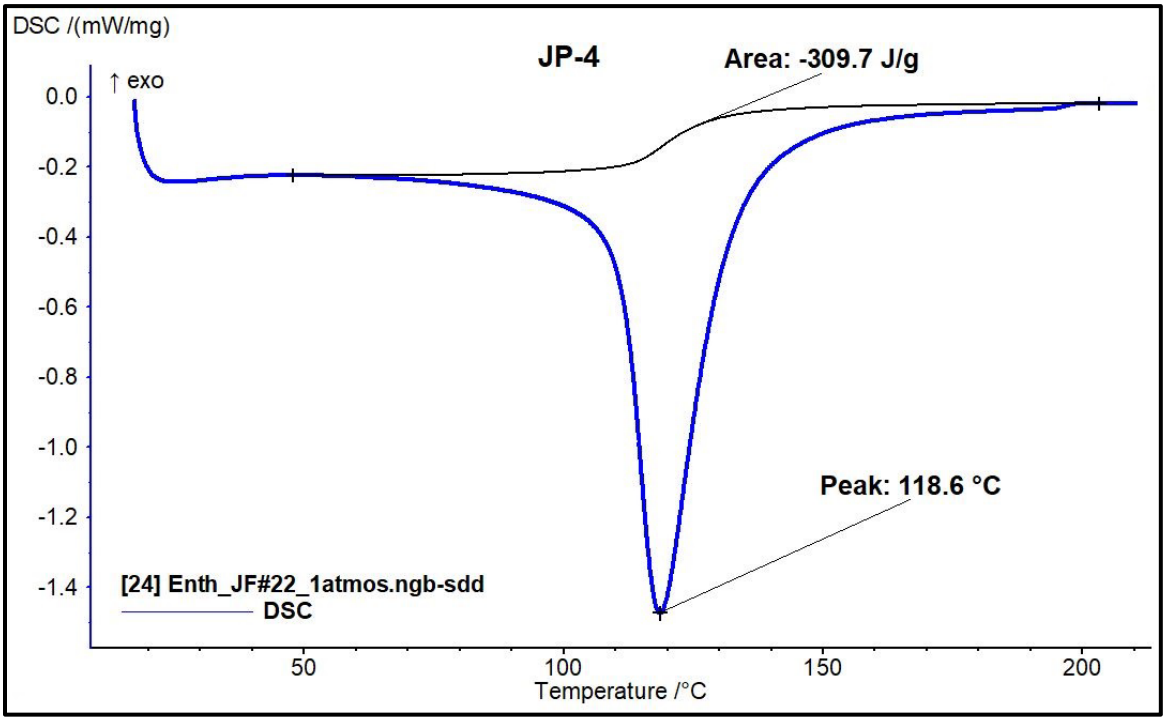

Figure 24: HOV analysis of JP-4, Nova Research, Chevron, USA (JF#22).

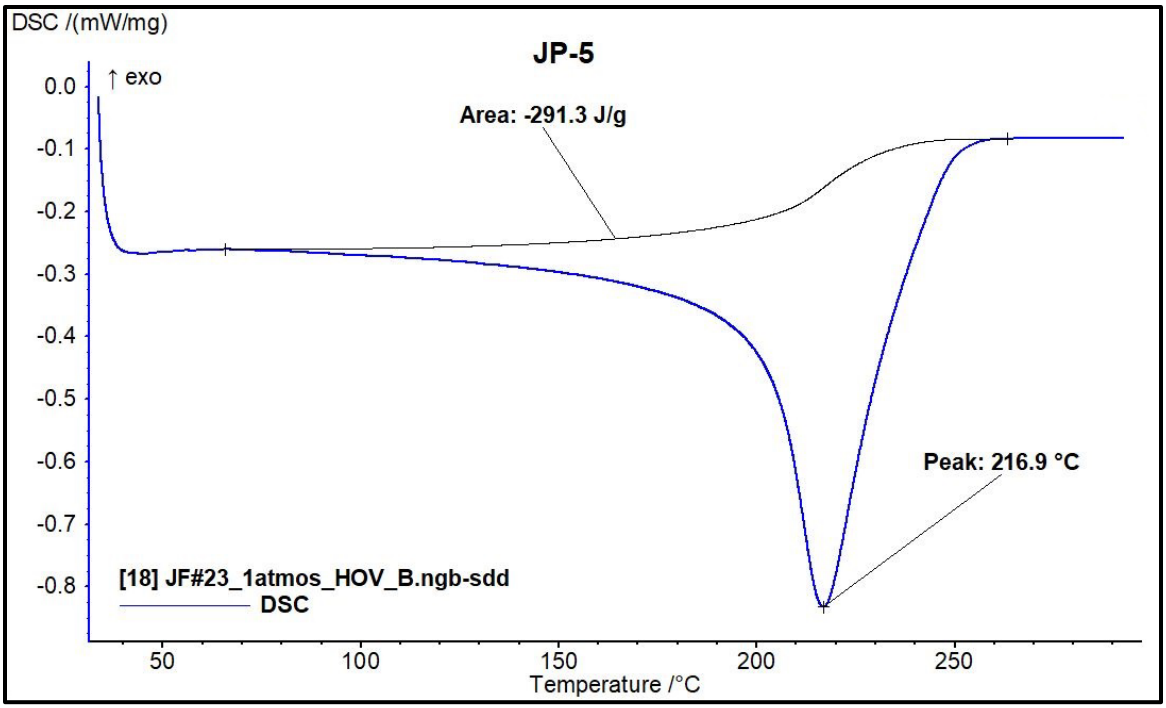

Figure 25: HOV analysis of JP-5, AVCAT, RNAS Culdrose, UK (JF#23).

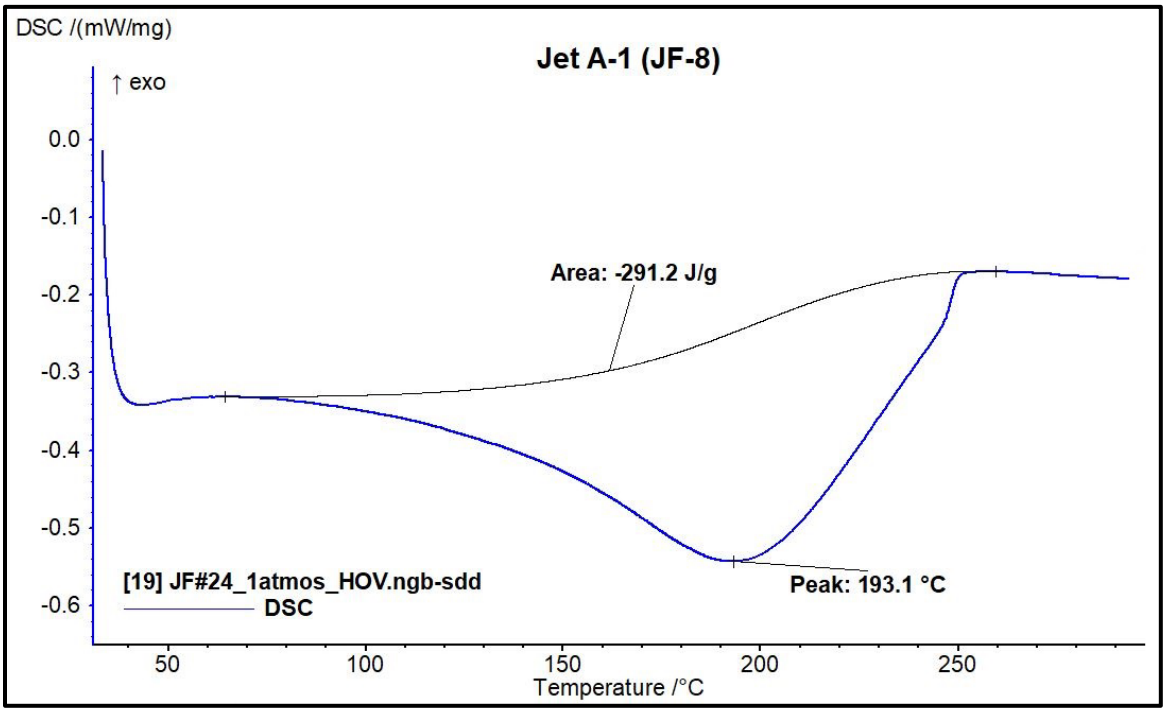

Figure 26: HOV analysis of Jet A-1 (JF-8), with MIL additives, Emo-Trans, Germany (JF#24).

5.5. Standard Deviation – HOV Results

No replicates were performed for this report, so there was no direct measure of the HOV standard deviation. An indirect measure of HOV standard deviation and average was calculated from all the Jet A-1 samples shown in Table 5 below. The average is 308.0 +/- 9.6 J/g for a +/- 3.1 % deviation from the average. The MIL spec jet fuels have a higher boiling point and a lower HOV than the commercial Jet A-1.

JF#12 (Blend) and JF#18 (JP-4) each had two peaks. This is not too surprising for a blend. If there are two components in a blend that have different boiling points, they will distill at different temperatures in the HPDSC experiment. This will give two HOV peaks or one larger peak and a shoulder. A similar observation was recorded for the Avgas samples. Two other blends JF#13 and JF#16 did not have a second peak. This would happen if the two components of the blend are similar in boiling point.

Table 5: Jet A-1 HOV Average and Std. Devi.

		HOV	Peak
Number	**Type**	**(J/g)**	**(°C)**
1	Jet A	329.2	208.4
2	Jet A-1	302.3	182.7
3	Jet A-1	314.5	190.1
4	Jet A-1	313.8	184.2
5	Jet A-1	311.8	185.7
14	Jet A-1	302.3	194.9
15	Jet A-1	298.1	190.2
19	Jet A-1	294.8	190.2
20	Jet A-1	310.6	193.6
21	Jet A-1	302.6	192.3
Average		**308.0**	**191.2**
Std Deviation		**9.6**	**6.9**

6. HOV Quasi-Isothermal (QI) Testing

The HPDSC needs to be set up differently for the HOV QI testing. The purpose of this test is to determine the HOV of the jet fuel at an isothermal temperature. This test is performed at several temperatures. The HOV will decrease as temperature increases until the HOV is zero at the critical temperature for the jet fuel. The HOV at several temperatures will be used to create a figure similar to Figure 27 [1]. The data will also be used to create the 'mix to gas' line in the enthalpy figures. The NETZSCH High-pressure DSC software can only integrate the area under an evaporation peak when there is a temperature ramp. This is the reason for the quasi-isothermal (QI) HPDSC test. A typical temperature versus time result is shown in Figure 29.

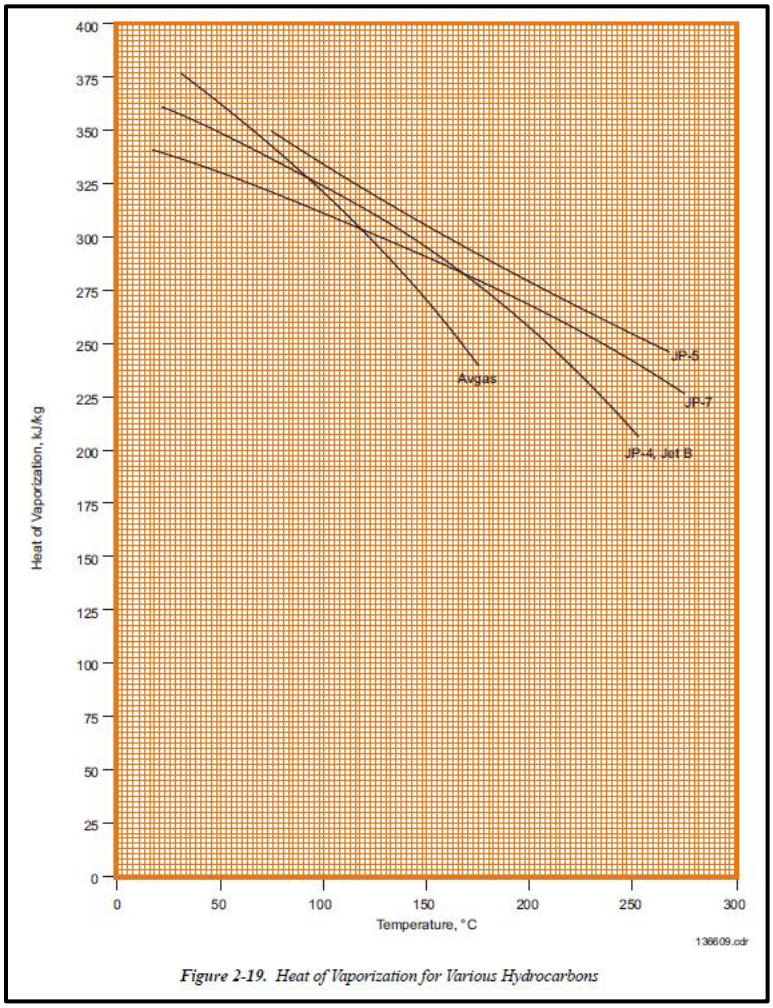

Figure 27: HOV for various hydrocarbons. CRC Handbook, Figure 2-19, [1].

6.1. Sample Preparation for HOV QI Testing

The same procedure as detailed in Section 5.1 was used to prepare samples for enthalpy testing.

6.2. HOV QI Testing Method

The sample was placed into the HPDSC, and the lid was secured, then the valve to the regulator was closed. The HPDSC was charged with nitrogen gas to 100 psi and released two times using the vent valve. The HPDSC was charged to 800 psi with nitrogen for the test. The heat flow sensitive and temperature calibration at one atm was used. No baseline subtraction was needed for these tests. Flowing tap water was used as the coolant for the HPDSC.

Test method

Initial Temperature: use the actual temperature as displayed.
Ramp temperature: 30°C/min to QI test temperature
Ramp temperature: 0.02 °C/min to 2°C above the QI test temperature

The method was started. I waited until the temperature reached the QI temperature. I waited a little longer until the heat flow signal stabilized close to zero W/g. I turned on the vacuum pump and set it to the maximum vacuum. I opened the outlet valve to the regulator. I waited for the method to finish or for the evaporation endotherm to finish. I turned off the vacuum pump. I opened the vent valve to equalize the pressure in the HPDSC to atmospheric pressure. I removed the lid nuts from the HPDSC by hand.

This test was repeated for several isothermal temperatures in the region of the enthalpy curve between the intersection of the 0.1 atm, 'Mix-to-Gas' and 68 atm lines, as shown in Figure 28. For the best precision, at least five temperatures should be run. In the case shown in Figure 28, seven tests were run from 175 to 325 °C in steps of 25°C.

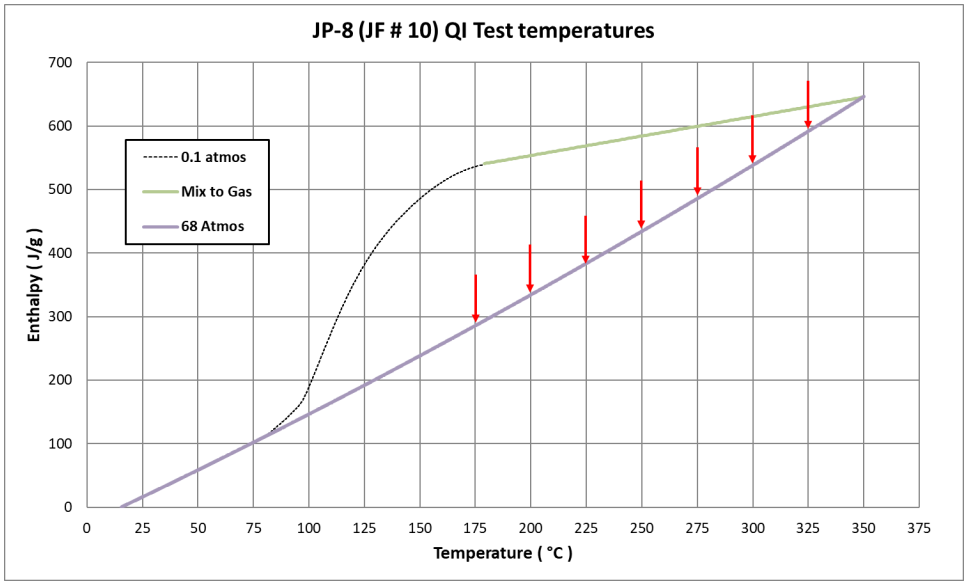

Figure 28: Typical enthalpy versus QI temperature. The QI temperatures for a HOV QI HPDSC experiment were 175, 200, 225, 250, 275, 300, and 325 °C.

A typical QI temperature ramp is shown in Figure 29. The peak temperature at the evaporation endotherm was used for the temperature of the evaporation that is used for the X axis value in the HOV versus temperature graphs.

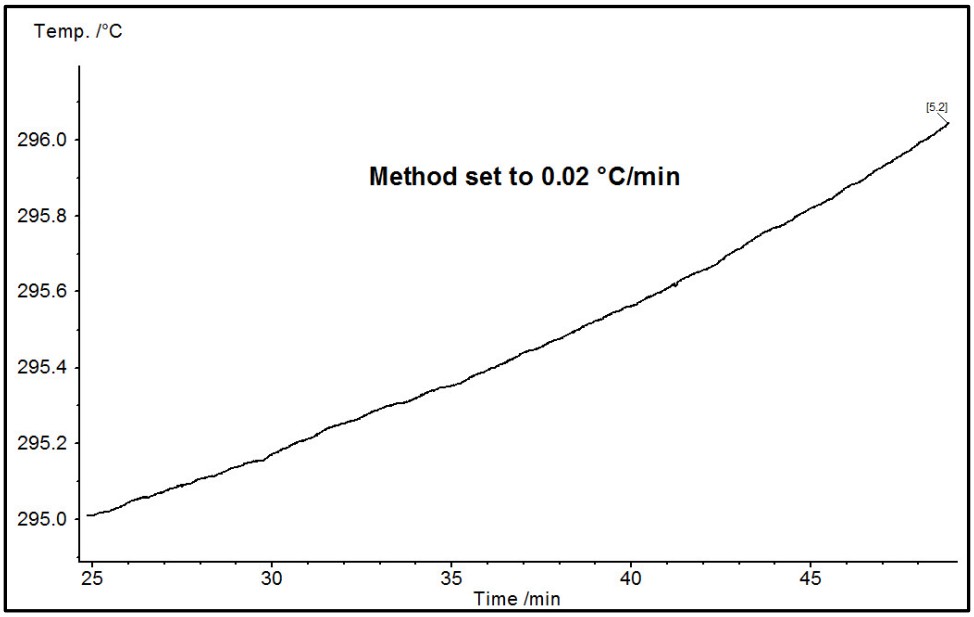

Figure 29: Temperature versus time for a HOV QI HPDSC experiment.

6.3. HOV QI Data Evaluation Procedure

The evaporation endotherm was integrated, as shown in Figure 30. The area under the peak is the HOV, 51.3 J/g, and the peak temperature, 321.2 °C, is the QI temperature for the evaporation, for the example shown.

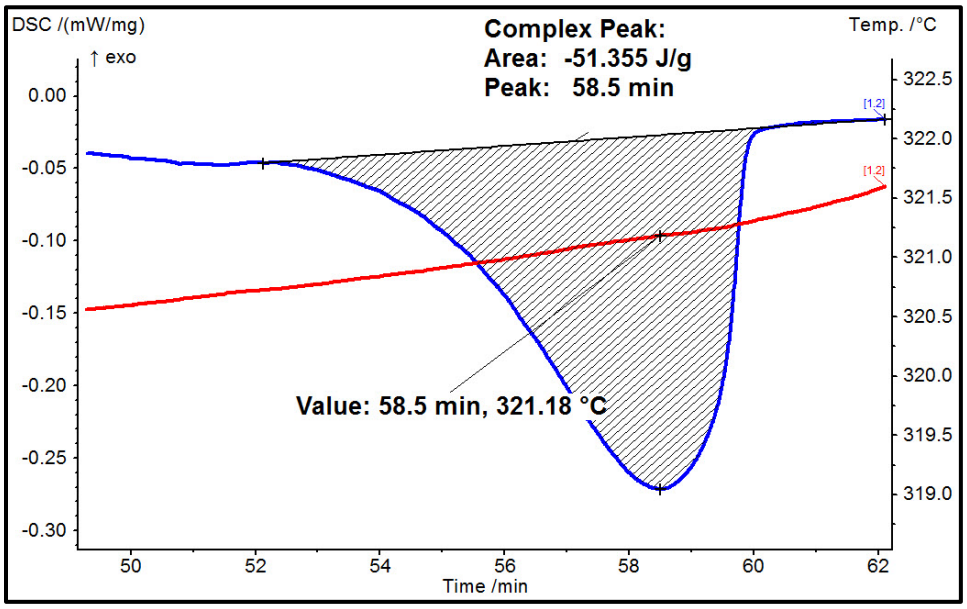

Figure 30: Integration of the evaporation of a JF during the QI HPDSC experiment.

7. HOV Quasi-Isothermal Diagrams

7.1. Tables of QI Heat Flow Data

Tables 6 to 25 show the data for the Peak Temperature and the HOV from the QI HPDSC experiments. The critical temperature, T_c, was obtained by extrapolating the peak temperature to zero HOV. The critical temperature is where the sample is a critical fluid, having the properties of a gas and a liquid, with no distinction between the two. Additionally, there is no heat of vaporization because there is no liquid to gas phase change above the critical temperature.

Table 6: Jet A Shell USA (JF#1)

	Peak Temperature	**HOV**
	(°C)	(J/g)
	246.7	108.8
	271.5	102.7
	296.3	67.34
	321.1	48.5
$T_{critical}$	397.4	0

Table 7: Jet A-1 SHELL Netherlands (JF#2)

	Peak Temperature	**HOV**
	(°C)	**(J/g)**
	247.2	202.9
	271.7	183.7
	296.4	156.8
	321.2	130.8
	346.1	92.34
	370.1	44.75
$T_{critical}$	379.9	0

Table 8: Jet A-1 A/S Dansk SHELL (JF#3)

	Peak Temperature	HOV
	(°C)	(J/g
	247.1	198.3
	271.8	189.9
	296.7	167.2
	321.4	144.5
	333.2	137.2
	339.2	126.5
	346.1	127.3
	370.8	63.3
	394.7	33.6
	346.1	60.0
	370.4	18.3
$T_{critical}$	405.4	0

Table 9: Jet A-1 SHELL Germany (JF#4)

	Peak Temperature	HOV
	(°C)	(J/g)
	221.8	176.6
	246.5	199.8
	271.8	190.0
	296.5	166.8
	321.2	149.6
	346.0	120.6
	370.8	53.4
	394.4	32.1
$T_{critical}$	428.4	0

Table 10: Jet A-1 SHELL Germany (JF#5)

	Peak Temperature	HOV
	(°C)	(J/g)
	222.0	187.4
	246.6	199.1
	271.4	188.2
	296.6	151.1
	321.3	135.2
	346.1	95.5
	370.3	16.5
$T_{critical}$	400.9	0

Table 11: Jet A WPAFB/Shell (JF#8)

	Peak Temperature	HOV
	(°C)	(J/g)
	196.9	231.3
	221.7	202.6
	247	171.5
	271.6	148.2
	296.4	81.2
	321.2	46.3
	345.7	6.04
$T_{critical}$	346.45	0

Table 12: JP-5 WPAFB/Valero (JF#9)

	Peak Temperature	HOV
	(°C)	(J/g)
	172.9	257.7
	197.7	226.8
	222.5	205.3
	247.2	185.0
	271.9	169.2
	297.7	110.6
	321.4	102.7
	346.3	61.8
	370.8	16.6
$T_{critical}$	379.175	0

Table 13: JP-8 WPAFB/NuStar (JF#10)

	Peak Temperature	HOV
	(°C)	(J/g)
	147.9	257.9
	172.6	259.3
	197.2	226.8
	222	161.2
	246.7	172.4
	271.5	133.5
	296	72.7
	320.9	39.2
	346.1	9.6
$T_{critical}$	349.15	0

Table 14: JP-TS WPAFB/Ashland (JF#11)

	Peak Temperature	HOV
	(°C)	(J/g)
	247.0	202.2
	271.8	178.8
	296.5	158.2
	321.4	133.5
	346.1	92.4
	369.9	37.6
$T_{critical}$	408.5	0

Table 15: Test Fld. WPAFB/AFRL (JF#12)

	Peak Temperature	HOV
	(°C)	(J/g)
	247.3	202.2
	272.0	179.7
	296.8	159.1
	321.5	172.6
	346.2	148.5
	370.3	108.7
$T_{critical}$	523.9	0

Table 16: HEFA/JP-8 WPAFB/AFRL (JF#13)

	Peak Temperature	HOV
	(°C)	(J/g)
	271.8	176
	296.6	161.6
	321.4	143.6
	346.1	107.7
	370.6	54.4
$T_{critical}$	420.6	0

Table 17: Jet A-1 Sasol/S. Africa (JF#14)

	Peak Temperature	HOV
	(°C)	(J/g)
	247.0	178.4
	271.6	173.9
	296.4	173.5
	321.0	140.2
	346.0	116.9
	370.5	53.4
$T_{critical}$	430.1	0

Table 18: Jet A-1 Sasol/S. Africa (JF#15)

	Peak Temperature	HOV
	(°C)	(J/g)
	246.9	178.6
	271.4	159.7
	296.4	147
	321.2	138.3
	346.0	108.3
	369.7	30.7
$T_{critical}$	410.1	0

Table 19: TS-1 AirBP/UK (JF#17)

	Peak Temperature	HOV
	(°C)	(J/g)
	123.4	291.2
	147.8	290.4
	172.8	254.5
	197.6	212.9
	221.8	191.7
	247	151.3
	271.8	77.2
	296.7	85.3
	321.6	15.9
$T_{critical}$	327.58	0

Table 20: Jet A-1 Total/France (JF#19)

	Peak Temperature	HOV
	(°C)	(J/g)
	246.9	196.9
	271.7	184.3
	296.4	201.8
	320.8	157.7
	345.8	114.5
	369.9	42.1
$T_{critical}$	408.0	0

Table 21: Jet A-1 Hydro-treated, Total/France (JF#20)

	Peak Temperature	HOV
	(°C)	(J/g)
	246.9	170.4
	271.3	185.4
	296.4	154.3
	320.8	91.9
	345.6	109.1
	370.6	3.4
$T_{critical}$	382.4	0

Table 22: Jet A-1 Meroxed™, Total/ France (JF#21)

	Peak Temperature	HOV
	(°C)	(J/g)
	247.0	180.3
	271.4	176.7
	296.6	163
	346.1	84.4
	370.6	42.4
$T_{critical}$	409.4	0

Table 23: JP-4 Nova Research/Chevron (JF#22)

	Peak Temperature	HOV
	(°C)	(J/g)
	74.2	292.9
	98.7	280.2
	123.4	193.4
	148	228.3
	172.6	190.3
	197.3	172.0
	221.8	104.7
	246.1	90.5
$T_{critical}$	320.22	0

Table 24: JP-5 RNAS Culdrose/UK (JF#23)

	Peak Temperature	HOV
	(°C)	(J/g)
	247.2	190.4
	271.8	178
	296.6	145.9
	321.2	145.4
	346.1	111
	370.8	71.0
$T_{critical}$	452.6	0

Table 25: Jet A-1 (JF-8) Emo-Trans/Germany (JF#24)

	Peak Temperature (°C)	HOV (J/g)
	246.9	170.5
	271.8	171.6
	296.6	150.8
	321.0	97.7
	345.9	83.6
	370.3	22.9
$T_{critical}$	396	0

7.2. HOV QI Diagram Results

The tabular data from the table in section 7.1 were used to generate the following Figures 31 to 50. The raw data points are shown as blue circles and the dashed blue line is a 1st or 2nd order polynomial line fit, whichever is the best fit. The polynomial fit was extrapolated to zero HOV to determine the critical temperature.

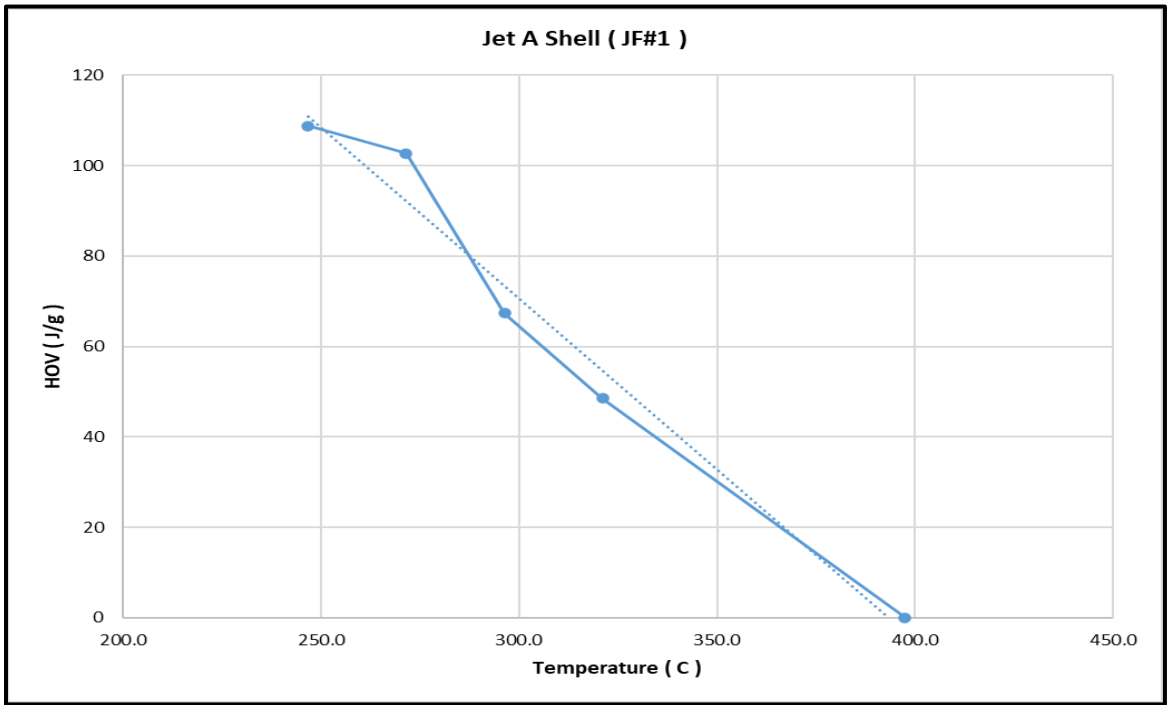

Figure 31: Jet A Shell USA from a QI HPDSC experiment.

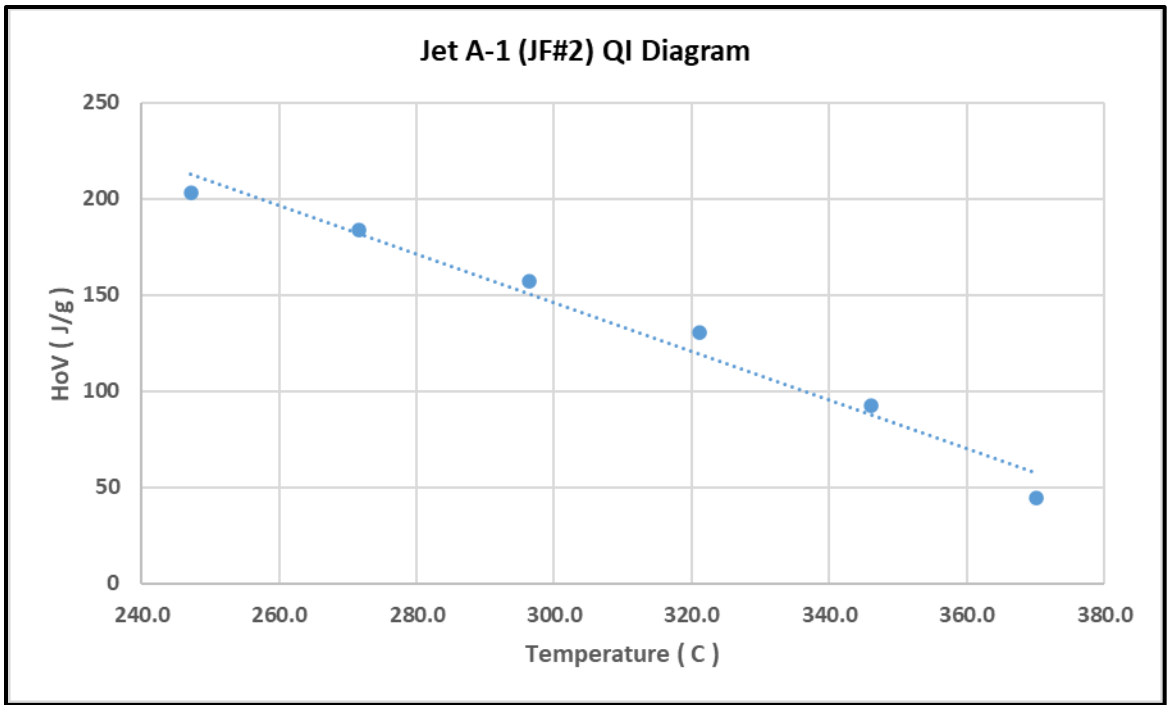

Figure 32: Jet A-1 Shell Netherlands HOV from a QI HPDSC experiment.

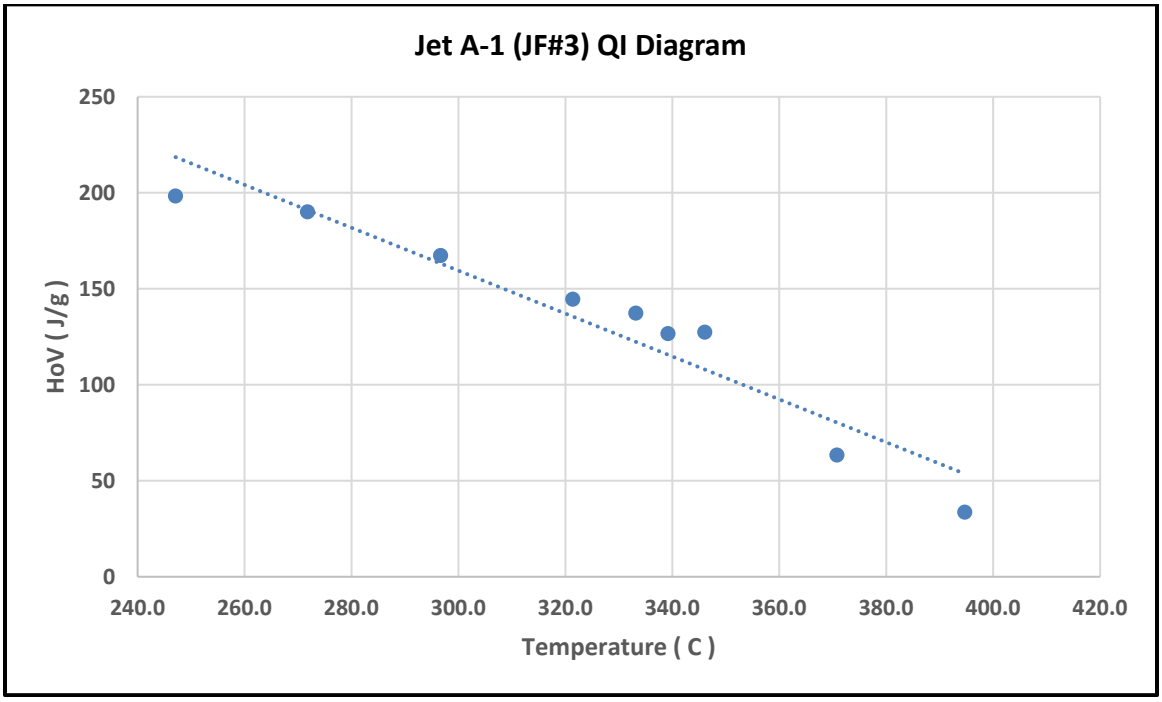

Figure 33: Jet A-1 A/S Dansk Shell HOV from a QI HPDSC experiment.

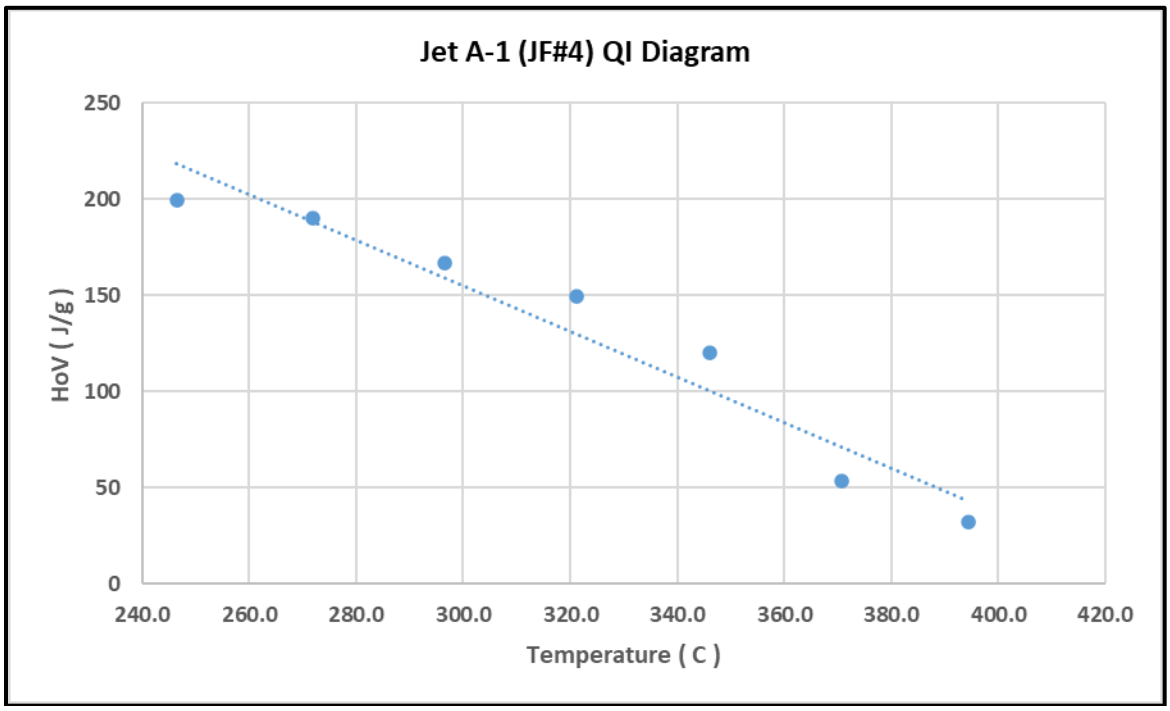

Figure 34: Jet A-1 T309 Shell Germany HOV from a QI HPDSC experiment.

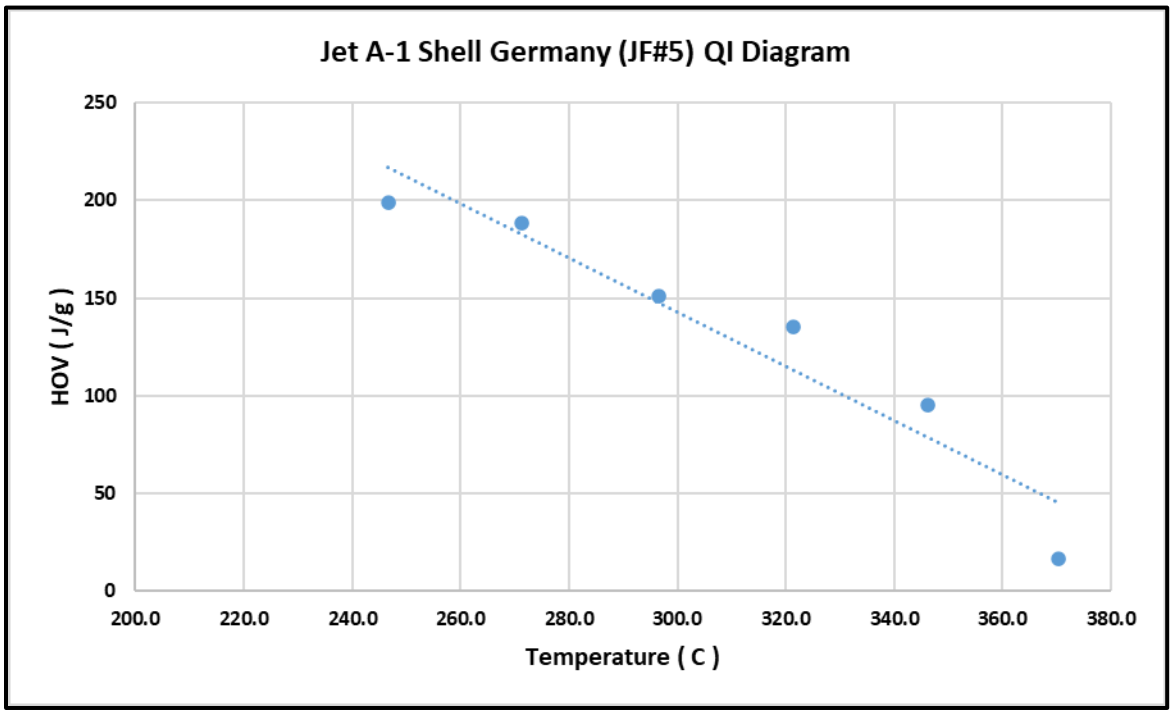

Figure 35: Jet A-1 Q92283 Shell Germany HOV from a QI HPDSC experiment.

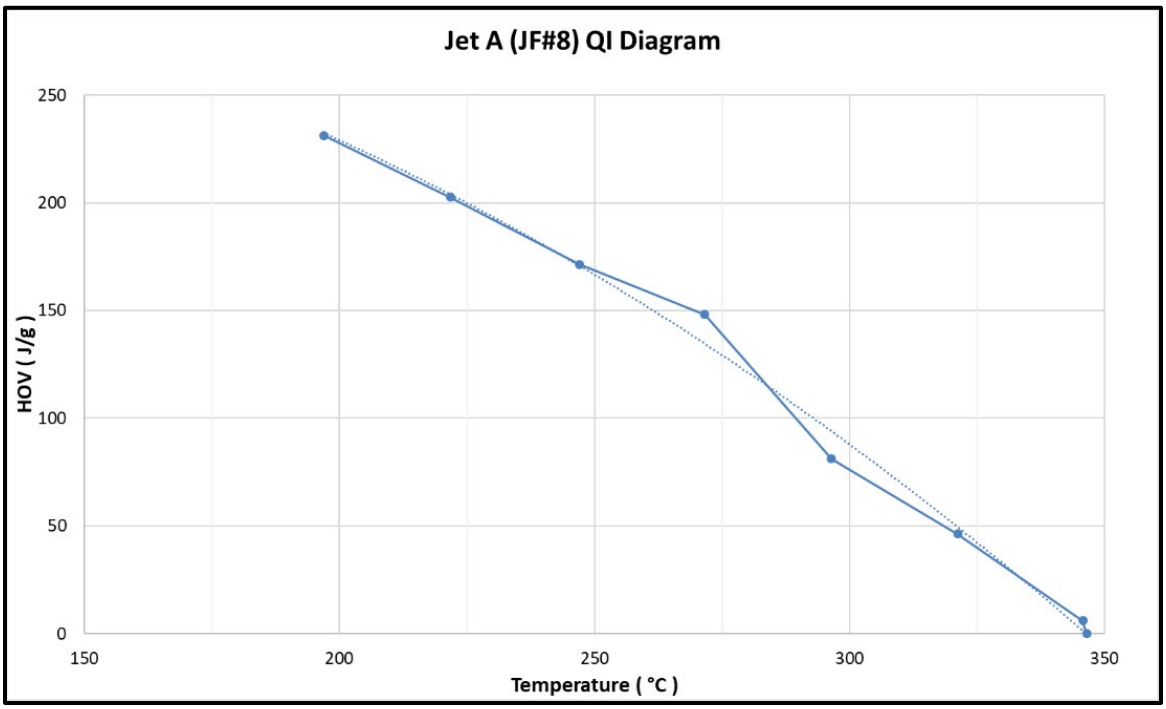

Figure 36: Jet A WPAFB USA HOV from a QI HPDSC experiment.

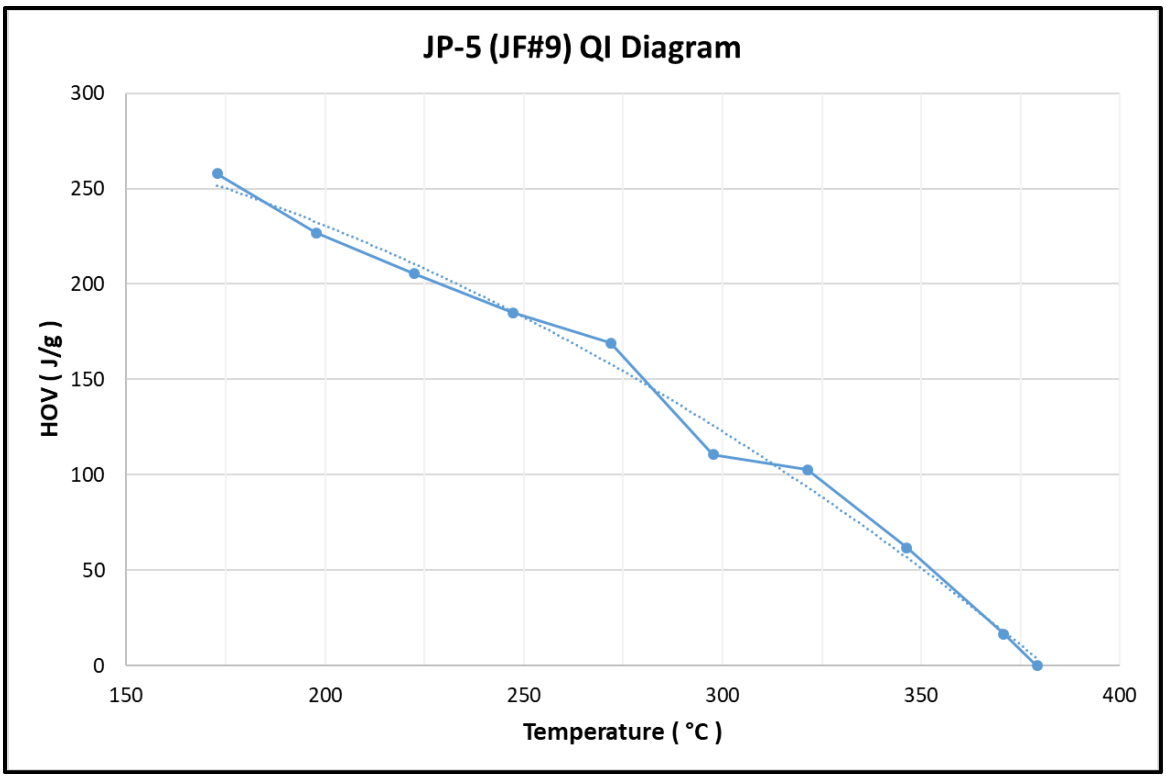

Figure 37: JP-5 WPAFB USA HOV from a QI HPDSC experiment.

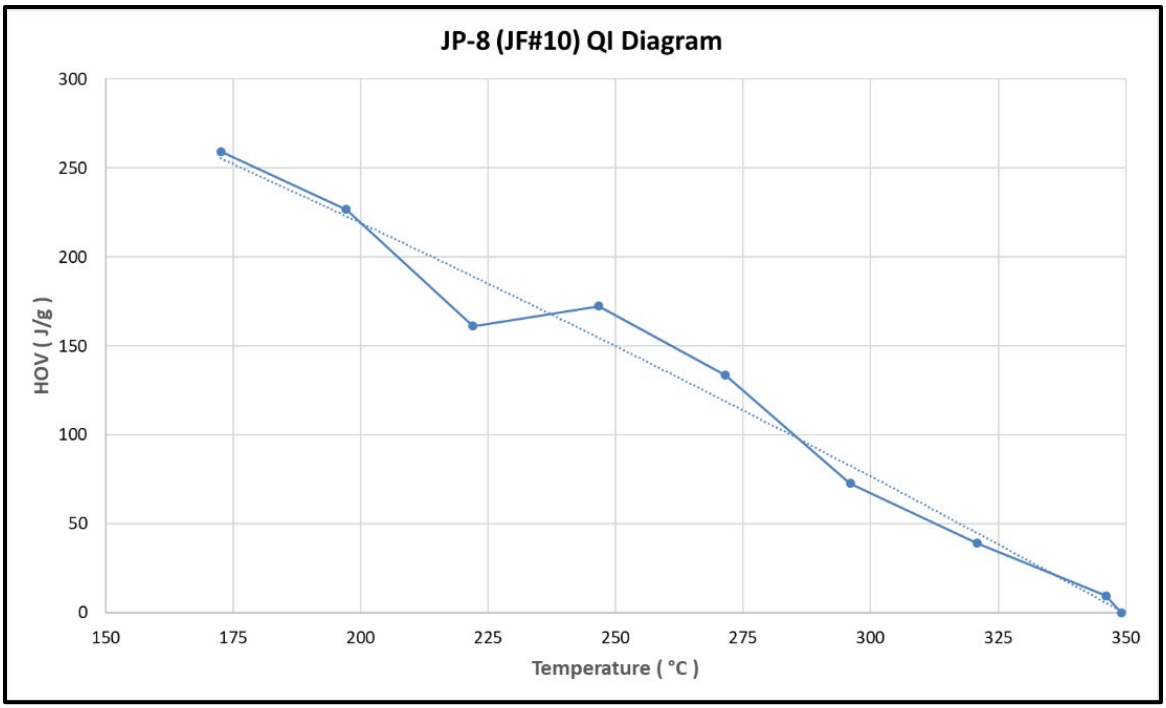

Figure 38: JP-8 WPAFB USA HOV from a QI HPDSC experiment.

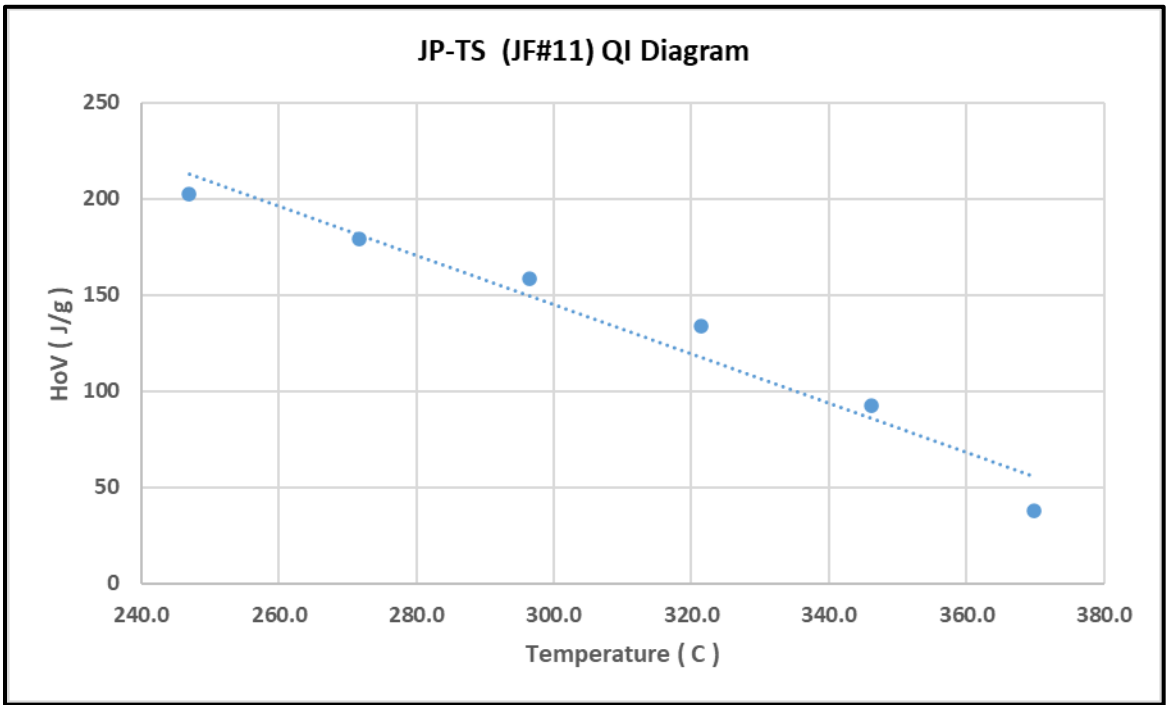

Figure 39: TP-TS WPAFB USA HOV from a QI HPDSC experiment.

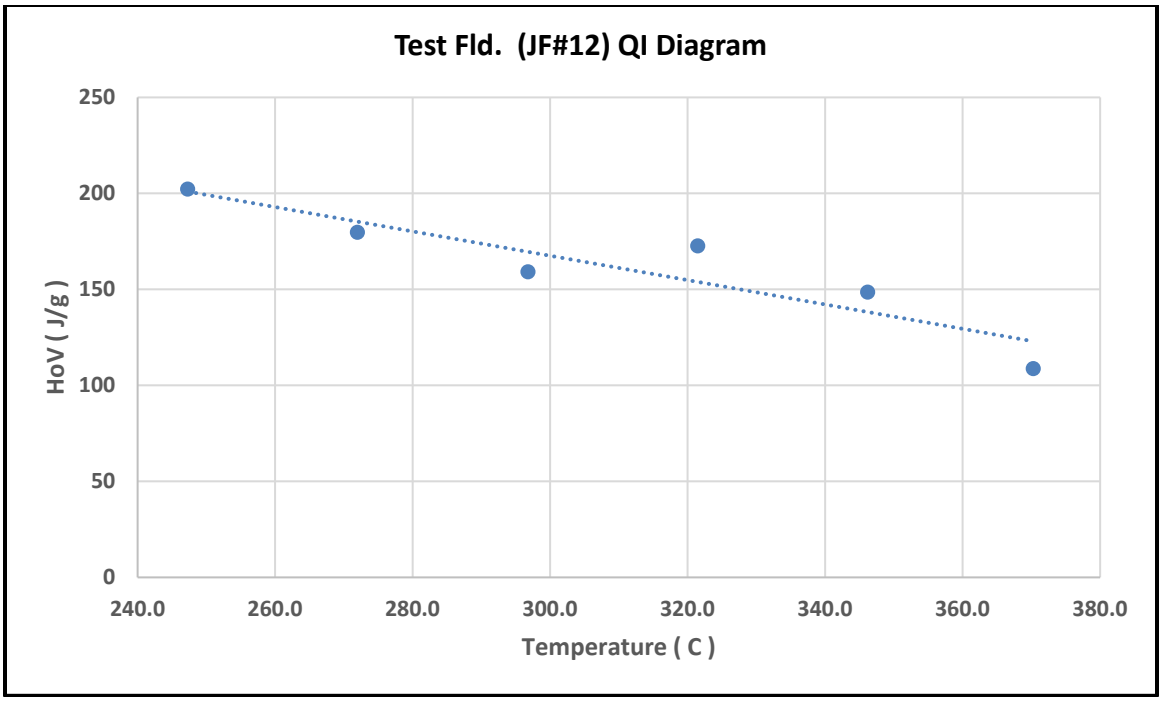

Figure 40: Test Fld. WPAFB USA HOV from a QI HPDSC experiment.

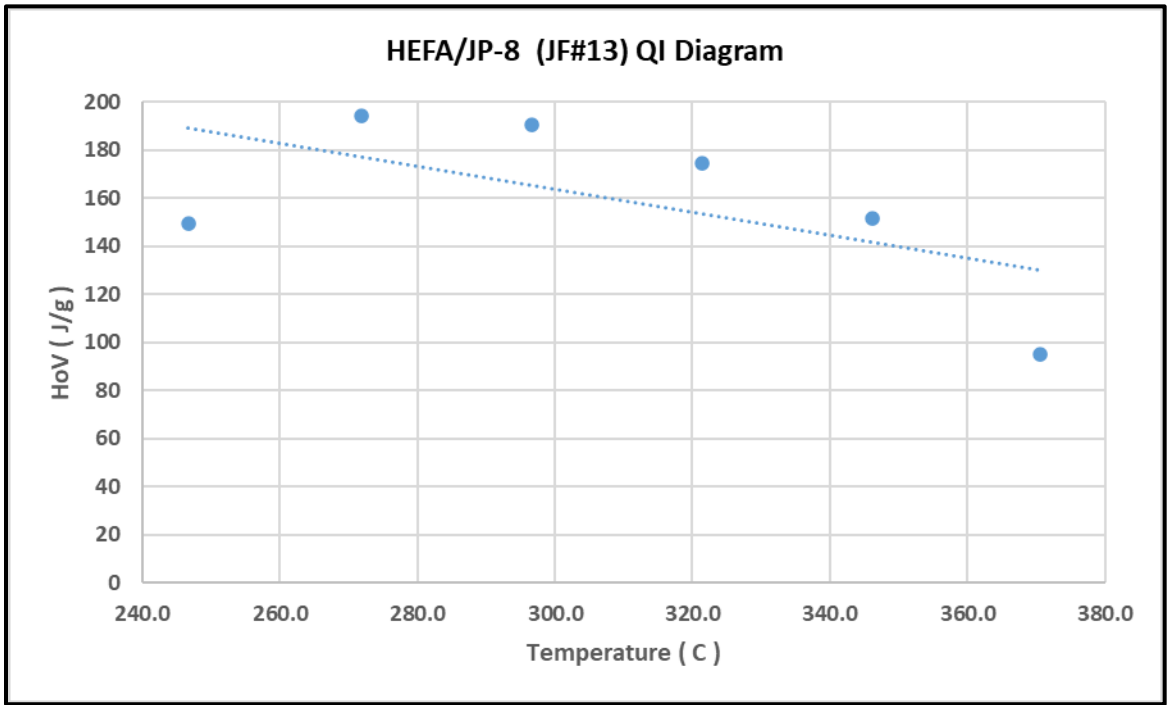

Figure 41: HEFA/JP-8 Blend WPAFB USA HOV from a QI HPDSC experiment.

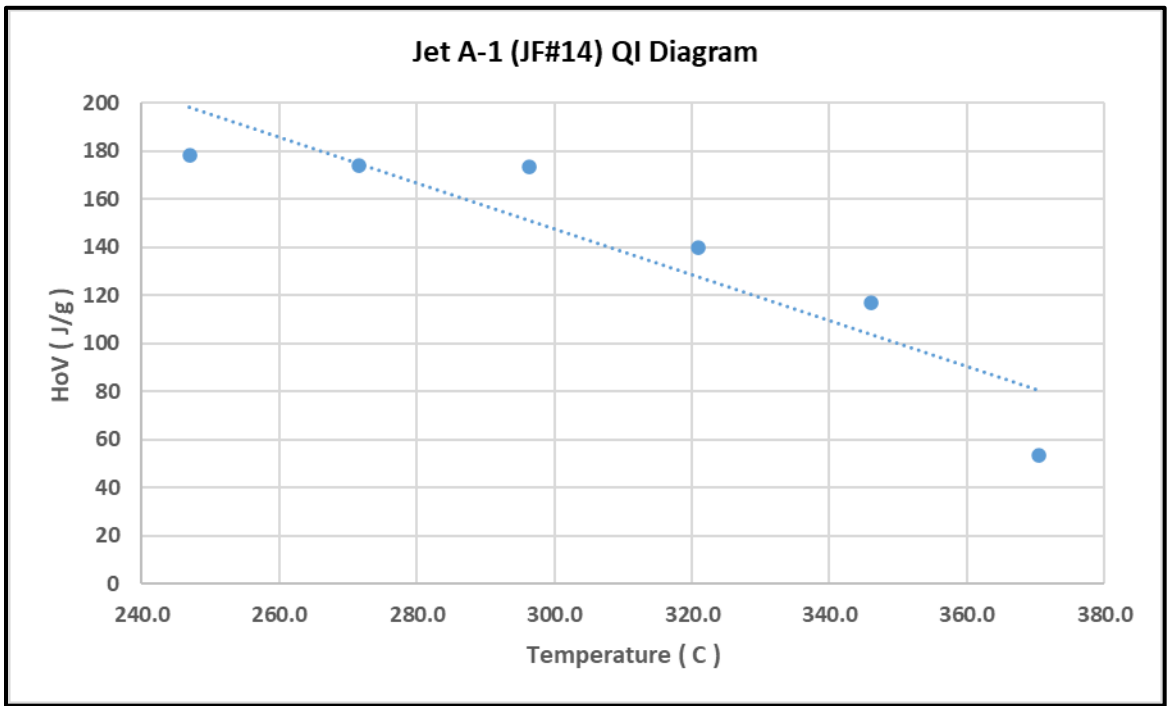

Figure 42: Jet A-1 Fully Synthetic SASOL S. Africa HOV from a QI HPDSC experiment.

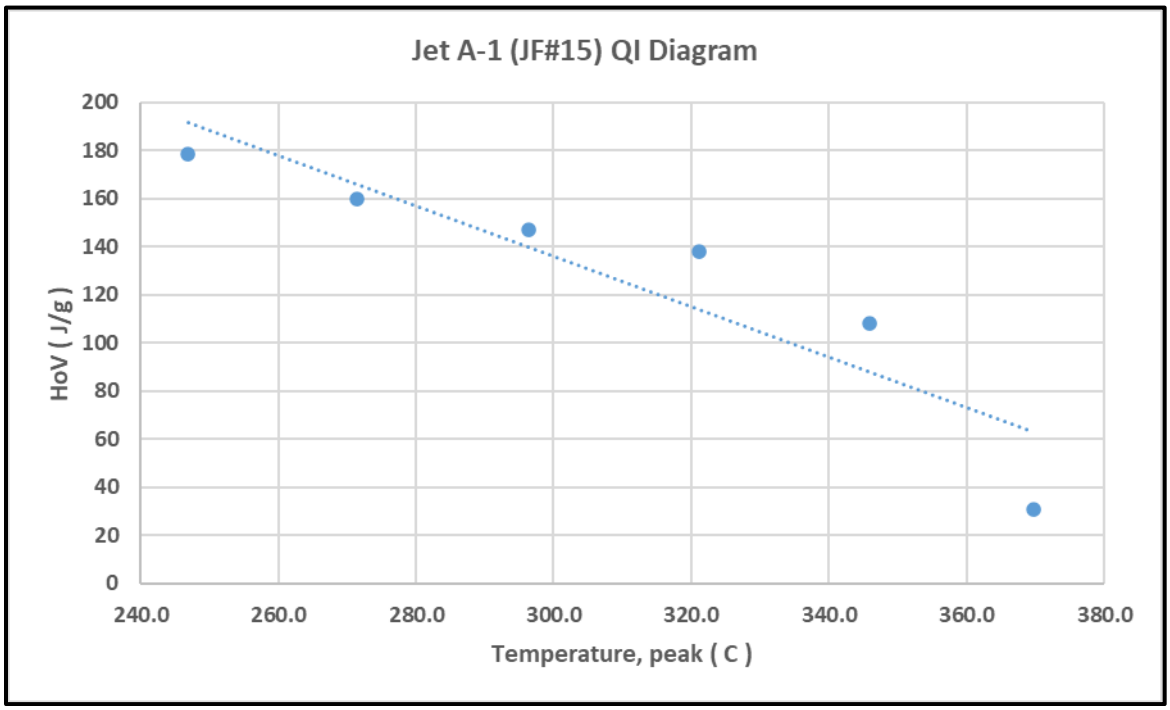

Figure 43: Jet A-1 Semi-Synthetic SASOL S. Africa HOV from a QI HPDSC experiment.

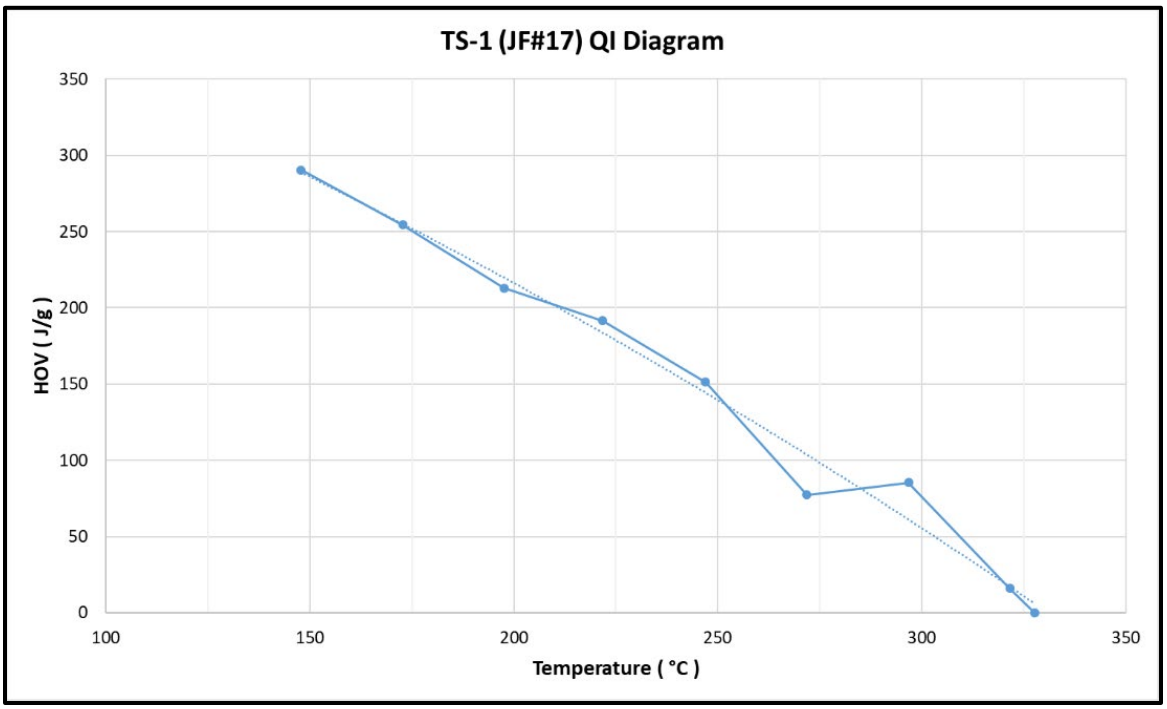

Figure 44: TS-1 Air BP UK HOV from a QI HPDSC experiment.

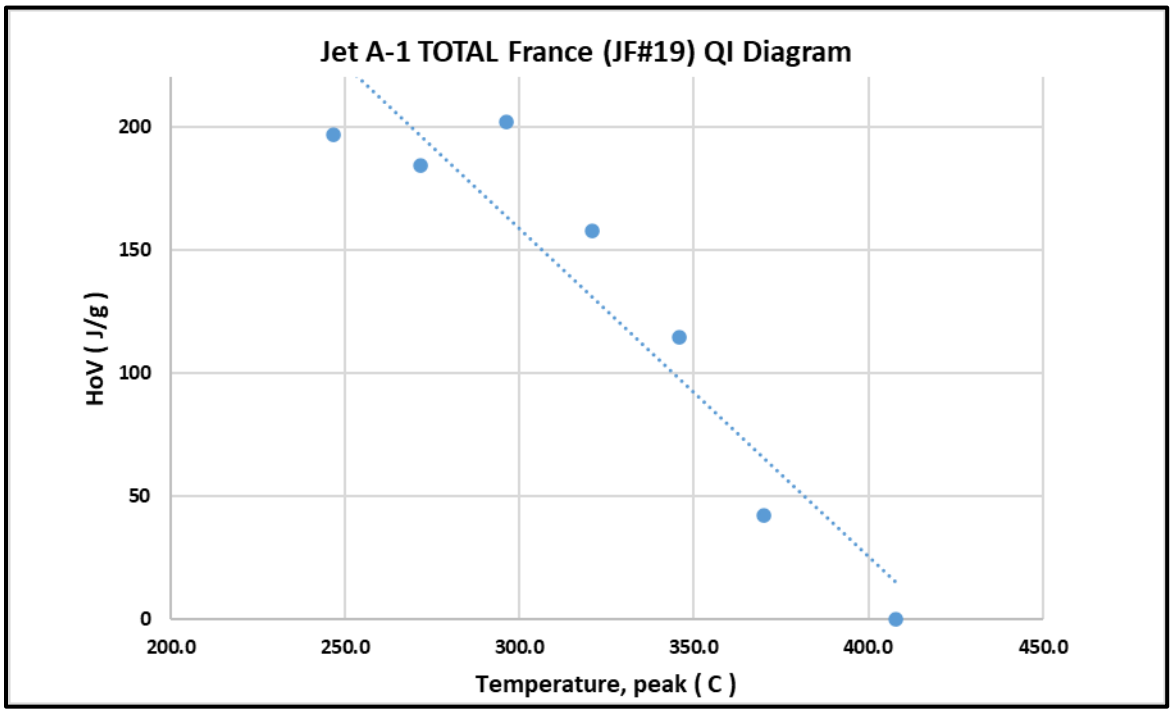

Figure 45: Jet A-1 TOTAL France HOV from a QI HPDSC experiment.

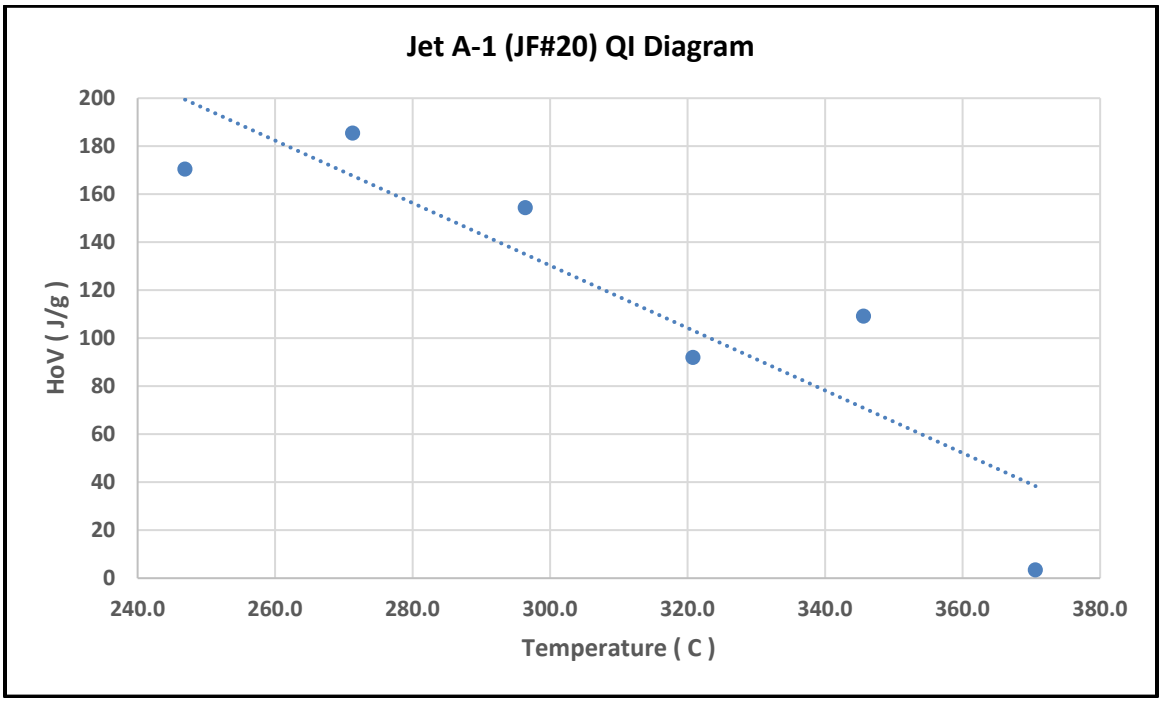

Figure 46: Jet A-1 hydro-treated, TOTAL France HOV, QI HPDSC experiment.

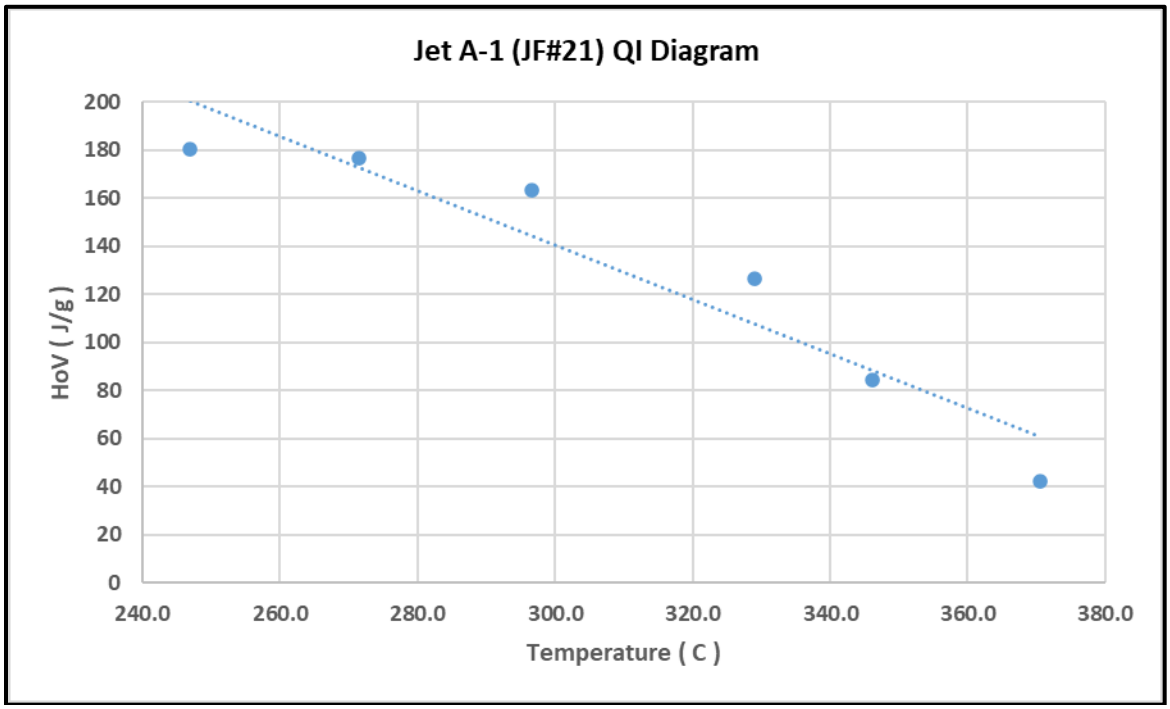

Figure 47: Jet A-1 Meroxed™, TOTAL France HOV from a QI HPDSC experiment.

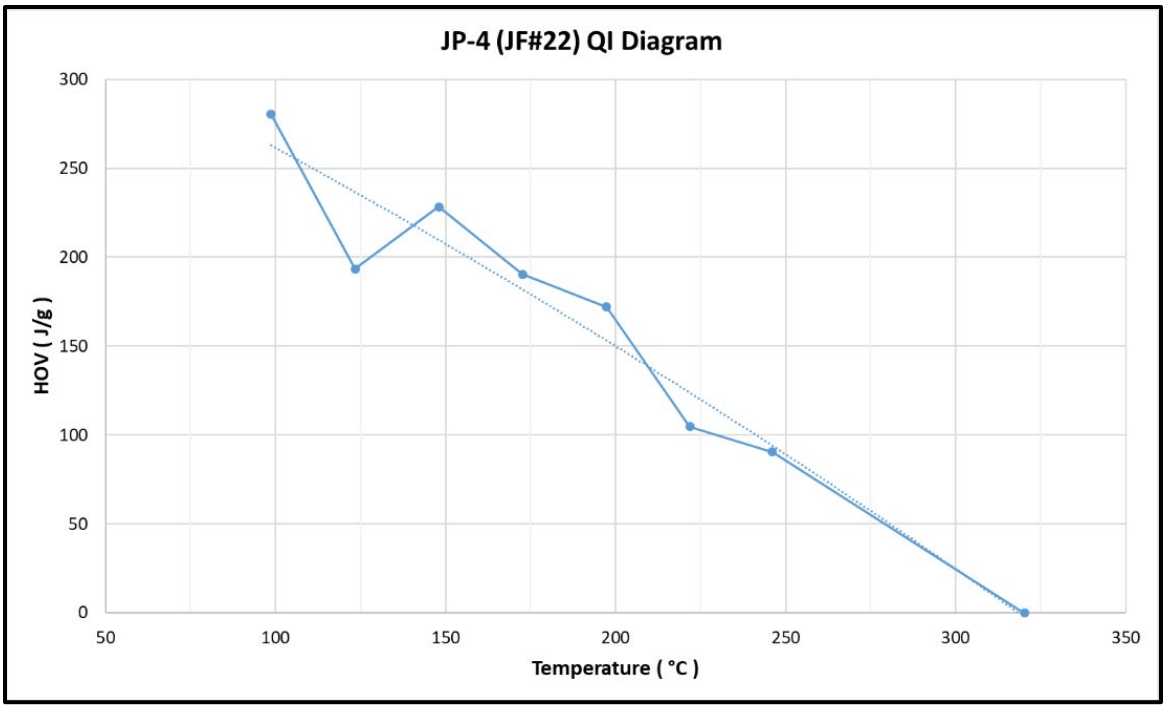

Figure 48: JP-4 NOVA Research Chevron USA HOV from a QI HPDSC experiment.

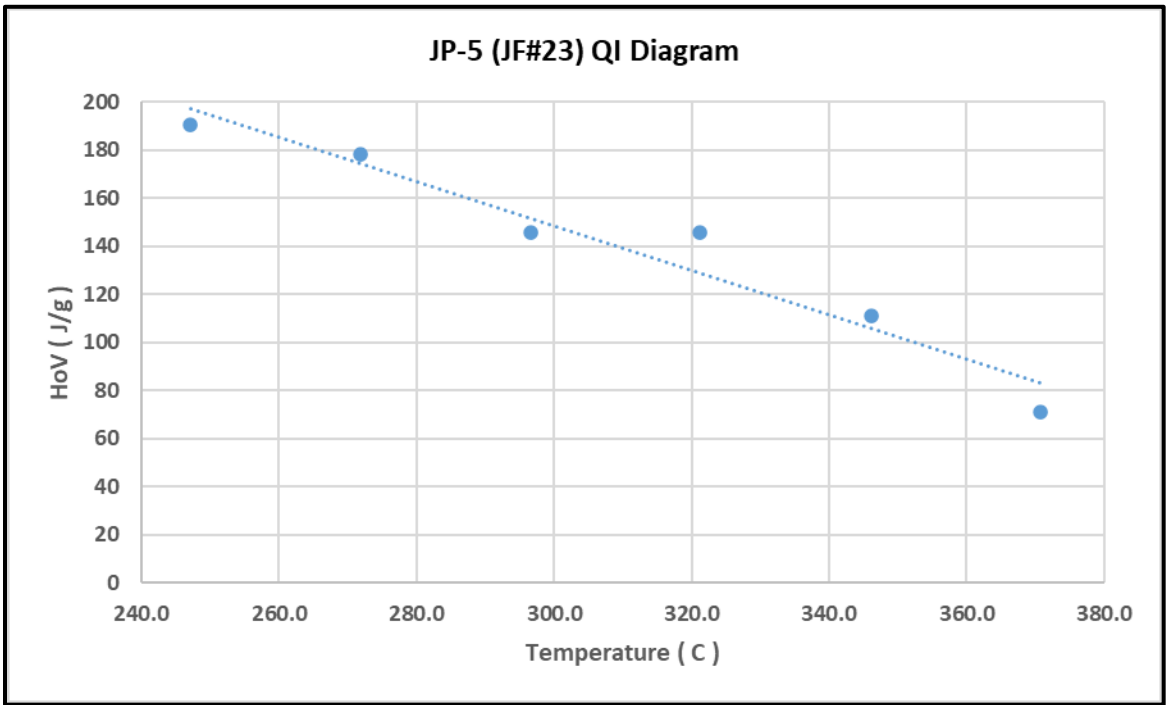

Figure 49: JP-5 RNAS Culdrose UK HOV from a QI HPDSC experiment.

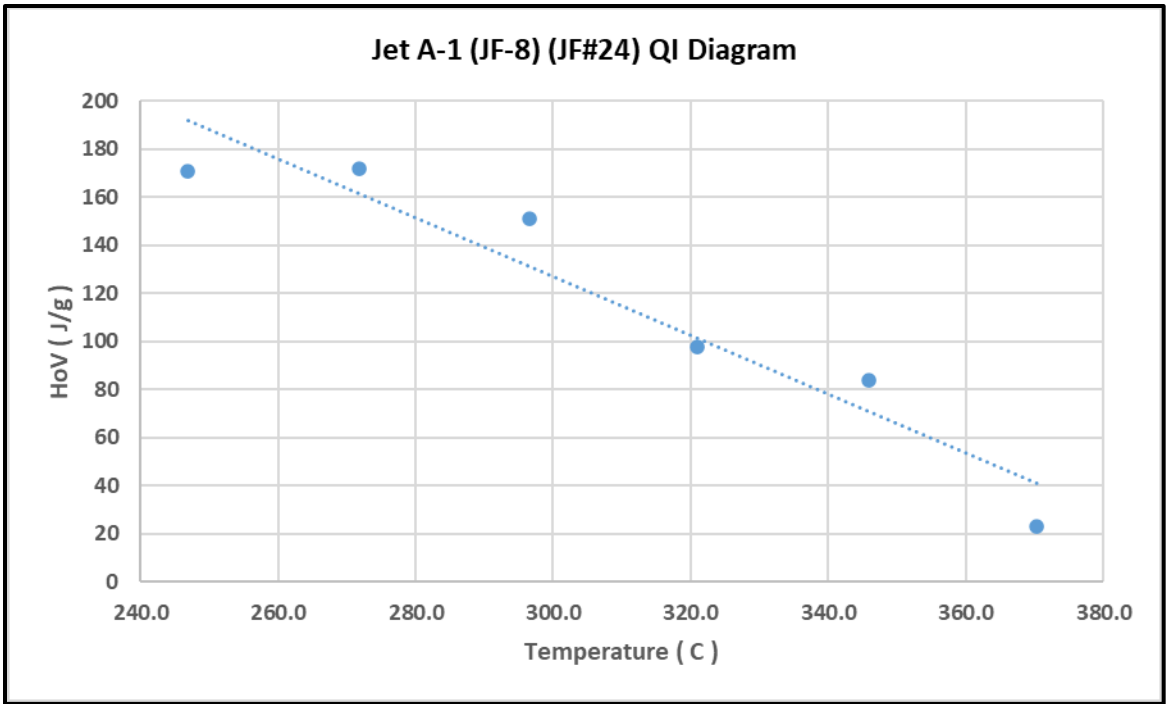

Figure 50: Jet A-1 Emo-Trans Germany (JF-8) HOV from a QI HPDSC experiment.

8. Enthalpy Diagram

8.1. Background on Enthalpy Diagrams

The HPDSC measures the instantaneous heat flow of the sample in watts per gram (W/g). The enthalpy is the cumulative integral of this heat flow from the beginning to the end of the scan. This integral requires a correct baseline to form one side of the boundary for this integration. The other side is the heat flow curve. The enthalpy calculation requires a baseline curve to be run under exactly the same conditions as the sample will be run. These conditions include: heating rate, type of gas, gas pressure and crucibles. The crucibles all had a 50 µm laser drilled hole in the lid to permit the jet fuel or Avgas to evaporate. The reference crucible was crimped to the lid and it was used for all future experiments. The sample crucible was not crimped for the blank run and then filled with the jet fuel and crimped shut for the sample test. Since the crimped sample crucible could not be reused, a blank had to be run for each sample/pressure pair that was tested.

8.2. Sample Preparation for Enthalpy Testing

The same procedure as detailed in Section 5.1 was used to prepare samples for enthalpy testing.

8.3. Enthalpy Testing Method

The HPDSC and samples were initially prepared as detailed in Section 5.2 for the test, again using the water chiller for the more volatile JP-4 (JF #22) and Avgas samples. Two crucibles, one sample and one empty, were used for all HPDSC tests. The reference crucible is crimped shut and can be used for all the HPDSC experiments. The sample crucible was run first with the lid not crimped closed. This is the baseline, which the software automatically subtracted for the next test, which is the sample run. The mass of the empty sample crucible was tared. The sample, 10 µL, was

pipetted into the sample crucible and promptly crimped shut. The sample was weighed until the mass was stable. The difference between the tare mass and the crucible with the sample is the sample mass. The crucible was put in the HPDSC. For tests ≥1 atm, the HPDSC was pressurized to 50 psig and released and refilled three times. This removes oxygen from the HPDSC that might react (exothermic combustion) with the jet fuel as it is coming out of the laser drilled hole in the lid. For tests at 68 atm, this purging was not required because the crucible is hermetically sealed, and does not have a laser drilled hole. For tests <1 atm, the vacuum removed enough of the oxygen so that combustion was not a concern. Then the HPDSC was pressurized, or evacuated, to the test pressure. A sample of JF#9 (JP-5) was pressurized/depressurized between 100 psi and atmospheric pressure three times and there was no mass loss of the JF. This is confirmation that the JF sample did not evaporate during the degassing process. The HPDSC temperature was allowed to settle to 15 °C +/- 0.5 °C. The method was started and heated at 5 °C/min to 350 °C or until the evaporation was complete, whichever happened first. The pressure was released from the HPDSC and the sample/crucible was removed. A new empty sample crucible was placed in the HPDSC and the HPDSC was closed. The HPDSC was stabilized at 15 °C +/- 1 °C before the next sample was prepared. This reduces the amount of sample evaporation that might happen in the HPDSC while waiting for the temperature to come back to 15 °C.

The 68 atm (1000 psi) sample test was prepared differently. A crucible and a solid lid were used to prevent the jet fuel from evaporating during the test. The high pressure was selected so that none of the jet fuel or Avgas sample would leak from the crucible during the test. This was confirmed by weighing each sample/crucible pair after the test. If the mass changed by more than 0.1 mg, a new sample was prepared and tested. The high pressure caused the crucible to collapse if there was a gas space above the sample. This problem was solved by inverting the lid so the convex side was down toward the liquid sample. The crucible was filled to overflowing with jet fuel. The lid was placed, concave side up, over the liquid such that it was floating on the jet fuel. The sample/crucible was placed in the crimper. The crimper arm was lowered to expel the excess jet fuel and allow the liquid to leave the crimping zone of the crucible and lid. This took about one minute. The crimper arm was lowered to complete the crimp. The sample was weighed several times over about one hour or until the sample mass was stable. This gave time for the excess jet fuel to evaporate from the outside of the crucible. The HPDSC temperature was allowed to settle to 15 °C +/- 0.5 °C. The method was started and the system was heated at 5 °C/min to 350 °C. At the end of the test, the pressure was released from the HPDSC and the sample/crucible was removed.

8.4. Integration of Heat Flow Data

The enthalpy is the integral of the heat flow curve versus seconds from the beginning to the end of evaporation, or 350 °C, whichever happens first. The software automatically integrates versus time in seconds even though the curve is plotted versus temperature. The baseline for this integration is a straight line at zero heat flow, Figure 51. The resulting enthalpy curve is shown as the green dash-dot line in Figure 52. One needs to inspect the heat flow curves carefully at this point. If the heat flow signal is oscillating (Figure 53), especially near the end of evaporation, this is an indication of combustion of the jet fuel reacting with residual oxygen in the HPDSC. Data such as this was discarded and the sample rerun.

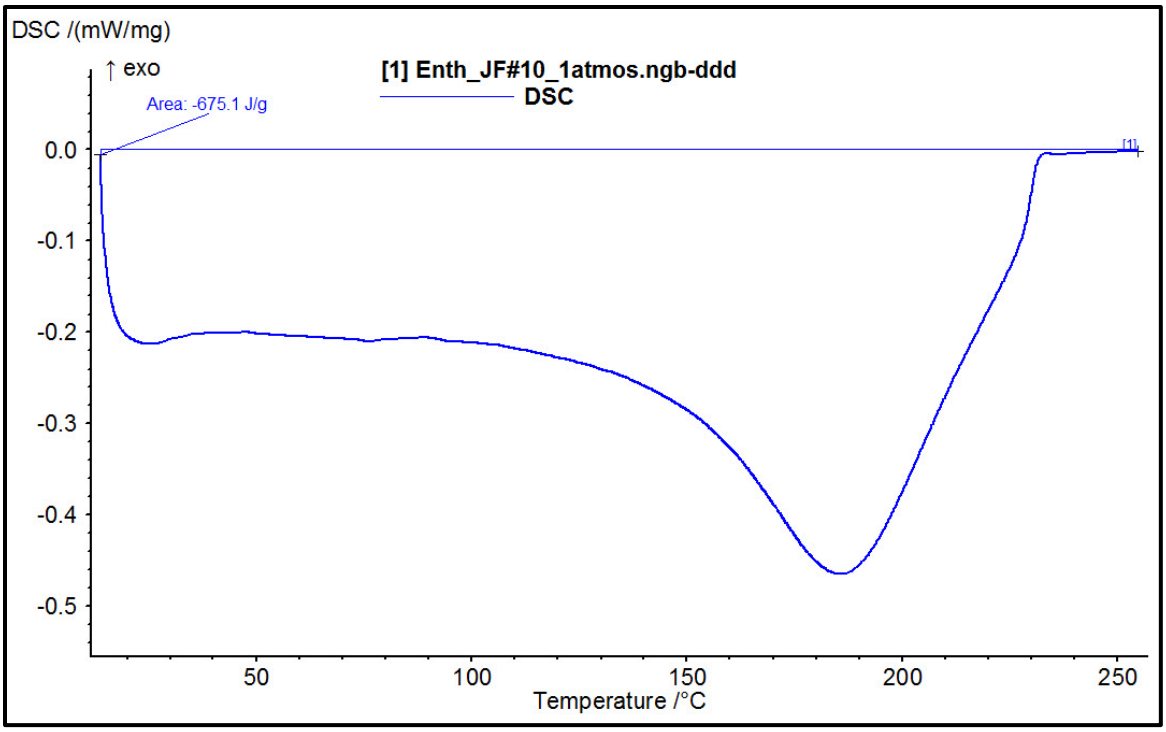

Figure 51: HPDSC raw data for JP-8 (JF#10) at 1 atm nitrogen pressure.

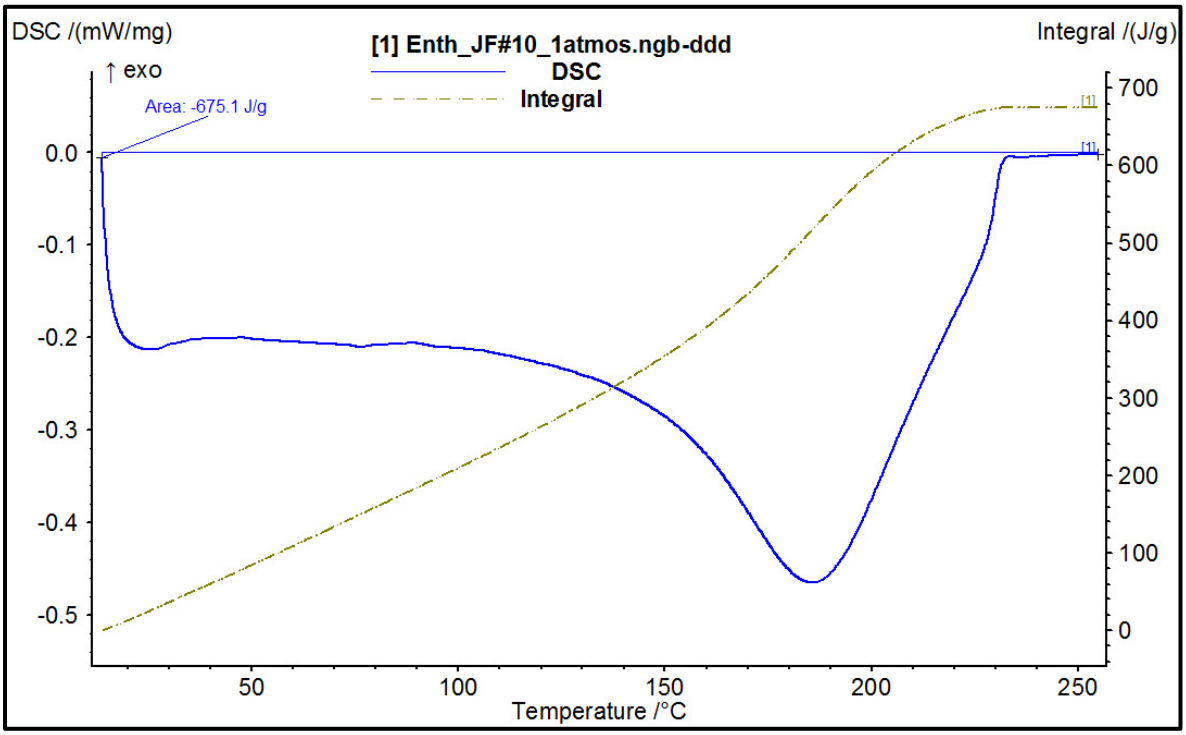

Figure 52: Heat flow integral (enthalpy) for JP-8 (JF#10) at 1 atm N_2 pressure.

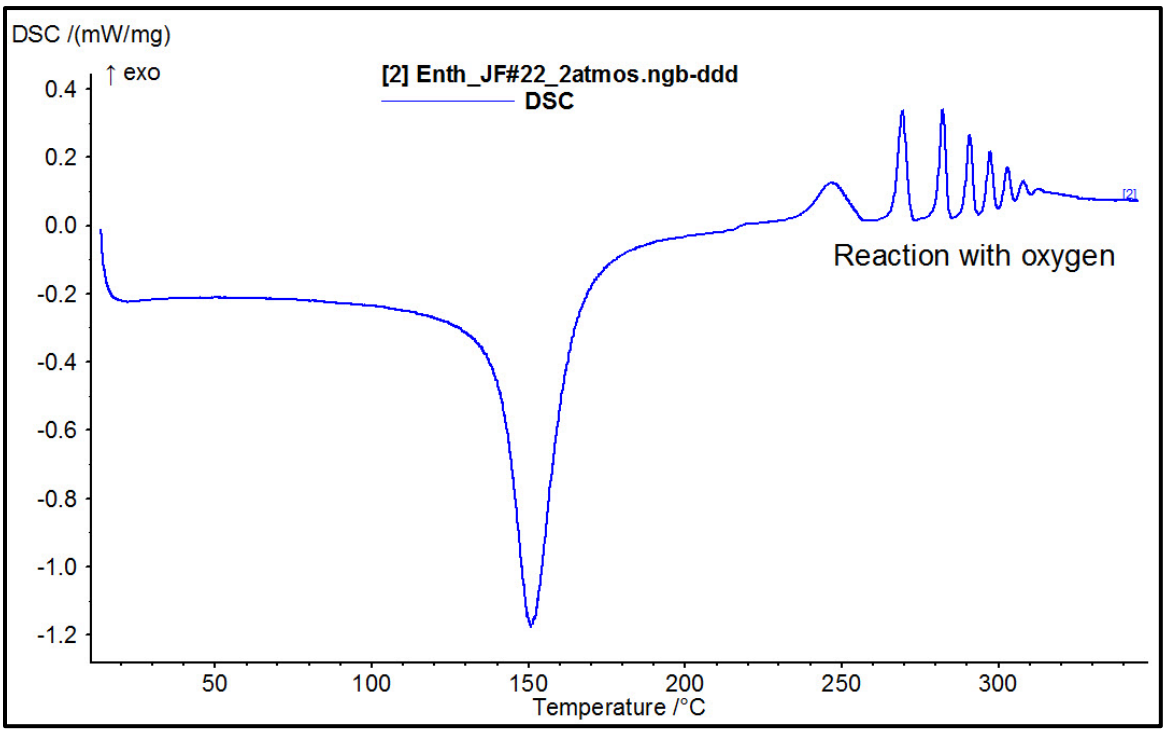

Figure 53: HPDSC raw data for JP-4 (JF#22) at 2 atm pressure without purging.

8.5. Construction of an Enthalpy Diagram

8.5.1. Plotting of All Enthalpy Data

The first look at the test results was done by plotting the curves at 68 atm and the QI HOV, as shown in Figure 54.

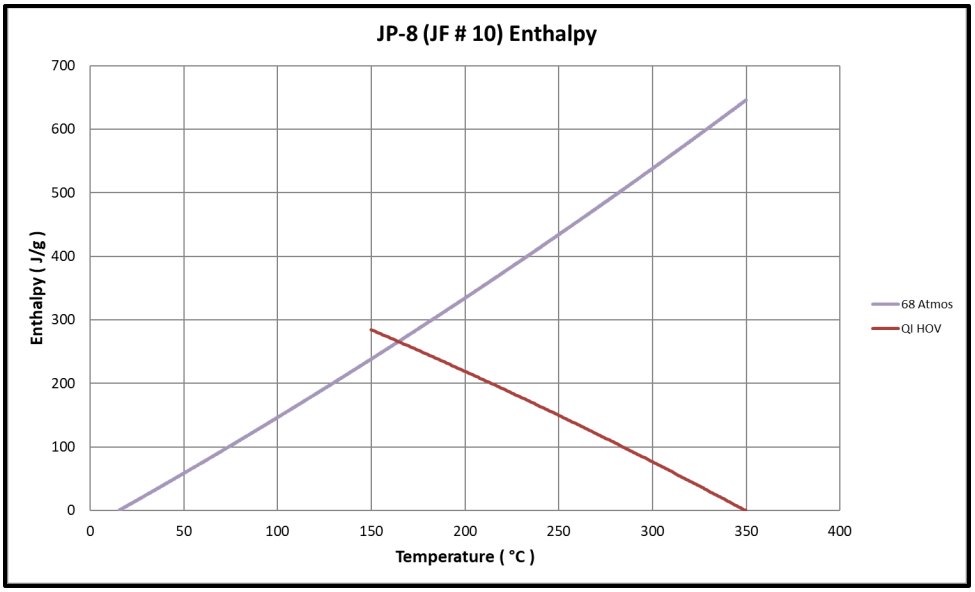

Figure 54: Raw enthalpy curves for JP-8 (JF#10).

The QI HOV and the 68 atm data were added to create the 'Mix to Gas' curve, as shown in Figure 55. The 68 atm and "Mix to Gas' curves were used as the standard curves that all other curves must match, so no adjustments were made to these two curves. This 68 atm curve must be a smooth curve with no sudden shifts in enthalpy. (A sudden shift is an indication of crucible rupture, and then the test must be rerun.) A mass loss between the start and end of the test was an indication of a slow leak of the jet fuel during the experiment and the test was rerun. Great care was taken in producing the 68 atm results because these data were the standard results that affect the accuracy of the final enthalpy plots. The 68 atm data line is replaced with the 3rd order polynomial equation. This removes the signal noise from the 68 atm data and permits a better fit with the lower pressure data.

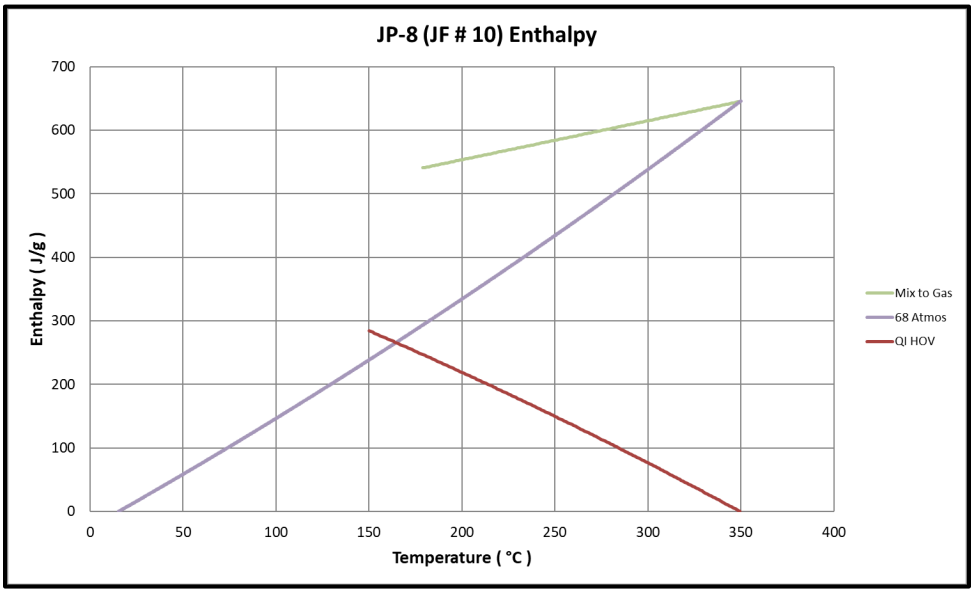

Figure 55: "Mix to Gas" curve, green line, for JP-8 (JF#10).

8.5.2. Matching Starting Enthalpies

There are two factors, the slope and offset, that were used to match the starting enthalpies, of different pressure curves, just prior to vaporization. The offset correction is used to correct errors that come from the experiments starting at slightly different temperatures. The raw data for the 0.1 atm curve are shown in Figure 56.

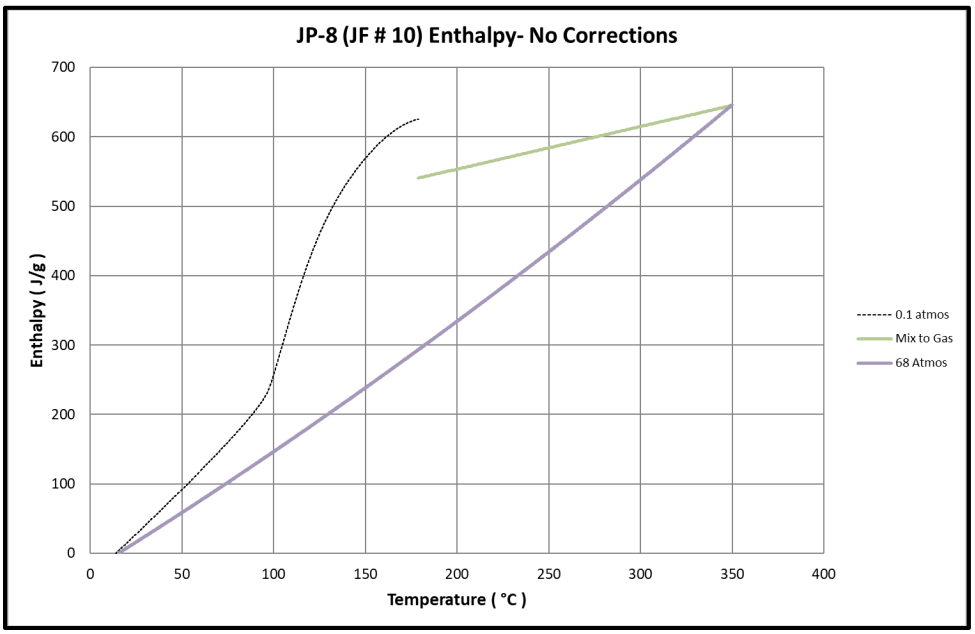

Figure 56: JP-8 0.1 atm with no corrections

At this point in the adjustments, only the slope is adjusted so the 0.1 atm line's curvature matches the 68 atm line's curvature. This determines the starting point of evaporation for the 0.1 atm line, see Figure 57. All data at lower temperatures were deleted.

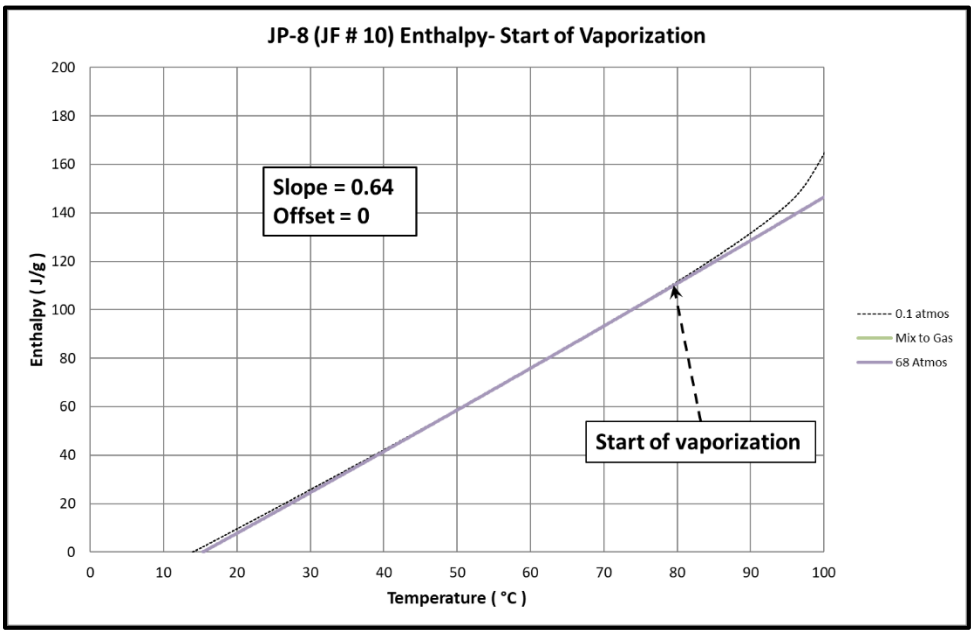

Figure 57: JP-8 0.1 atm matching curvature at low temperatures, near the start of vaporization.

8.5.3. Fitting Data to the 68 atm and 'Mix to Gas' Lines

The slope and offset of the 0.1 atm curve were adjusted so the 0.1 atm line matched with the 68 atm curve, at low temperature, and with the 'Mix to Gas' line at high temperature, the end of vaporization, shown in Figure 58.

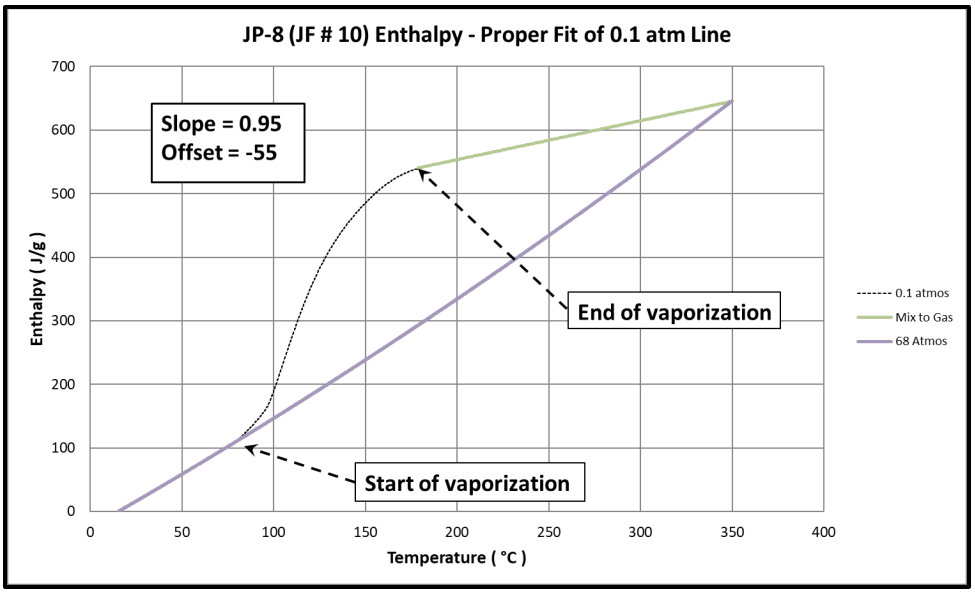

Figure 58: JP-8 0.1 atm matching with the 68 atm curve at low temperature and with the 'Mix to Gas' line at high temperature, the end of vaporization.

The steps 8.5.2 and 8.5.3 are repeated from lower pressures to higher pressures. The slope and offset are adjusted for each of the 0.25 to 8 atm data so that the beginning of evaporation matches the 68 atm line, at low temperature, and the 'Mix to Gas' line. Data points for the 0.1 to 8 atm lines that are at higher temperature than the 'Mix to Gas' line were deleted. This results in the final enthalpy graph for JP-8 shown in Figure 59.

Additionally, one must verify that the lines at different pressures do not cross in the region of about 50% evaporation. If this happens, the sample tests at both of those pressures need to be rerun. The enthalpy plot should look similar to the plot shown in Figure 59.

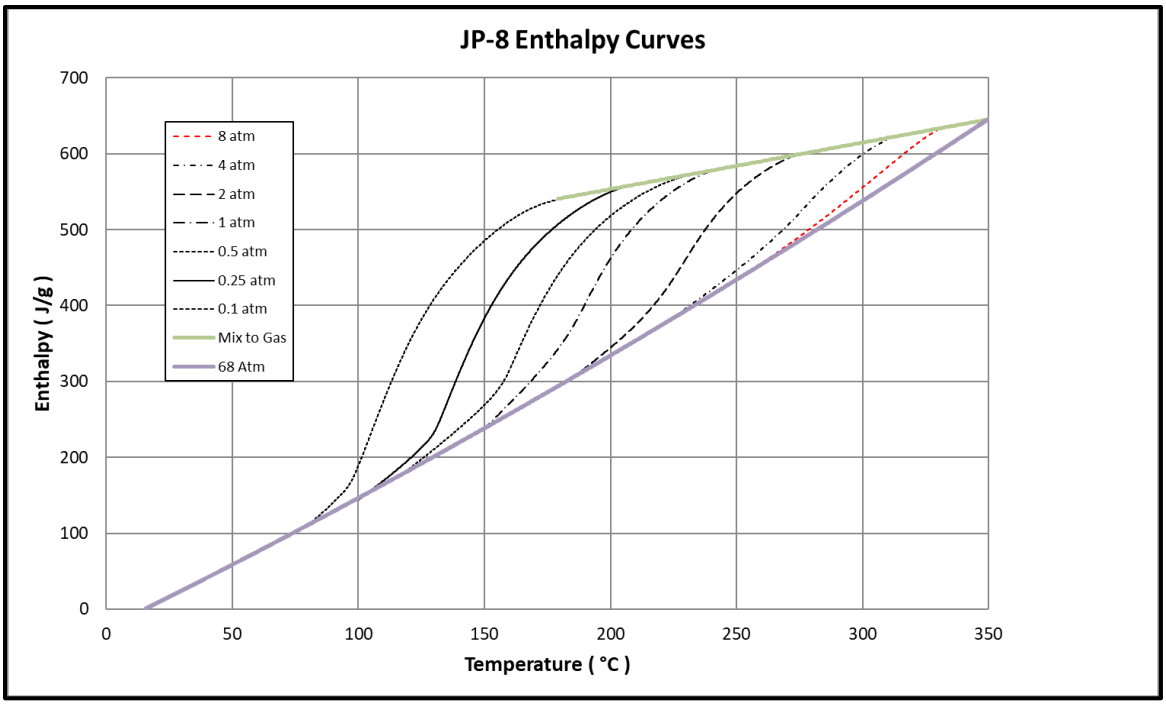

Figure 59: Final enthalpy diagram for JP-8 (JF#10).

8.5.4. Comparison of Enthalpy Curves with Literature

The data generated in this work were validated by correlating to historical data. For example, the enthalpy plot for JP-5 from this work was compared to CRC Handbook Figure 2-18, the enthalpy plot of JP-5. In Figure 60, the dashed lines are manually digitized from Figure 2-18 in the CRC Handbook [1]. The solid lines, in Figure 60, are data from this work. The two sets of data are very similar below about 225 °C. The 'Mix to Gas' lines were shifted in about the same enthalpy through the entire temperature range. The beginning of vaporization for each of the pressure curves, 0.1 to 8 atm, are very similar in both data sets. The temperature of the end of vaporization is different in the two data sets. The vaporization results in this work are probably the most correct since the data were taken from actual jet fuel under pressure in the high-pressure DSC.

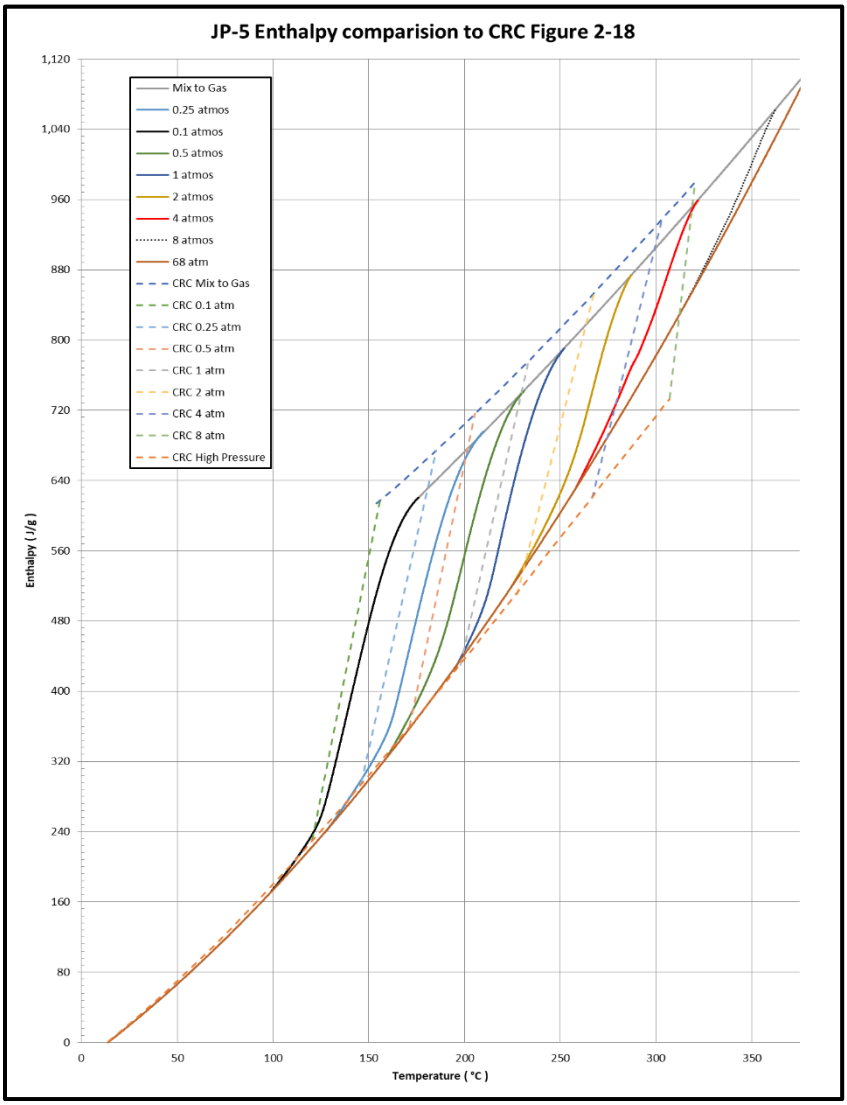

Figure 60: Comparison of the enthalpy diagram for JP-5. The dashed lines are from CRC Handbook [1], Figure 2-18. The solid lines are data from this work.

8.6. Enthalpy Diagram Results

The enthalpy diagram plots are shown in Figures 61 to 66. Equations for these enthalpy curves are in Appendix B.

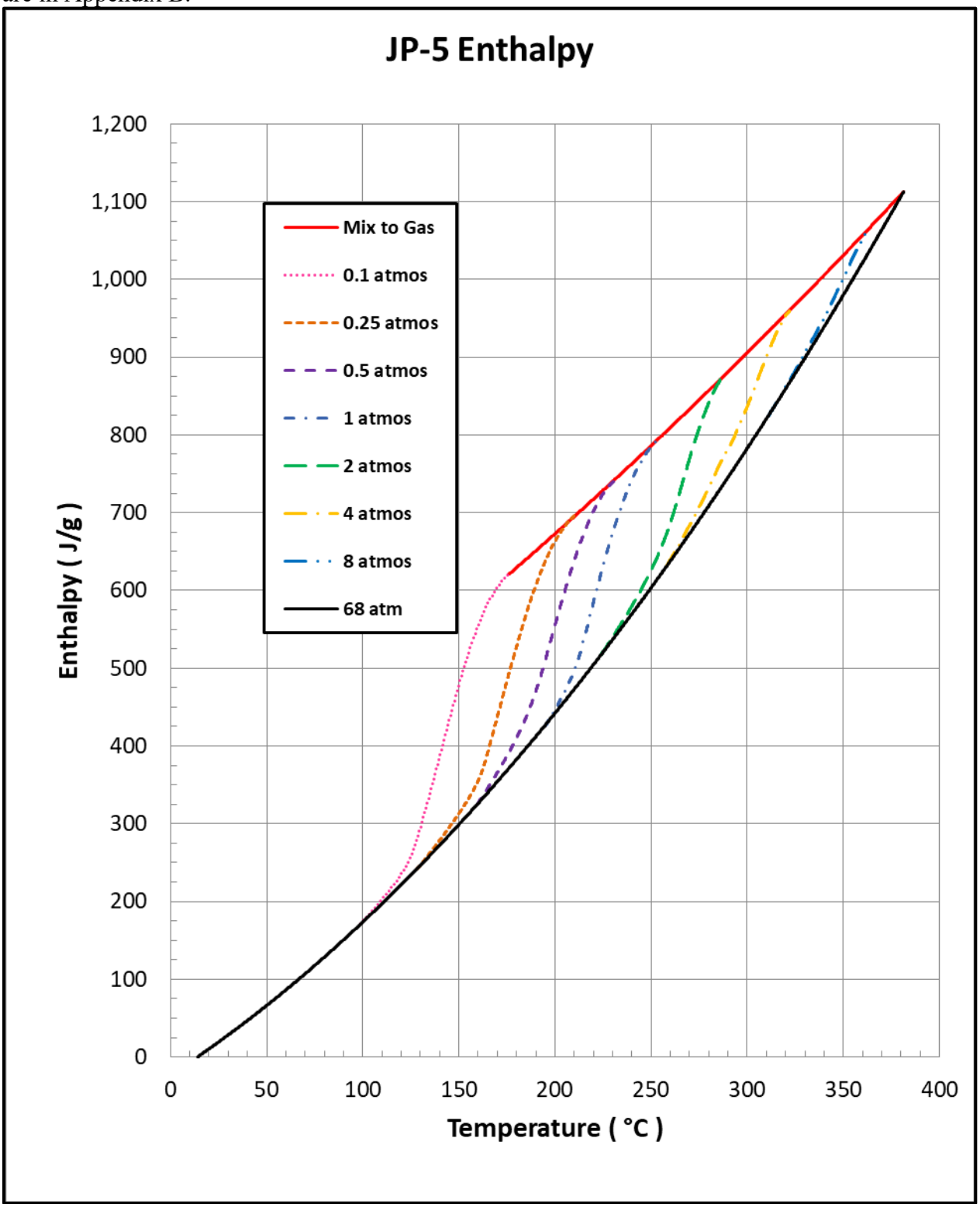

Figure 61: Enthalpy diagram for jet fuel JP-5 (WPAFB, OH, USA).

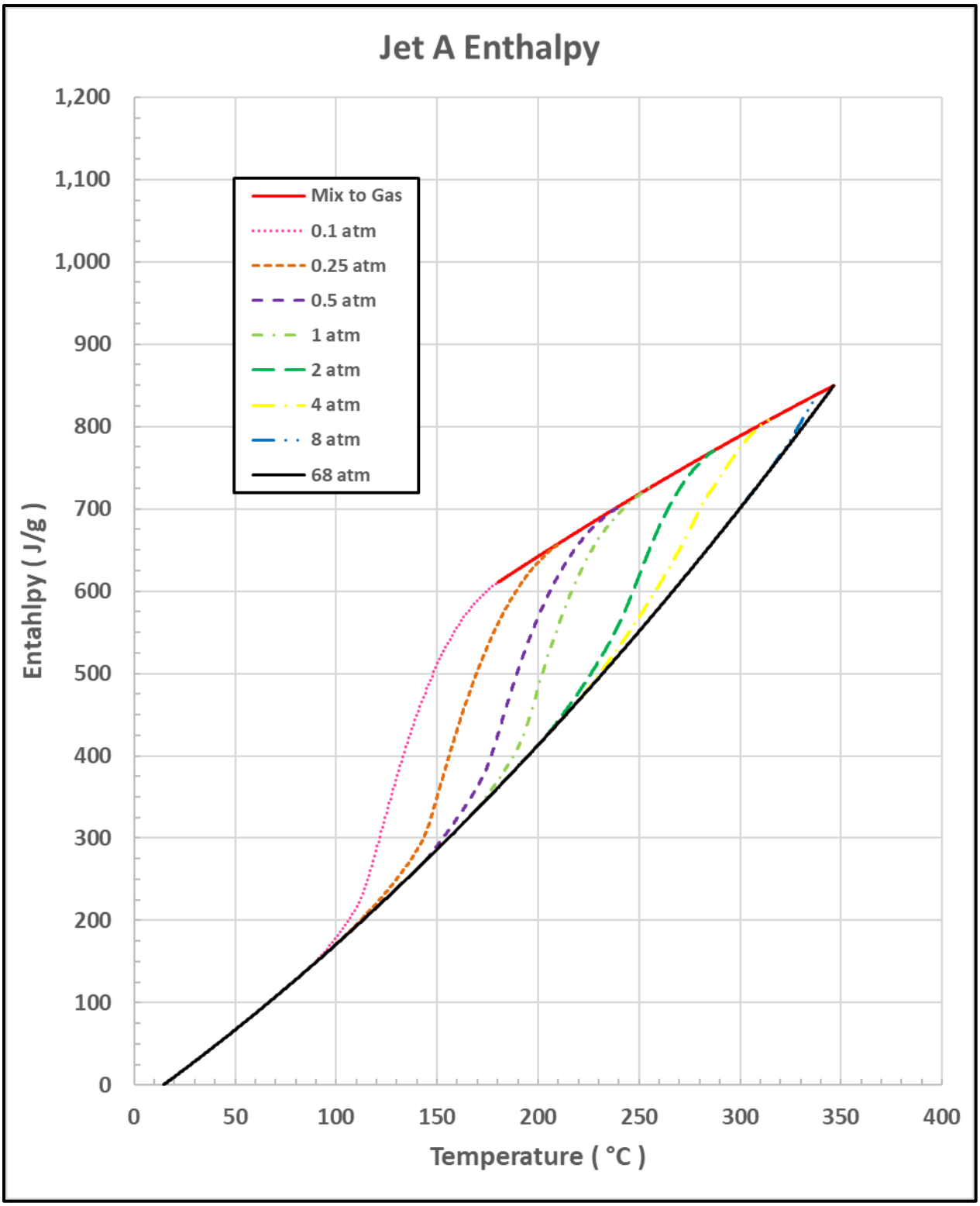

Figure 62: Enthalpy diagram for jet fuel Jet A (WPAFB, OH, USA).

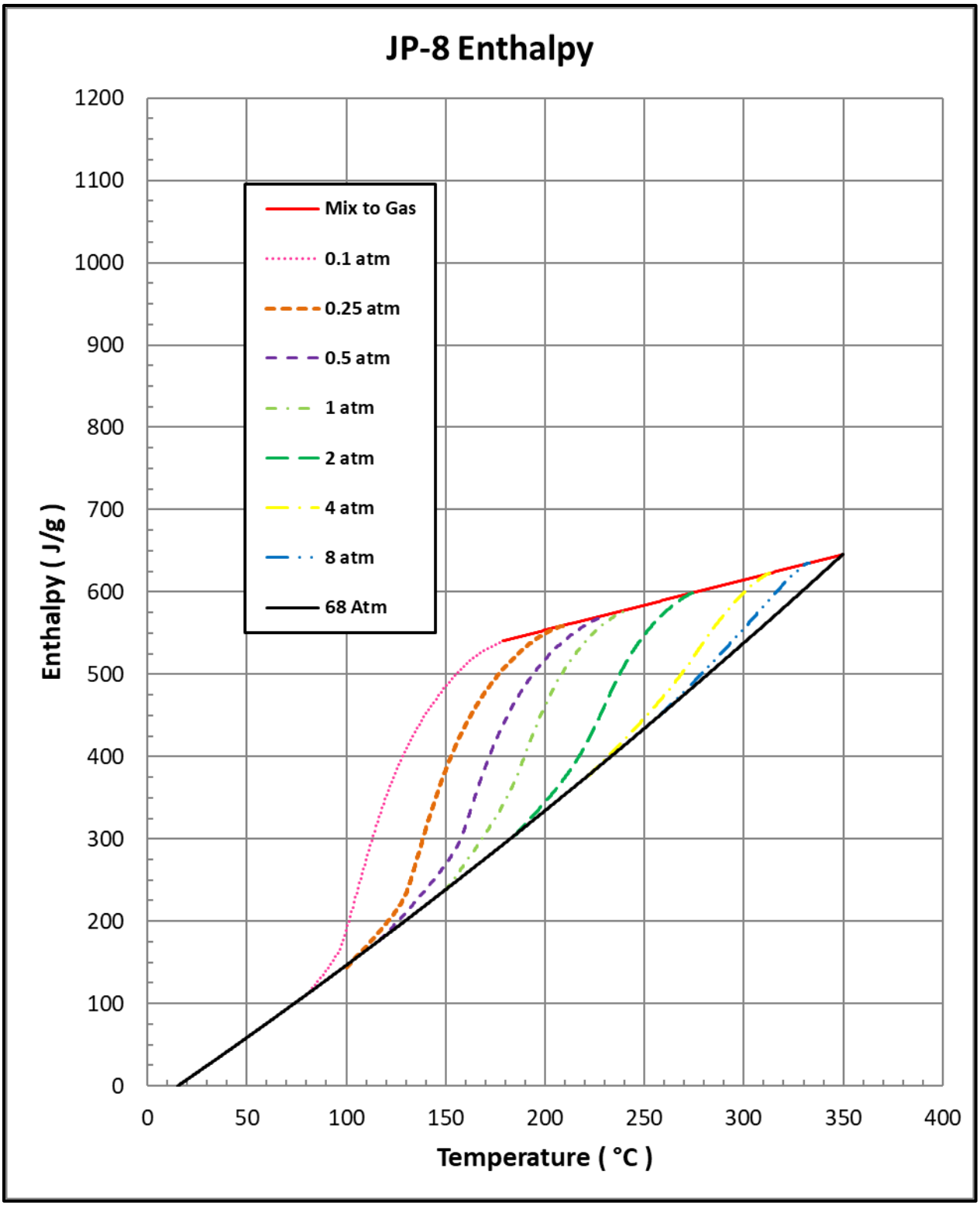

Figure 63: Enthalpy diagram for jet fuel JP-8 (WPAFB, OH, USA).

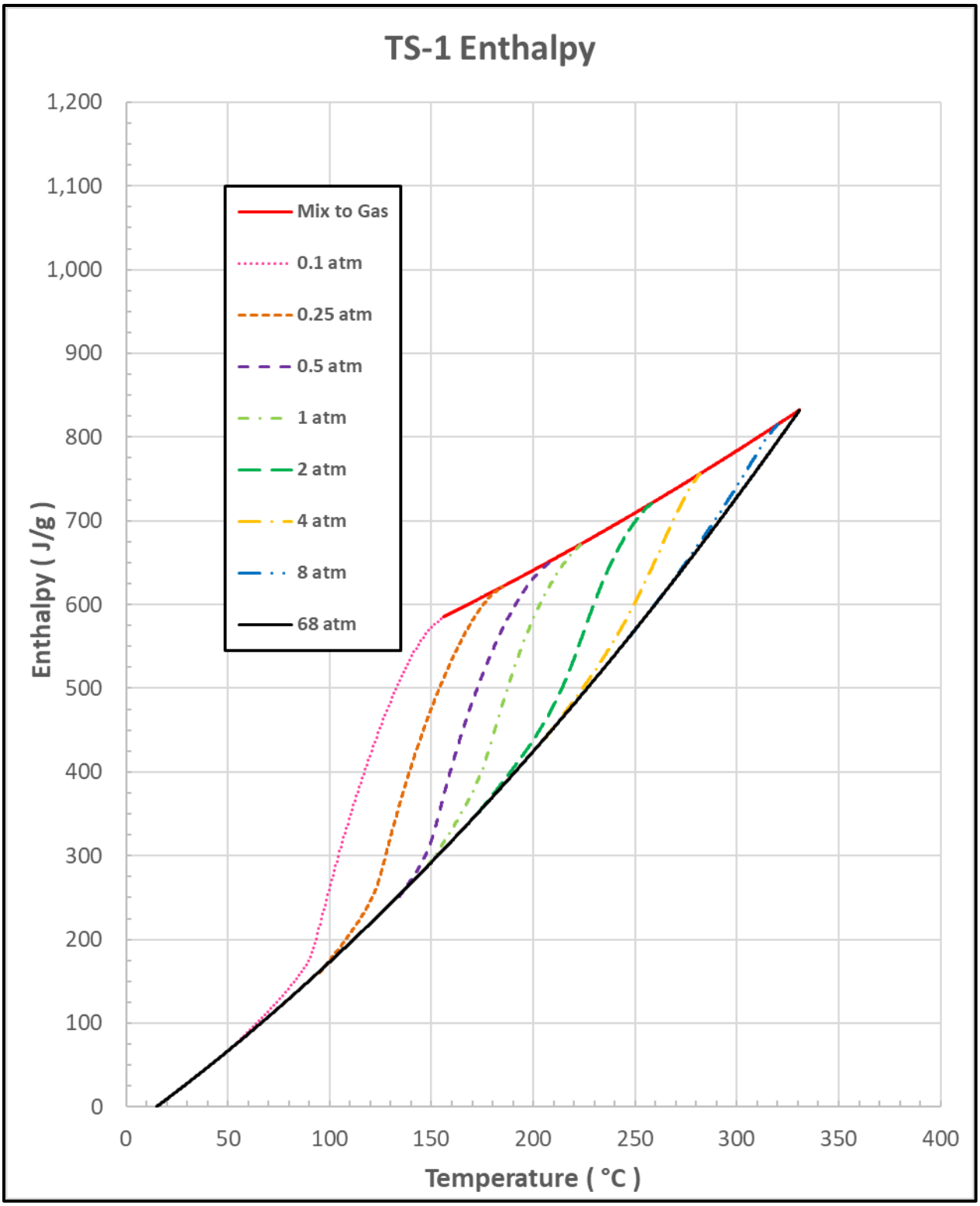

Figure 64: Enthalpy diagram for jet fuel TS-1 (GOST, AirBP, Kent, UK).

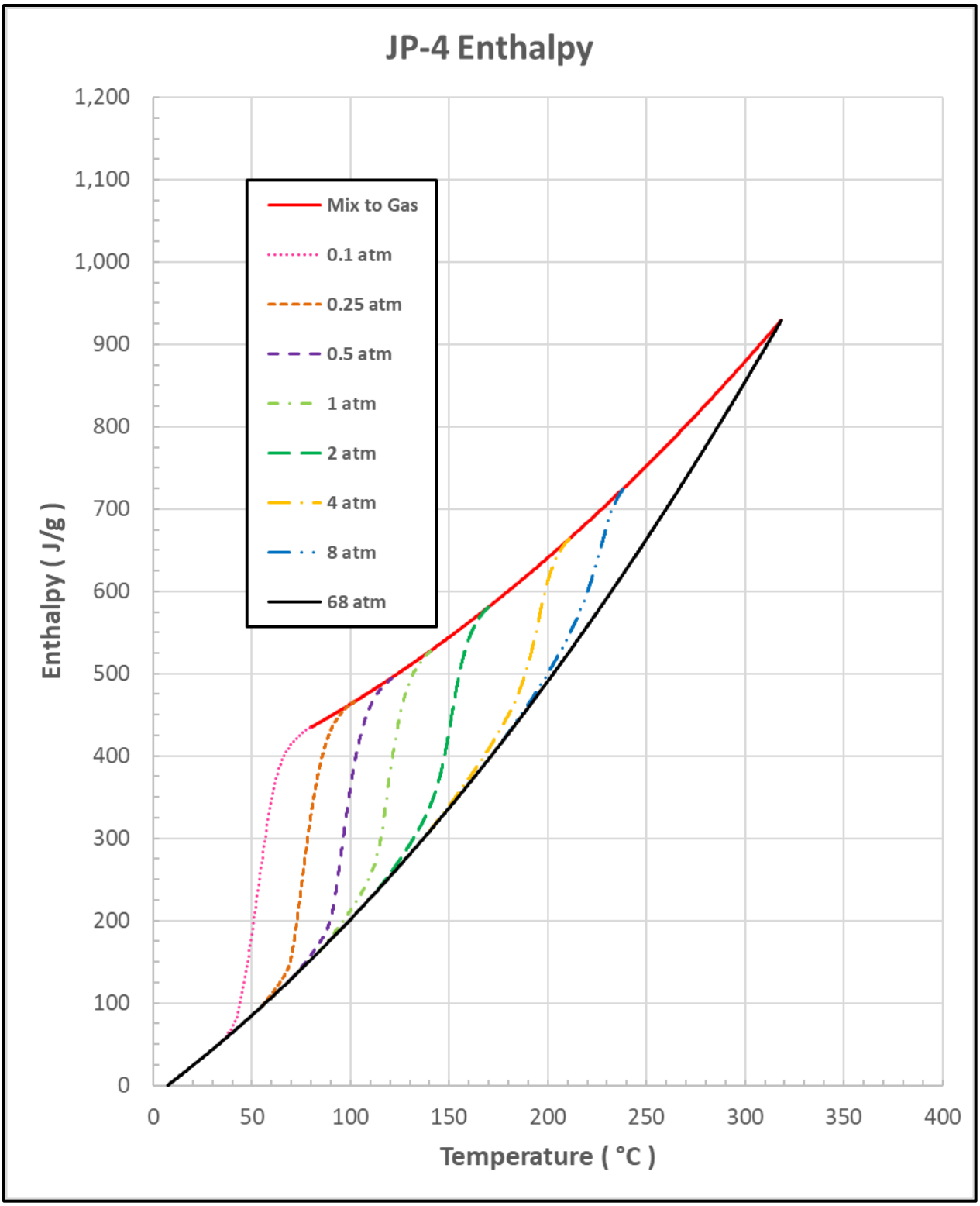

Figure 65: Enthalpy diagram for jet fuel JP-4 (Nova Research, VA, USA).

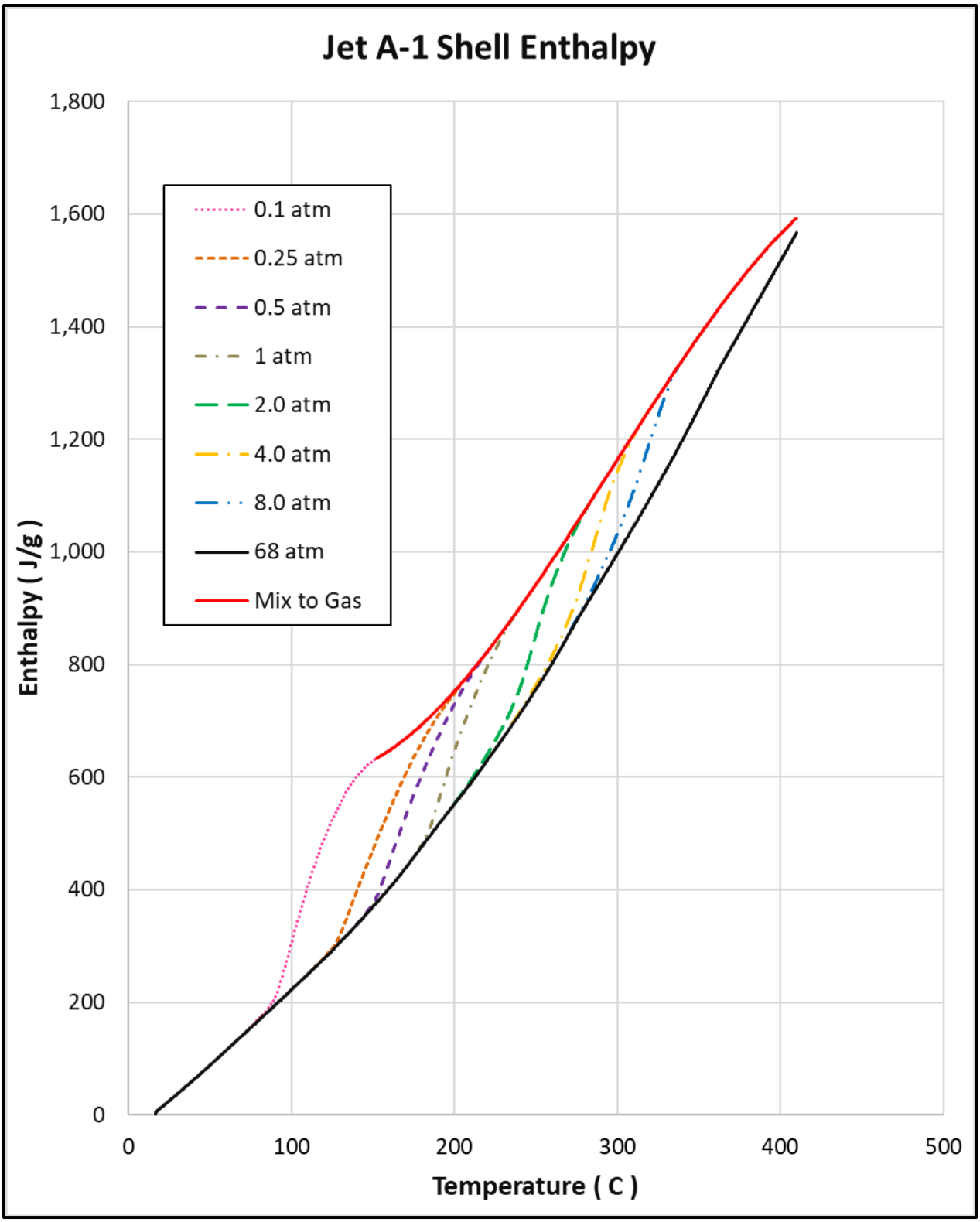

Figure 66: Enthalpy Diagram for jet fuel Jet A-1 Shell-Netherlands (JF#2).

8.7. How to use Enthalpy Diagrams

8.7.1. Determining the HOV

First, select the enthalpy diagram that is the closest match to the fuel type for which the HOV is required, for example Jet A. You will need to know the fuel storage tank-pressure. In this case, we will assume the pressure is 120 psi, so use the 120 psi curve (blue dash-dot-dot line) in Figure 67. The starting temperature should be the temperature of the fuel in the fuel tank. By example, the starting temperature will be 25 °C, red circle on Figure 67. The enthalpy at this starting point is 20 J/g.

Let us assume that the temperature at the nozzle is 350 °C. From Figure 68, one sees that the enthalpy at 350 °C is 815 J/g. So the total heat required to heat the Jet A from 25 to 350 °C is 795 J/g. Next we would like to calculate the wattage needed to heat the Jet A under actual conditions. We assume that the fuel delivery rate is 10 g/s. The wattage is calculated from the following equation.

$$795\ {}^{J}/_{g} \times 10\ {}^{g}/_{s} = 7{,}950\ {}^{J}/_{s} = 7{,}950\ Watts$$

Of course, this is just one example. The flow rate needs to be correct for each engine and each throttle setting. Units can be converted to meet the end use requirements. If there is too much heating (wattage), the fuel will start to evaporate before it gets to the nozzle. The excess temperature may cause the fuel to decompose in the fuel line and leave deposits, which will reduce the fuel line inside diameter. Then if there is not enough heating, the JF will enter the combustion chamber as a liquid. This may slightly reduce the engine efficiency since the residual HOV will take away from the heat of combustion and reduce the amount of expansion work done during combustion.

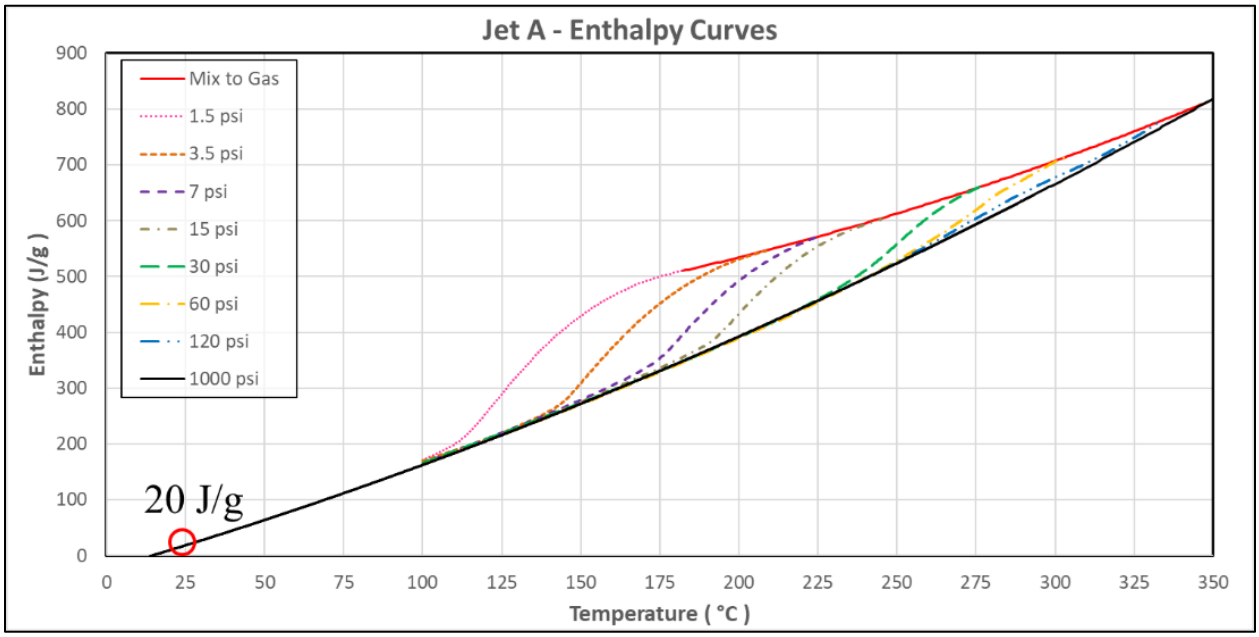

Figure 67: Jet A enthalpy at 25 °C is 20 J/g.

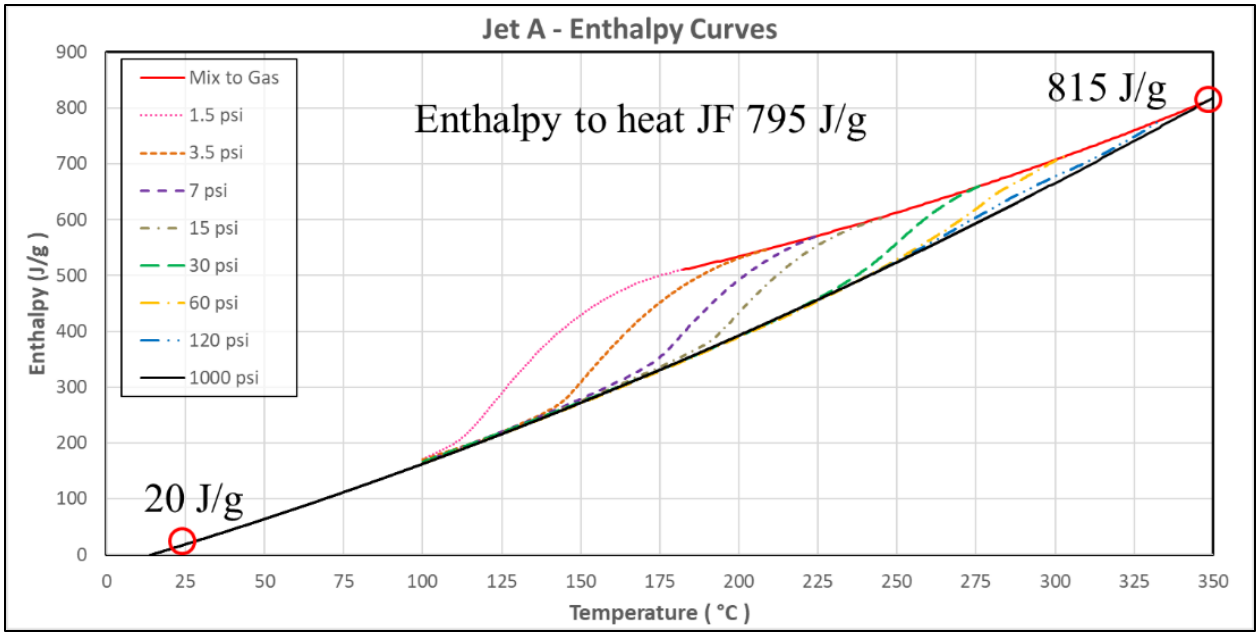

Figure 68: Jet A enthalpy at 350 °C is 815 J/g.

8.7.2. Optimal JF Pressure and Nozzle Temperature

Again, one must select the enthalpy diagram that is the closest match to fuel type for which the information is required, for example Jet A. The starting temperature should be the temperature of the JF in the fuel tank. By example, the starting temperature will be 25 °C, red circle on Figure 69. The enthalpy at this starting point is 20 J/g.

You will need to know the fuel delivery pressure. In this case, assume the pressure is 30 psi, so use the 30 psi curve (green dashed line) in Figure 70. Now find the intersection of the 30 psi curve (green dashed line) with the 'Mix to Gas' curve (red solid line) in Figure 71. The temperature at this intersection is 275 °C and the enthalpy is 657 J/g. So the total heat required to heat the Jet A from 25 to 275 °C is 637 J/g.

If the nozzle temperature is greater than 275 °C, the fuel will convert to vapor before it comes out of the nozzle. If the nozzle temperature is below/or equal to 275 °C, only liquid fuel will be coming out of the nozzle and into the combustion chamber. In the design of jet fuel systems, it is better if the nozzle temperature is below 275 °C at all throttle positions. This ensures that the fuel is always a liquid when it goes through the nozzle and the atomization of the JF will be consistent through all throttle positions.

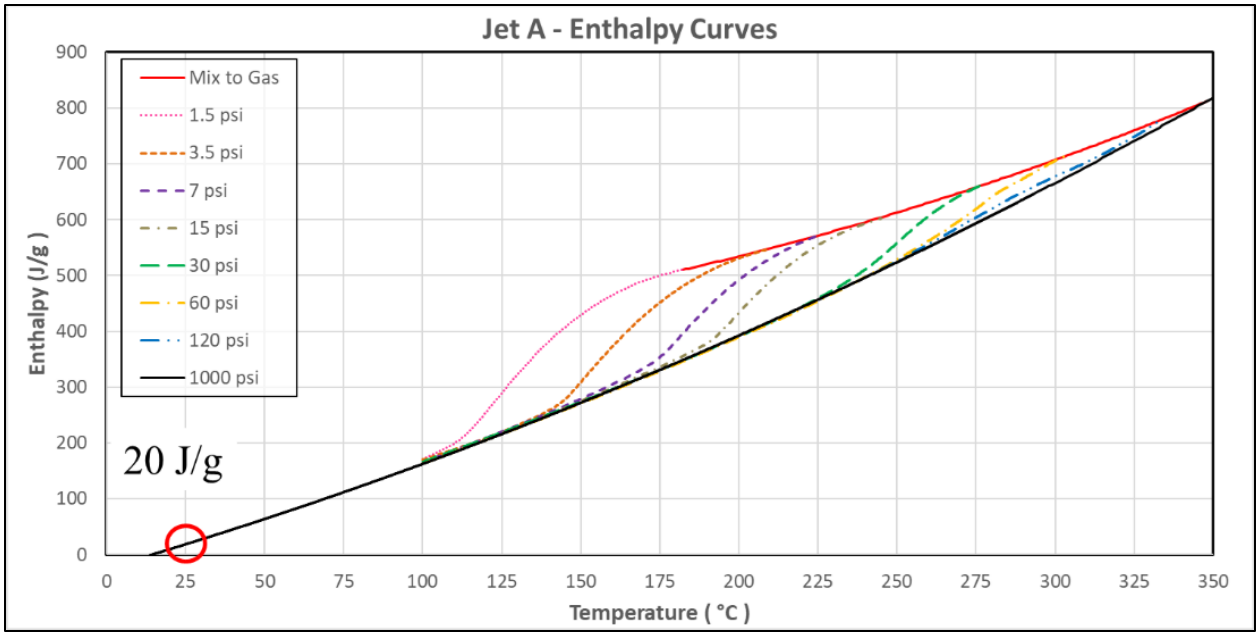

Figure 69: Jet A enthalpy at 25 °C is 20 J/g.

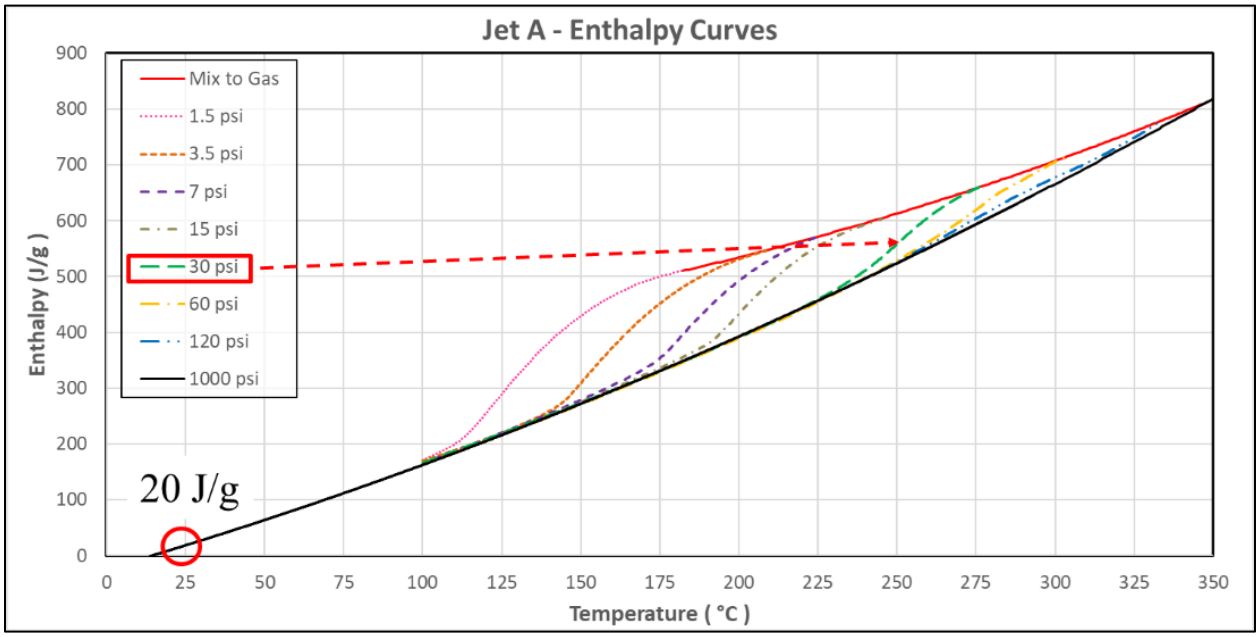

Figure 70: Enthalpy curve for Jet A. The 30 psi isobaric line is the green dashed line.

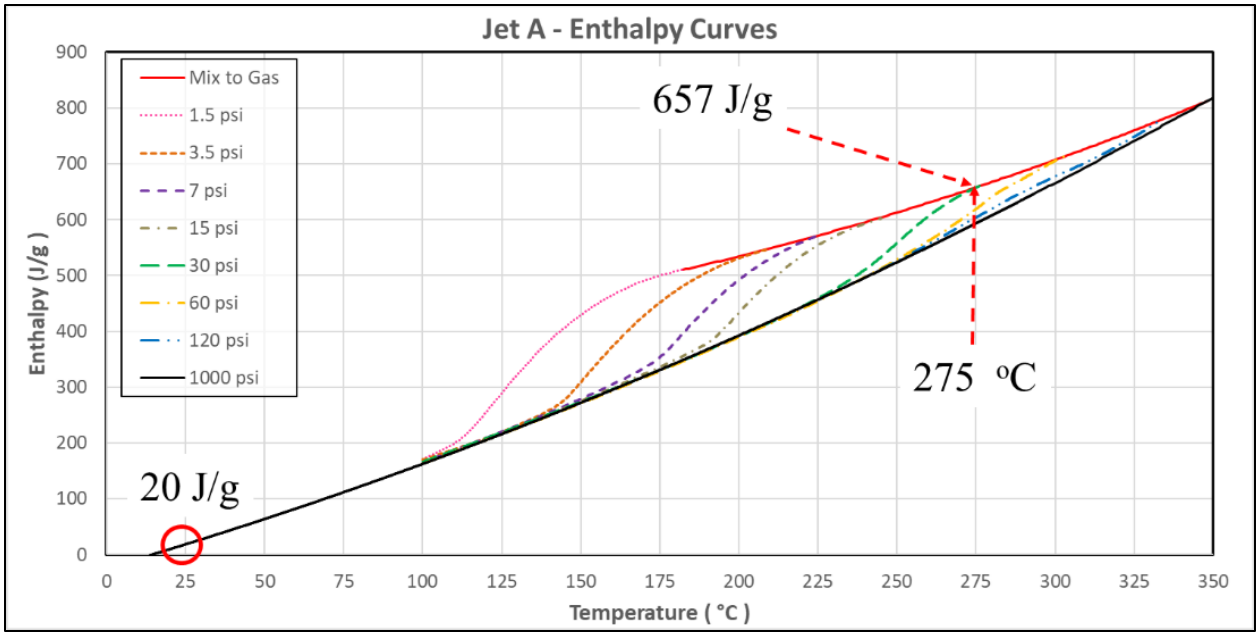

Figure 71: Enthalpy curve for Jet A. The Jet A is finished evaporating at 275 °C under 30 psi of pressure. The enthalpy at this point is 657 J/g.

9. Aviation Gasoline

9.1. Background

In addition to the jet fuel study, the Coordinating Research Council (CRC) has sponsored this testing for the "Determination of Heat of Vaporization and Creating Enthalpy Diagram for Several Aviation Gasolines" (CRC Project No. AV-20-20). Avgas (aviation gasoline) is an aviation fuel used in aircraft with internal combustion (IC) spark ignition piston engines. *Avgas* is distinguished from conventional gasoline used in motor vehicles by having specific volatility and other characteristics for flight use.

The most commonly used grades of Avgas, 100LL still contain tetraethyllead (TEL), a toxic additive used to achieve a very high octane quality (≥99.6 MON) and prevent detonation within the combustion chamber. Various proposals are being assessed by the Aviation Industry to allow transition from leaded to unleaded Avgas for environmental benefit. While jet fuel turbine engines dominate commercial and military aviation, Avgas aircraft represent a significant proportion of the flying fleet (About 200,000 aircraft in the US) performing important training, commercial and recreational roles. Current Industry studies suggest that for high octane, Grade 100LL Avgas, unleaded fuels will not be 'drop in' replacements. Changes in volatility distribution have been suggested for some proposals and having HOV data for current Grades is important to help with comparison and understanding. For example, Avgas volatility is important to ensure correct fuel vaporization in the engine. An appropriate fuel: air mixture is required for distribution to the cylinders and combustion. For carburetor units this is achieved using heat from the intake section, which under certain conditions, can even result in ice formation. This is a serious condition, which, if not quickly rectified by application of hot air from the exhaust manifold, can result in an irrecoverable loss of power. The best way to reduce this hazard is to use Avgas formulations that have an appropriate heat

of vaporization, carefully balancing vapor lock risk in fuel systems with volatility for hot and cold day operation.

The determination of Enthalpy Diagrams and HOV QI Curves for a volatile product such as Avgas is non-trivial. The work reported here is a proof-of-concept study using two representative market samples of Avgas 100LL, one with low aromatics (AG-LA) and one with high aromatics (AG-HA). The data generated offer a useful baseline for comparison with future, possibly non-standard, unleaded Avgas proposals.

Enthalpy charts are used for determining the state of the fuel in the design of fuel systems for, and performance of, carburetors in general aviation IC engines. These charts provide a source of information when trying to understand what has happened in an aircraft accident and its aftermath, or a fuel spill and fire investigation. Heat of Vaporization mismatch is one of the causes of carburetor icing. The heat of vaporization cools the inside of the carburetor. When humid air is pulled into the carburetor, ice forms on the inside near the venturi. This ice reduces air intake and lowers the power of the engine. This will happen most often on takeoff when the pilot needs the most power. Carburetor heating is one technique to reduce icing. It brings hot air into the carburetor; this removes ice and reduces further icing. Carburetor heating also reduces engine power because the air expands upon heating. The best way to reduce icing is to use Avgas formulations that have a lower heat of vaporization. And this information can be found with tests that are included in this report.

Heat of Vaporization

The heat of vaporization (HOV, also symbolized as ΔH_{vap}) is the energy that is needed to completely convert a given quantity of a substance from a liquid to a gaseous state at a given temperature and pressure, usually measured at atmospheric pressure. More details can be found in section 2. Background, page 12. The HOV from raw DSC data at 1 atmosphere for the two Avgas samples are shown in the following Figures 73 and 73.

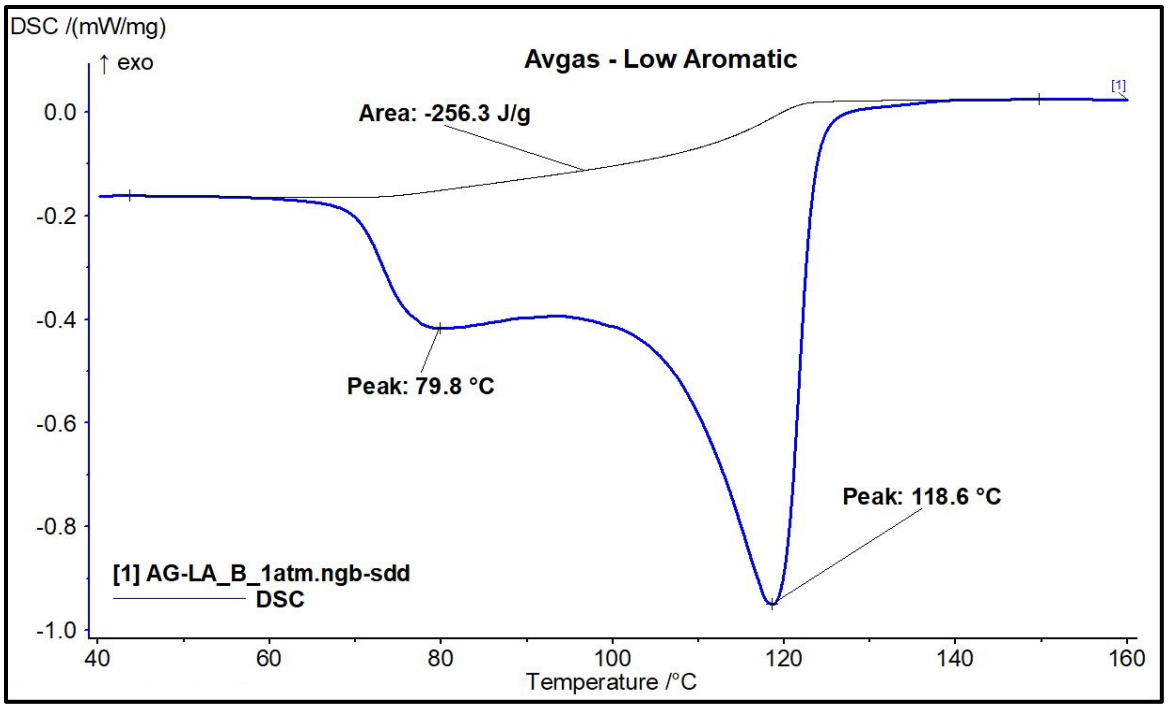

Figure 72: HOV analysis of Avgas Low Aromatic (AG-LA).

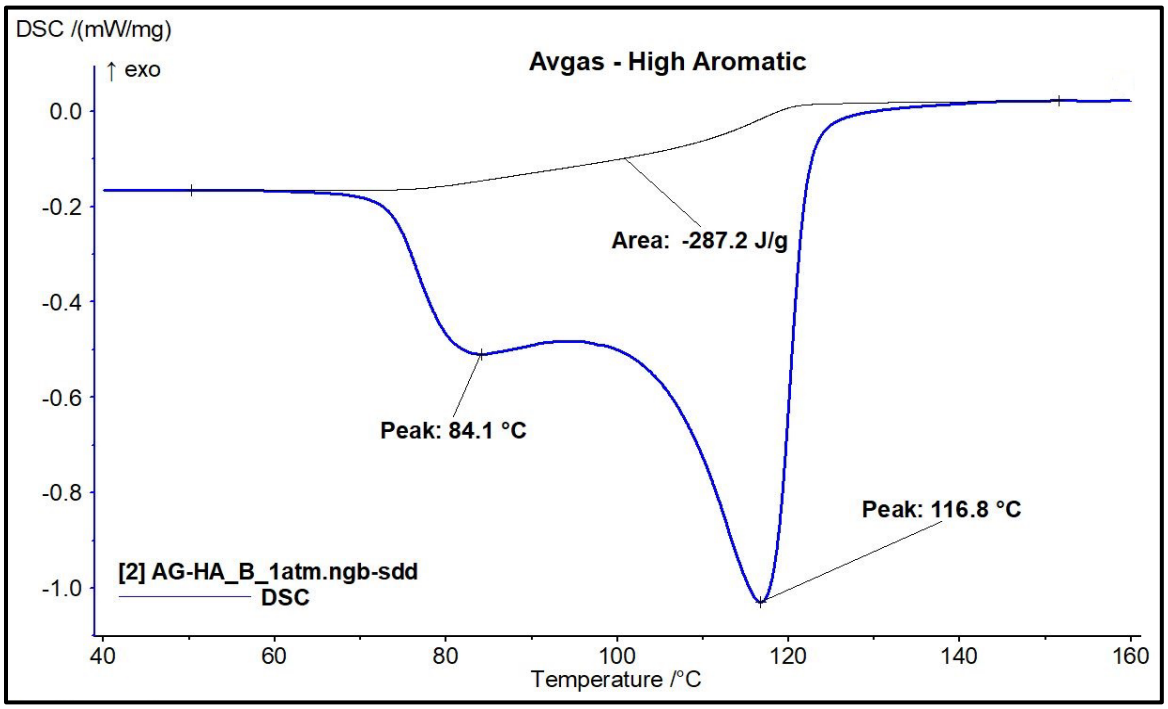

Figure 73: HOV analysis of Avgas High Aromatic (AG-HA).

9.2. HOV QI Diagrams

The HPDSC needs to be set up differently for the HOV QI testing as detailed in Section 6. Similar to Jet Fuel, the purpose of this test is to determine the HOV of the avgas at an isothermal temperature. This test is performed at several temperatures. The HOV will decrease as temperature increases until the HOV is zero at the critical temperature for the avgas. More details on this test method can be found in section 6. HOV Quasi-Isothermal (QI) Testing, page 33.

The HOV at several temperatures will be used to create a figure similar to Figure 59 [1]. The data will also be used to create the 'mix to gas' line in the enthalpy figures. The NETZSCH High-pressure DSC software can only integrate the area under an evaporation peak when there is a temperature ramp. This is the reason for the quasi-isothermal (QI) HPDSC test. The enthalpy (QI) versus temperature for avgas with a low aromatic content (AG-LA) is shown in Figure 74, below, and the data for avgas with a high aromatic content (AG-HA) are shown in Figure 75. The data points are tabulated in Tables 26 and 27.

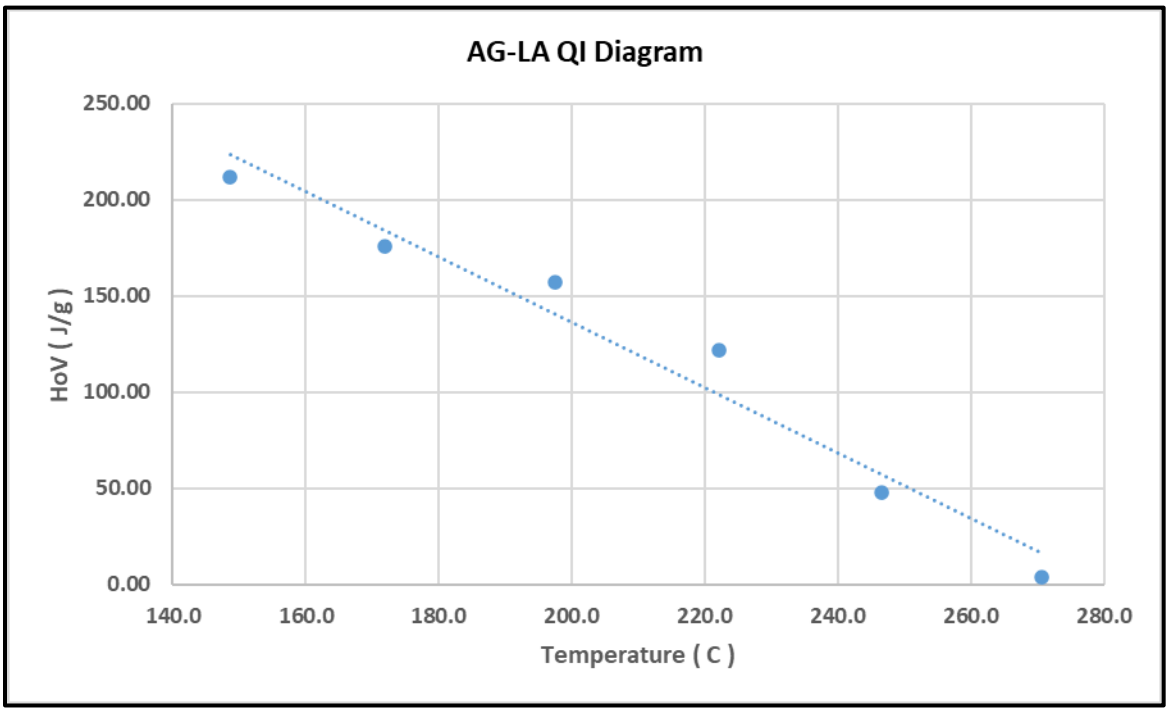

Figure 74: AG-LA HOV from a QI HPDSC experiment.

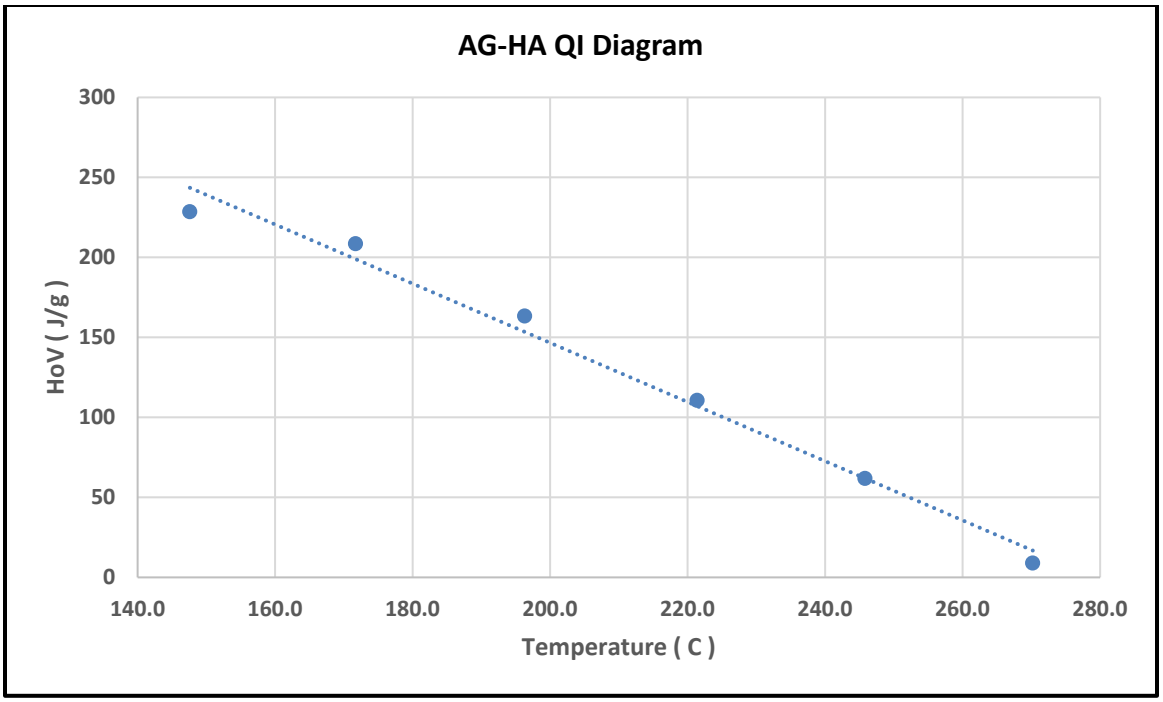

Figure 75: AG-HA HOV from a QI HPDSC experiment.

Table 26: Avgas Low Aromatics (AG-LA)

	Peak Temperature	HOV
	(°C)	(J/g)
	148.7	211.8
	172.0	175.7
	197.6	157.0
	222.1	121.8
	246.5	48.0
	270.6	3.5
$T_{critical}$	227.1	0

Table 27: Avgas High Aromatics (AG-HA)

	Peak Temperature	HOV
	(°C)	(J/g)
	147.6	228.5
	171.7	208.5
	196.3	163.3
	221.4	110.6
	245.8	61.8
	270.2	8.9
$T_{critical}$	278.3	0

9.3. Enthalpy Diagrams

9.3.1 Background on Enthalpy Diagrams

The HPDSC measures the instantaneous heat flow of the sample in watts per gram (W/g). The enthalpy is the cumulative integral of this heat flow from the beginning to the end of the scan. More detail on Enthalpy Diagrams can be found in section 8.1, page 54.

9.3.2 Sample Preparation for Enthalpy Testing

The same procedure as detailed in Section 5.1 was used to prepare samples for enthalpy testing. The determined mass was entered into the software as the sample mass for the test.

9.3.3 Enthalpy Testing Method

The HPDSC was cooled using refrigerated water (1 ºC setpoint) running through the lid of the high-pressure chamber. The sample was placed in the HPDSC as quickly as possible after weighing, an aspect particularly important for a volatile fuel such as Avgas. The HPDSC pressure lid was fastened down. The HPDSC cell was filled with nitrogen gas to 50 psi and emptied three times. Sample analysis was performed in a static nitrogen environment. The HPDSC cell was initially stabilized at 15 °C, then heated at 5 °C/min to 400 °C.

For Avgas, which was too volatile to run at 0.1 atmospheres, the water chiller was used and set to 1 °C. The HPDSC was allowed to stabilize at 15 °C +/- 0.1 °C before the sample was prepared. This reduces the amount of sample evaporation that could occur in the HPDSC while waiting for the temperature to come back to 15 °C. The test was started when the HPDSC cell stabilized at 15 °C. The 68 atm (1000 psi) sample test for AvGas was prepared differently than was described in section 8.3, page 55. The 25 µL crucibles could not be crimped securely with a closed, inverted lid. Presumably, the AvGas wet the aluminum sealing edges of the pan and lid so a complete seal could not be made in the presence of the liquid AvGas. So for AvGas, a larger crucible was used; a100 µL pan (PN ME-51119872 Mettler Toledo) with the same laser pierced lid (PN 6.239.2-64.801 Netzsch) positioned with the concave side down. The sample volume was increased to around 80 µL with these crucibles. The larger volume meant that an insignificant amount of AvGas would leave the crucible during the 68 atm test. More details on the crimping press sealing are available on page 91, after Figure C8. The enthalpy

diagram for Low Aromatic Avgas is found below in Figure 76. The enthalpy diagram for High Aromatic Avgas is found in Figure 77. Overall, the reported experimental technique and resultant data proved successful given the challenges associated with this volatile product.

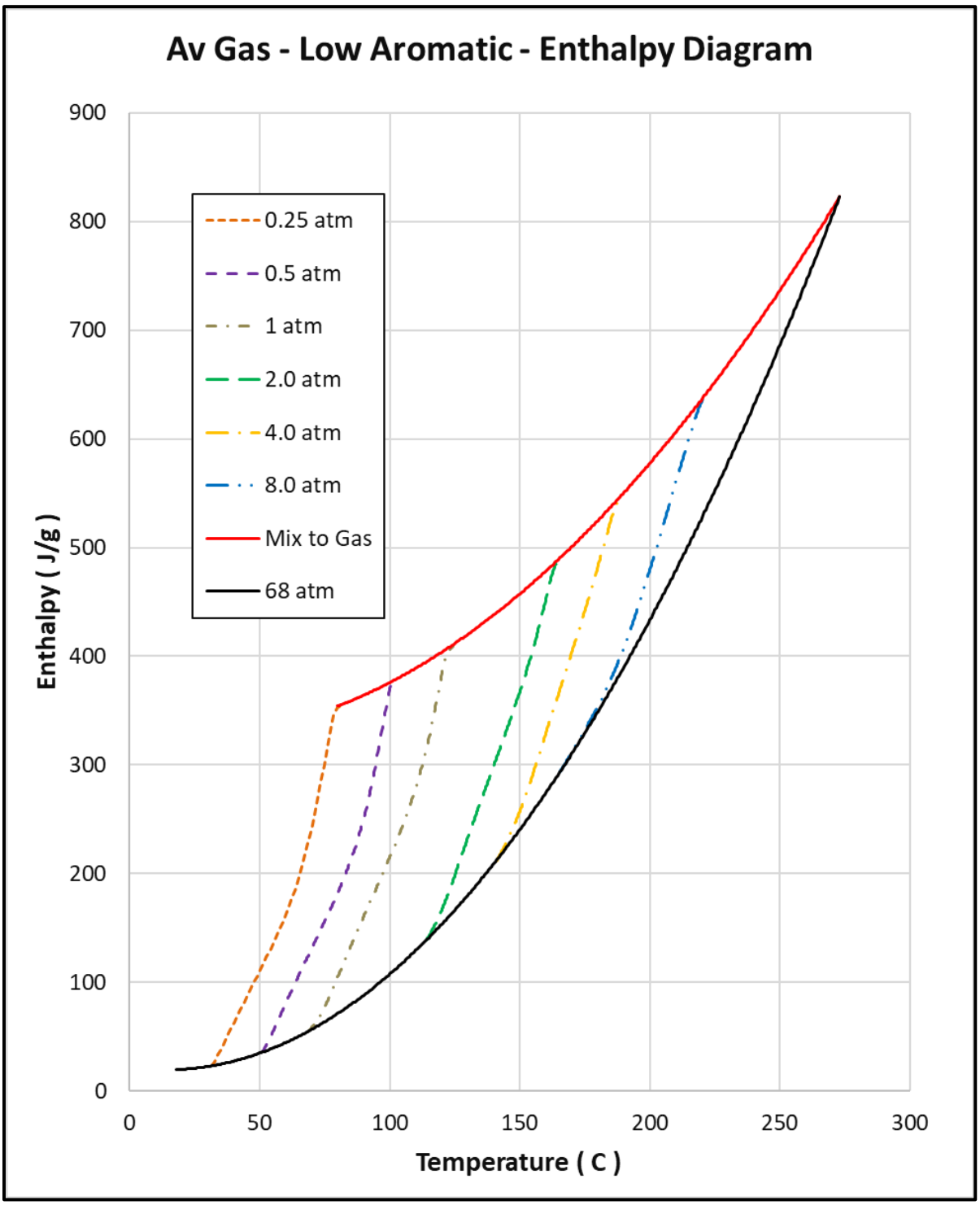

Figure 76: Enthalpy Diagram of Avgas Low Aromatic (AG-LA).

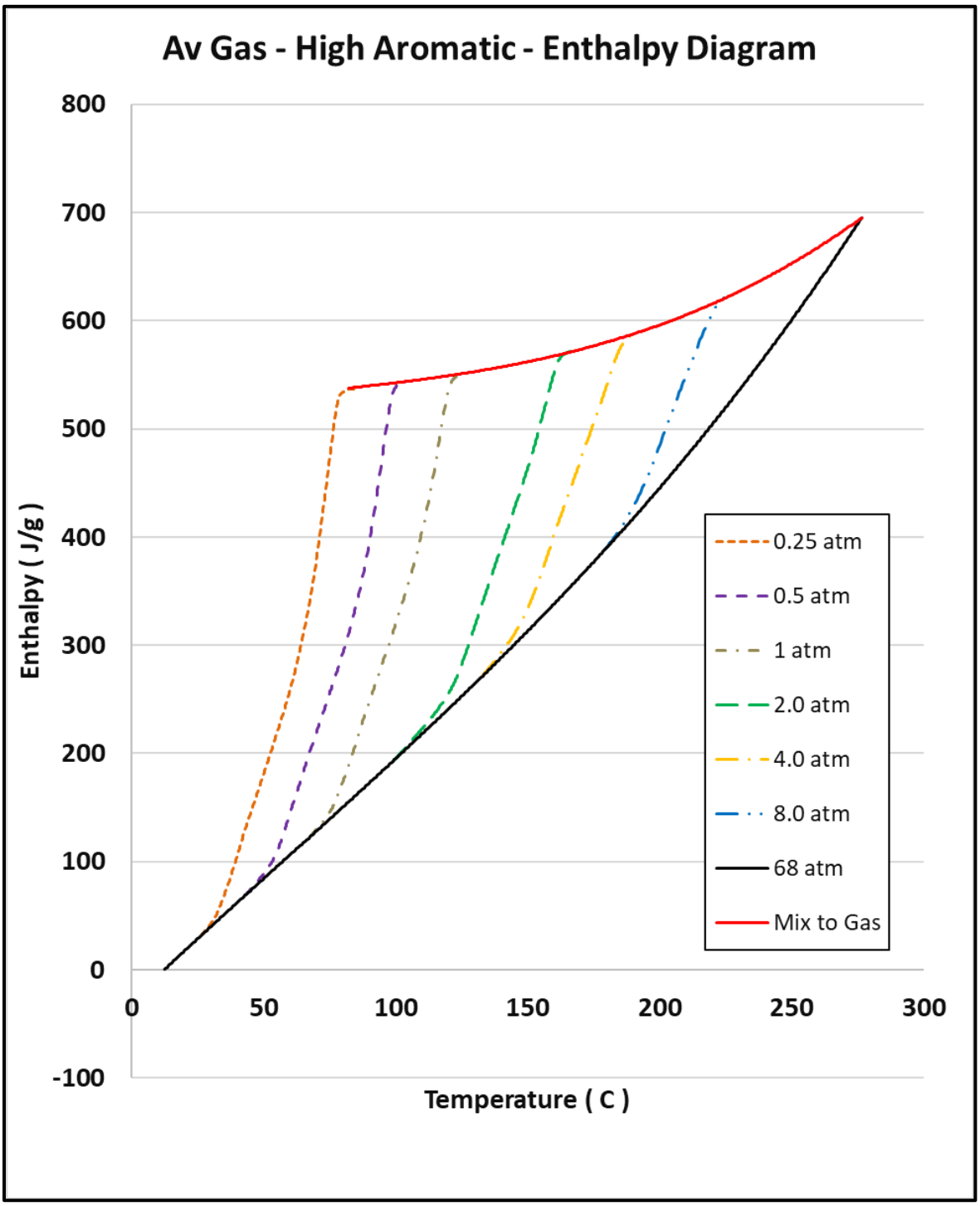

Figure 77: Enthalpy Diagram of Avgas High Aromatic (AG-HA).

10. Concluding Remarks

10.1. Heat of Vaporization of Jet Fuel (HOV)

Premature sample evaporation is a concern for this test. The correct HOV is dependent on the sample mass that is weighed before the experiment being the same as the sample mass at the beginning of the experiment. This error was minimized by weighing the sample after the crucible was sealed. Additionally, the crucible was sealed as soon as possible after the aliquot of sample was added to the crucible. Jet fuel is a petroleum distillate and, as such, the liquid evaporates over a range of temperatures. Some jet fuels were found to evaporate as two separate endothermic peaks: JP-4 and JF#12 from WPAFB. The HOV is the total heat of vaporization over the entire evaporation process. The largest source of uncertainty is determining the baseline at the onset of vaporization. The best measure of standard deviation is from the multiple Jet A-1 samples which gave an average HOV of 308 J/g with +/- 9.6 J/g standard deviation, or about 3% error.

10.2 Heat of Vaporization of Avgas (HOV)

The HOV of the two Avgas samples are very similar, 256.3 and 287.2 J/g. Also, the first endothermic peaks in the HOV curve, Figures 72 and 73, are very close to each other, 84.1 and 79.8 °C. This indicates that either Avgas sample will perform about the same with regards to fuel: air mixture formation, cylinder distribution and the carburetor and/or venturi icing risk. The two peaks observed may reflect the chemical composition of Avgas 100LL which tends to feature iso-pentane (boiling point 28 °C) for front-end volatility and higher boiling (90 – 120 °C) iso-octanes and aromatics for octane.

10.3. HOV of Jet Fuel using Quasi-Isothermal Testing

This test was the best way to measure the HOV versus temperature. The instrumental setup allows the jet fuel to experience a constant ramp down in pressure. This gave very smooth heat flow curves from the HPDSC as the fuel vaporized. The critical temperature, T_c , was also determined by extrapolating the temperature to zero HOV, the definition of the critical temperature. The critical temperatures are summarized in Table 28, shown below. In all five of the jet fuels shown, the critical pressure, P_c , is equal or greater than 1000 psi. These jet fuels behave as supercritical fluids when they are equal or greater than the Tc and equal or greater than the P_c .

Table 28: Critical Temperature of Selected Jet and Avgas Fuels

Jet Fuel	Critical Temperature (°C)
JP-4	320.2
TS-1	327.6
Jet A	346.5
JP-8	349.2
JP-5	379.2
Avgas Low Aromatic	227.1
Avgas High Aromatic	278.3

10.4 HOV of Avgas using Quasi-Isothermal Testing

The critical temperature of the high aromatic is higher than for the low aromatic, Table 28. The critical temperature is the temperature and pressure where there is no HOV for the transition from liquid to vapor. Since this only happens at high pressures, it is of no importance to aviation gasoline piston engines when a carburetor is the source of fuel vapor. If the engine featured a fuel injection system, then the critical temperature and pressure would be more important for the fuel delivery into the cylinder. The vaporization of the fuel, after injection, would proceed faster if the Avgas were preheated to the critical temperature prior to the injectors provided sufficient pressure could be applied to prevent vapor lock.

10.5. Enthalpy Diagrams of Jet Fuel

Premature sample evaporation is also a concern for energy diagrams, for the same reason as mentioned in section 8.3. In addition, care must be taken to ensure the sample does not evaporate during the pressurization (or evacuation) of the HPDSC cell prior to the test. A blank test must be run using the exact same reference and sample crucibles. The high pressure curve, 68 atm in these tests, is the standard curve where no sample evaporates. The data from all the other pressure curves must match the 68 atm curve at temperatures below the start of evaporation. High vapor pressure samples, such as JP-4, must be started at a low temperature, 15 °C in this case. This prevents early evaporation. The "mixture to vapor" line is a best fit third order polynomial fit to the HOV, as measured in quasi-isothermal HPDSC tests. The HPDSC provided high quality data for the construction of the Enthalpy Diagrams.

10.6. Enthalpy Diagrams of Avgas

The Avgas Enthalpy Diagrams are shown in Figures 76 and 77. You will notice that the 0.1 atmosphere data are missing from the figures. This is because both Avgas samples have too high of a vapor pressure at 15 °C for them not to vaporize at 0.1 atmosphere. The 15 °C starting point is the lowest temperature that the HPDSC was capable of acheiving. An accurate measure of the HOV enthalpy is very dependent on the sample mass being constant before the heating ramp starts in the HPDSC. This is not a concern for general aviation because 0.1 atmosphere pressure (vacuum) only occurs at around 50,000 ft altitude, which is above the service ceiling for a performance piston engine aircraft such as the Cessna 340, 29,800 feet. More typical for the current fleet is the recommended crusing altitude for a Cessna 172 of 4,500 to 9,500 ft. For these altitudes the air pressure is 0.85 to 0.71 atmospheres, respectively, well above the lowest pressure, 0.25 atmospheres used in this study.

11. References

1. CRC Aviation Fuel Properties Handbook, 2014 Fourth Edition, CRC Report No. 663.
2. Clausius, R. (1850). "Ueber die bewegende Kraft der Wärme und die Gesetze, welche sich daraus für die Wärmelehre selbst ableiten lassen" [On the motive power of heat and the laws which can be deduced there from regarding the theory of heat]. *Annalen der Physik* (in German) **155**: 500–524 (1850).
3. Clapeyron, M. C. (1834). "Mémoire sur la puissance motrice de la chaleur". *Journal de l'École polytechnique* (in French) **23**: 153–190 (1834).
4. ASTM E2071, "Standard Practice for Calculating Heat of Vaporization or Sublimation from Vapor Pressure Data", 2000.
5. ASTM E1782, "Standard Test Method for Determining Vapor Pressure by Thermal Analysis".
6. Seyler, R.J., "Parameters affecting the determination of vapor pressure by differential thermal methods," Thermochimica Acta., Vol 11, 1976, pp. 129-136.
7. Brozena, A., "Vapor Pressure of 1-octanol below 5 kPa using DSC," Thermochimica Acta, Vol 561, 2013, pp. 72—76.
8. Chappelow, C.C., "Density of Liquid n-Octane", J. Chem. Eng., Vol 16, No. 4, 1971, pp 440-442.

Appendices

Appendix A: Enthalpy of Liquid Volumetric Change

The enthalpy due to the change of the liquid density as a function of temperature is caused by the work that the air pressure exerts against the liquid as the liquid density changes. The question to be answered is, "Is the enthalpy due to the liquid density change versus temperature and pressure significant enough that it needs to be considered?" The pure liquid n-octane was selected as a model for this enthalpy. The density of n-octane was taken from Chappelow, et. al. [8].

Table A1: Density of n-octane and Enthalpy of JP-4

Temperature (°C)	n-octane Density [8] (g/mL)	JP-4 Enthalpy at 68 atm (J/g)
26.103	0.69788	23.148
122.575	0.614554	210.3309
Delta Values	-0.08333	187.1829

The JP-4 was selected for this calculation because it has the lowest delta enthalpy of all the jet fuels. This makes it the worst-case jet fuel with a delta enthalpy of 187.1829 J/g. It was also assumed that the jet fuel sample mass was 10 mg. This mass is larger than all the jet fuel samples tested. Again, this is a worst-case scenario. The delta volume for a 10 mg sample is calculated in the equation below.

$$Vol = \left(\frac{mass}{\Delta density}\right) = \left(\frac{10\ mg}{-0.08333\ g/mL}\right) = -120\mu L = -120\ mm^3 = -120 \times 10^{-9}\ m^3$$

Volume change against a constant pressure work is in the units of energy, Joules, as shown below.

$$P \times V = \left(\frac{force}{area}\right) \times volume = \frac{N}{m^2} \times m^3 = N \cdot m = Joules$$

The largest work is done with the highest pressure. So 68 atmospheres was selected for this calculation. The pressure is converted to Pascals, shown below.

$$68\ atmos = 68.901\ \times 10^5\ Pa$$

The pressure times the delta volume gives the enthalpy, in Joules, for the decreasing volume of 10 mg of n-octane over about a 100 °C range.

$$work = (68.901 \times 10^5\ Pa) \times (120 \times 10^{-9} m^3) = 0.8268\ Joules\ for\ 10\ mg$$

$$error = \left(\frac{0.8268}{187.18}\right) \times 100 = 0.44\%\ error$$

This error is too small to be significant to the enthalpy diagrams generated in this work, and therefore was ignored.

Appendix B: Jet Fuel Enthalpy Equations

The equations for all the curves in the Enthalpy Diagrams are given below. Some of the lines are best fit to a 2nd order equation, but most are best fit to a 6th order equation shown here.

$$y = A * x^6 + B * x^5 + C * x^4 + D * x^3 + E * x^2 + F * x + G$$

Where:
X = temperature (°C)
Y = enthalpy (J/g)

Table B1: Jet A Enthalpy Curve Equations

Coefficients	$A*X^6$	$B*X^5$	$C*X^4$	$D*X^3$	$E*X^2$	F *X	G	Temperature (°C)	
Line								Start	End
Mix to Gas					-1.003811E-03	1.966122E+00	2.890430E+02	180.0	346.4
0.1 atm	-1.876693E-08	1.556853E-05	-5.310071E-03	9.513997E-01	-9.428265E+01	4.899176E+03	-1.042235E+05	90.0	180.0
0.25 atm	9.952192E-10	-5.903398E-07	8.839911E-05	1.092190E-02	-4.424364E+00	4.445478E+02	-1.490168E+04	100.0	211.0
0.5 atm	-1.132994E-08	1.351371E-05	-6.666677E-03	1.739981E+00	-2.532498E+02	1.948565E+04	-6.190075E+05	145.0	240.0
1 atm	-2.177274E-08	2.817081E-05	-1.510923E-02	4.298470E+00	-6.839452E+02	5.770205E+04	-2.016309E+06	170.0	256.0
2 atm	1.067156E-08	-1.534743E-05	9.153187E-03	-2.898051E+00	5.138549E+02	-4.838525E+04	1.890772E+06	205.0	287.0
4 atm	1.833616E-09	-2.866600E-06	1.855796E-03	-6.369606E-01	1.222856E+02	-1.245170E+04	5.257067E+05	222.0	314.0
8 atm					2.401582E-02	-1.173219E+01	2.060761E+03	303.0	338.0
68 atm					2.280039E-03	1.736222E+00	-2.542010E+01	14.4	346.4

Table B2: JP-5 Enthalpy Curve Equations

Coefficients	$A*X^6$	$B*X^5$	$C*X^4$	$D*X^3$	$E*X^2$	F *X	G	Temperature (°C)	
Line								Start	End
Mix to Gas					1.221325E-03	1.715016E+00	2.809821E+02	176.0	381.0
0.1 atm	-3.819284E-09	4.352679E-06	-1.926441E-03	4.311183E-01	-5.192467E+01	3.215110E+03	-8.027385E+04	99.0	176.0
0.25 atm	1.598759E-08	-1.534416E-05	6.049858E-03	-1.253786E+00	1.440317E+02	-8.692702E+03	2.153804E+05	128.0	210.0
0.5 atm	2.001654E-08	-2.242488E-05	1.037796E-02	-2.539302E+00	3.464797E+02	-2.499446E+04	7.448338E+05	160.0	231.0
1 atm	-1.174028E-07	1.604400E-04	-9.117482E-02	2.757529E+01	-4.680803E+03	4.227789E+05	-1.587278E+07	195.0	252.0
2 atm	5.348816E-08	-8.264087E-05	5.306341E-02	-1.812546E+01	3.473980E+03	-3.542524E+05	1.501664E+07	224.0	287.0
4 atm	-1.278040E-08	2.103060E-05	-1.437387E-02	5.222209E+00	-1.063491E+03	1.150811E+05	-5.168044E+06	258.0	322.0
8 atm					1.507716E-02	-5.441220E+00	1.058318E+03	311.0	362.0
68 atm					3.592181E-03	1.607851E+00	-2.303045E+01	14.0	381.0

Table B3: JP-8 Enthalpy Curve Equations

Coefficients	$A*X^6$	$B*X^5$	$C*X^4$	$D*X^3$	$E*X^2$	F *X	G	Temperature (°C)	
Line								Start	End
Mix to Gas					3.903300E-06	6.111130E-01	4.311041E+02	150.0	350.0
0.1 atm		-3.194423E-07	2.279597E-04	-6.420548E-02	8.862823E+00	-5.910334E+02	1.527381E+04	87.0	179.0
0.25 atm	-9.677213E-09	9.149585E-06	-3.552437E-03	7.238747E-01	-8.154080E+01	4.814692E+03	-1.163786E+05	104.0	201.0
0.5 atm	-4.202801E-09	4.628419E-06	-2.095827E-03	4.987069E-01	-6.568495E+01	4.540226E+03	-1.285746E+05	119.0	231.0
1 atm	-5.773134E-09	7.195068E-06	-3.704336E-03	1.007801E+00	-1.527405E+02	1.222791E+04	-4.039194E+05	152.0	242.0
2 atm	4.949408E-10	-3.063749E-07	-4.363201E-05	8.022504E-02	-2.500552E+01	3.274695E+03	-1.599993E+05	185.0	274.0
4 atm	2.681084E-09	-4.277935E-06	2.830964E-03	-9.946994E-01	1.957574E+02	-2.046123E+04	8.877541E+05	221.0	313.0
8 atm				-1.488641E-04	1.330275E-01	-3.692636E+01	3.681049E+03	258.0	333.0
68 atm					8.012991E-04	1.637700E+00	-2.526129E+01	15.0	350.0

Table B4: TS-1 Enthalpy Curve Equations

Coefficients	$A*X^6$	$B*X^5$	$C*X^4$	$D*X^3$	$E*X^2$	F *X	G	Temperature (°C)	
Line								Start	End
Mix to Gas					1.168861E-03	8.433773E-01	4.255899E+02	156.0	330.0
0.1 atm	-6.168142E-09	4.378708E-06	-1.263274E-03	1.881163E-01	-1.512445E+01	6.233344E+02	-1.023674E+04	75.0	156.0
0.25 atm	-1.942815E-08	1.679645E-05	-5.983948E-03	1.122757E+00	-1.168418E+02	6.392155E+03	-1.435178E+05	97.0	185.0
0.5 atm	-2.627817E-08	2.659309E-05	-1.112392E-02	2.459847E+00	-3.030320E+02	1.970932E+04	-5.284426E+05	133.0	209.0
1 atm	-1.754187E-08	2.062955E-05	-1.004667E-02	2.592100E+00	-3.735149E+02	2.849699E+04	-8.991231E+05	144.0	224.0
2 atm	1.365022E-08	-1.746226E-05	9.253474E-03	-2.600266E+00	4.087478E+02	-3.408513E+04	1.178427E+06	173.0	258.0
4 atm		-2.654881E-07	3.103240E-04	-1.445699E-01	3.357528E+01	-3.885931E+03	1.795983E+05	205.0	282.0
8 atm				-7.268141E-05	6.889589E-02	-1.792889E+01	1.882213E+03	247.0	320.0
68 atm					2.603396E-03	1.734519E+00	-2.627016E+01	15.0	330.0

Table B5: JP-4 Enthalpy Curve Equations

Coefficients	$A*X^6$	$B*X^5$	$C*X^4$	$D*X^3$	$E*X^2$	F *X	G	Temperature (°C)	
Line								Start	End
Mix to Gas					3.034821E-03	8.666529E-01	3.460561E+02	80.0	319.0
0.1 atm	-1.016809E-06	3.650146E-04	-5.330811E-02	4.038423E+00	-1.668128E+02	3.564188E+03	-3.080007E+04	34.0	80.0
0.25 atm	-9.924691E-07	4.997876E-04	-1.035329E-01	1.127935E+01	-6.808981E+02	2.158774E+04	-2.808015E+05	63.0	102.0
0.5 atm	4.097645E-07	-2.121783E-04	4.471815E-02	-4.895570E+00	2.925398E+02	-8.994741E+03	1.102043E+05	71.0	119.0
1 atm	5.604652E-07	-3.768212E-04	1.046549E-01	-1.536943E+01	1.259054E+03	-5.456258E+04	9.776176E+05	84.0	143.0
2 atm	4.122329E-07	-3.533489E-04	1.255209E-01	-2.365440E+01	2.494375E+03	-1.395701E+05	3.237979E+06	114.0	172.0
4 atm	-1.459591E-08	1.325679E-05	-4.907608E-03	9.432850E-01	-9.850356E+01	5.229580E+03	-1.073092E+05	140.0	206.0
8 atm	-5.527939E-08	6.678765E-05	-3.354899E-02	8.969495E+00	-1.346231E+03	1.075601E+05	-3.574006E+06	177.0	240.0
68 atm					3.724737E-03	1.774588E+00	-1.308158E+01	7.0	319.0

Table B6: Jet A-1 Shell-Netherlands (JF#2) Enthalpy Curve Equations

Coefficients	$A*X^6$	$B*X^5$	$C*X^4$	$D*X^3$	$E*X^2$	F*X	G	Temperature (C)	
Line								Start	End
Mix to Gas				-4.637126E-05	4.119663E-02	-7.673668E+00	1.010439E+03	152	409.8
0.1 atm	-3.429798E-08	2.324049E-05	-6.448866E-03	9.350284E-01	-7.447229E+01	3.086915E+03	-5.191357E+04	76	152
0.25 atm	-1.254620E-09	9.855209E-07	-2.899475E-04	3.588127E-02	-7.630224E-01	-1.942833E+02	1.192128E+04	114	202.6
0.5 atm	-9.453211E-10	5.942527E-07	-5.105753E-05	-4.553789E-02	1.469351E+01	-1.712582E+03	7.183995E+04	140	220
1 atm	3.829865E-08	-4.946905E-05	2.658814E-02	-7.611012E+00	1.223738E+03	-1.047666E+05	3.730515E+06	178	239
2 atm	2.685629E-08	-3.838455E-05	2.276444E-02	-7.171122E+00	1.265668E+03	-1.186797E+05	4.619884E+06	200	282.9
4 atm	2.596853E-08	-4.260821E-05	2.904235E-02	-1.052679E+01	2.140147E+03	-2.314101E+05	1.039811E+07	235	311.1
8 atm			-2.755971E-05	3.304792E-02	-1.479834E+01	2.939712E+03	-2.180909E+05	271	337
68 atm			-4.145774E-08	3.391928E-05	-4.026321E-03	2.733736E+00	-4.123937E+01	16.4	410

Table B7: Avgas Low Aromatic - Enthalpy Curve Equations

Coefficients	$A*X^6$	$B*X^5$	$C*X^4$	$D*X^3$	$E*X^2$	F*X	G	Temperature (C)	
Line								Start	End
Mix to Gas					-4.271022E-03	4.123693E-02	3.068732E+02	80	273
0.1 atm	NA	NA	NA	NA	NA	NA	NA	NA	NA
0.25 atm	-3.656660E-07	1.149856E-04	-1.472029E-02	9.836733E-01	-3.622396E+01	7.022372E+02	-5.617340E+03	31.5	80.9
0.5 atm	-2.359183E-07	1.046373E-04	-1.907314E-02	1.830714E+00	-9.766805E+01	2.752851E+03	-3.209141E+04	51.1	101.4
1 atm	-1.800408E-07	1.002601E-04	-2.300726E-02	2.785058E+00	-1.875701E+02	6.668945E+03	-9.787096E+04	68.9	124.3
2 atm		-3.664236E-06	2.597426E-03	-7.331431E-01	1.030199E+02	-7.201423E+03	2.002968E+05	114	165.3
4 atm			3.918101E-05	-2.651563E-02	6.735849E+00	-7.535780E+02	3.139323E+04	141	188
8 atm			-4.481772E-05	3.390056E-02	-9.527737E+00	1.185016E+03	-5.491070E+04	165.4	220.9
68 atm					1.201517E-02	-3.457867E-01	2.199764E+01	18	273

Table B8: AvGas High Aromatic - Enthalpy Curve Equations

Coefficients	$A*X^6$	$B*X^5$	$C*X^4$	$D*X^3$	$E*X^2$	F*X	G	Temperature (C)	
Line								**Start**	**End**
Mix to Gas			3.122502E-17	1.068126E-05	-1.860955E-03	3.457470E-01	5.159719E+02	82	276.5
0.1 atm	NA	NA	NA	NA	NA	NA	NA	NA	NA
0.25 atm	-1.552944E-07	3.993752E-05	-3.839366E-03	1.644778E-01	-2.469380E+00	-1.690004E+01	5.821349E+02	26.6	86
0.5 atm	-3.156052E-07	1.321652E-04	-2.260302E-02	2.019258E+00	-9.925396E+01	2.547225E+03	-2.664700E+04	43	104.8
1 atm		-8.497512E-06	4.087549E-03	-7.788381E-01	7.352671E+01	-3.434085E+03	6.351568E+04	68.1	126.9
2 atm	-9.352653E-08	7.457256E-05	-2.465097E-02	4.322810E+00	-4.239325E+02	2.203762E+04	-4.741566E+05	99	165.9
4 atm	-1.695474E-07	1.639835E-04	-6.590855E-02	1.408838E+01	-1.688919E+03	1.076476E+05	-2.849480E+06	133	189.8
8 atm				-2.665706E-03	1.633353E+00	-3.270537E+02	2.188790E+04	179.2	224.8
68 atm			1.734723E-18	1.068126E-05	-1.860955E-03	2.313915E+00	-2.816535E+01	12.5	276.5

Appendix C: Instrumental Details

C.1. HPDSC and Sample Preparation Details

Figures C1 through C17 show pictures for the 'step by step' process for preparing the jet fuel sample to be run in the HPDSC.

Figure C1: DSC pan resting on the crimping press lower die.

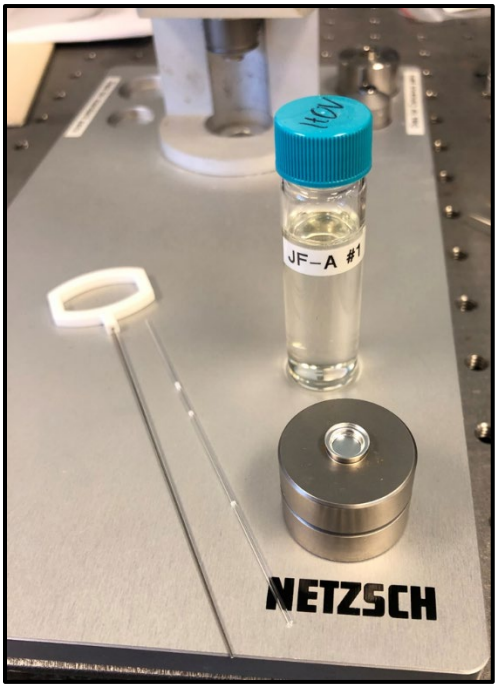

Figure C2: Micropipette and JF sample.

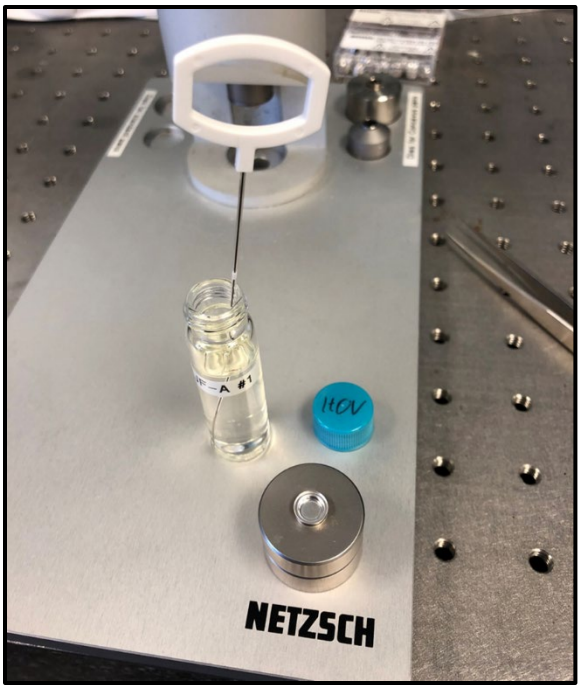

Figure C3: Micropipette in JF sample.

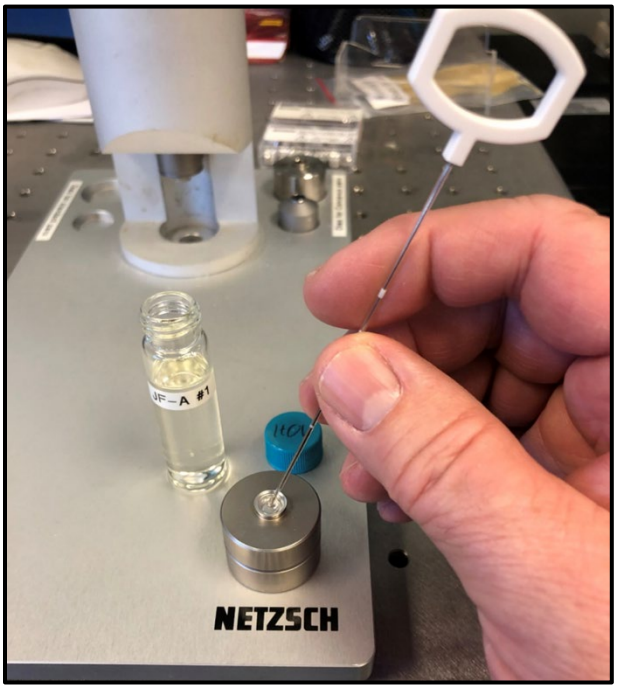

Figure C4: Micropipette depositing JF sample in DSC pan.

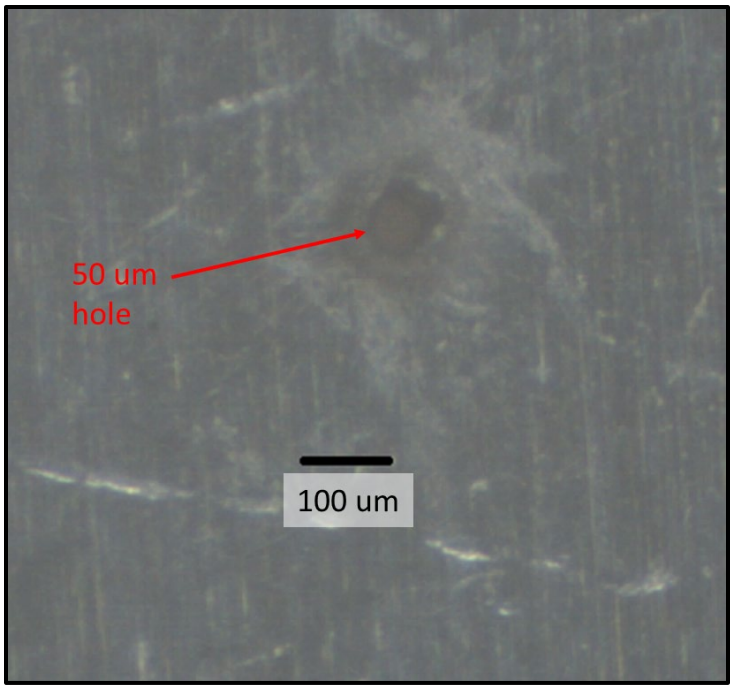

Figure C5: Microscope image of the 50 µm laser-drilled hole in the DSC lid.


Figure C6: Laser-drilled lid placed on DSC pan.

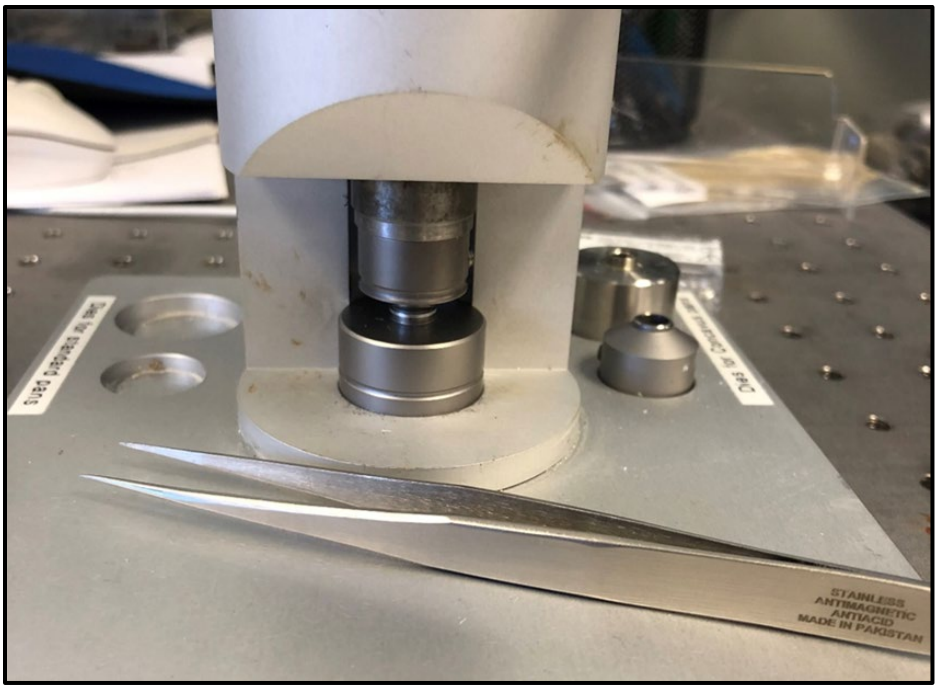

Figure C7: DSC pan/lid being pressed in the crimper. The pressing makes a hermetically sealed cold weld of the aluminum pan and lid. The only escape route for the JF is through the 50 µm orifice.

Figure C8: DSC pan/lid after crimping

Note: The crimping dies were subject to damage if the lower die was not placed evenly into the bottom of the press. If the lower die was tilted ever so slightly when it was put in the bottom of the press and the lever was pulled down, both dies would scratch each other. These scratches prevented the crucibles from completely sealing when crimped. There were two ways to solve

this problem. First was to purchase new top and bottom dies. Second, the scratched dies could be used to crimp the crucible multiply times while rotating the bottom die slightly in between each crimp. After doing this, a complete seal was made and the sample could only escape through the laser drilled hole in the lid.

Figure C9: Inside of the HPDSC cell, with an empty pan/lid on the reference side of the HPDSC cell.

Figure C10: Inside of the HPDSC cell, with a JF sample on the sample side of the HPDSC cell.

Figure C11: Inside of the HPDSC cell, with the inner silver lid installed.

Figure C12: Inside of the HPDSC cell, with the outer silver lid installed.

Figure C13: The HPDSC cell, with the water-cooled stainless steel (SS)lid.

Figure C14: The HPDSC cell, with the SS lid installed and retaining nuts tightened.

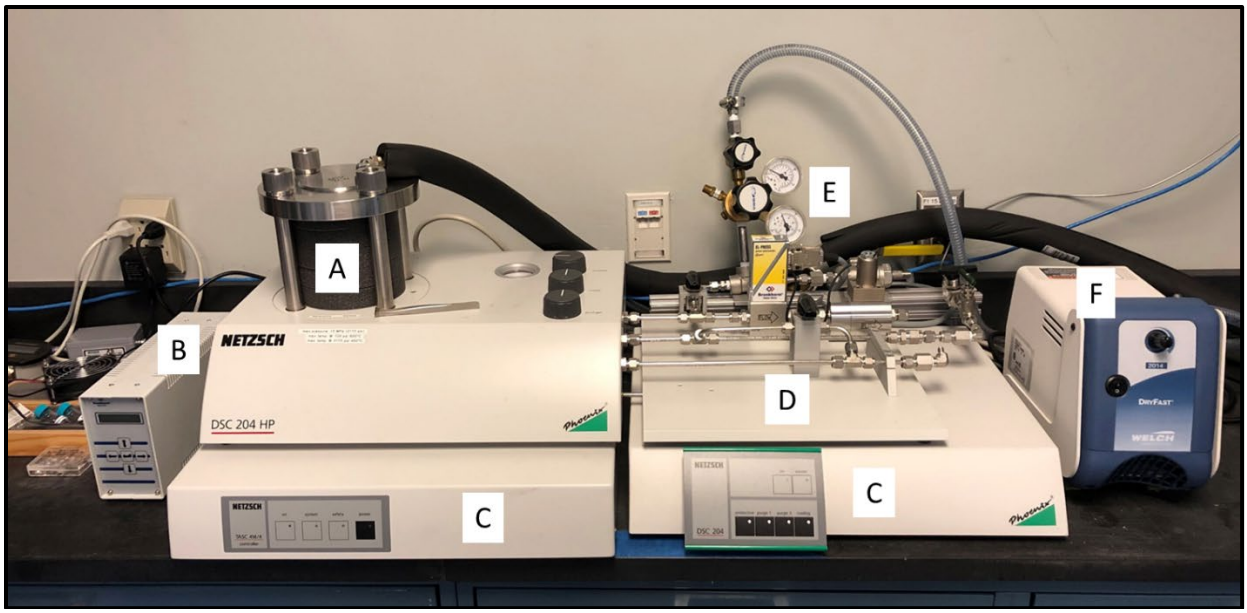

Figure C15: The complete HPDSC instrument setup. Parts included are A) the HPDSC cell, B) the pressure signal amplifier, C) the HPDSC electronics, D) the HP gas distribution connections, E) the QI regulator, F) the vacuum pump.

C.2. QI HPDSC Setup

The HPDSC was set up differently for this experiment so that the pressure inside the HPDSC was decreased linearly versus time. This is shown in Figures C16 and C17. The regulator was set so the high-pressure inlet faces the HPDSC and the low-pressure outlet faces the vacuum pump. A 10 µm orifice (E) is placed between the regulator (C) and vacuum pump (D) so that the pressure decrease rate is not too fast. A regulator is needed so that the rate of pressure change in the HPDSC is constant. The outlet pressure of the regulator controls the rate of pressure change. An outlet pressure of 5 psi gave a pressure change of about 1.75 atm/min; see Figure C18. The vacuum pump is needed to get HOV data for low-temperature tests.

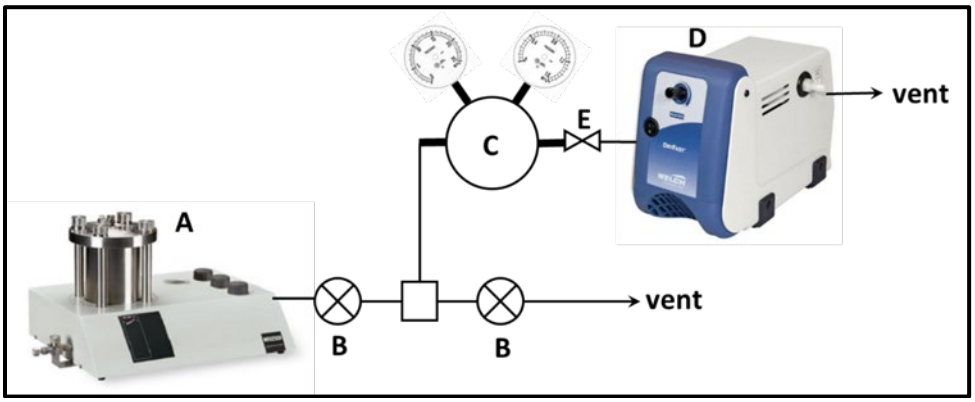

Figure C16: HOV QI HPDSC setup, where A is the HPDSC, B is a valve, C is a regulator set to 5 psi output, E is a 10 µm orifice and D is the vacuum pump.

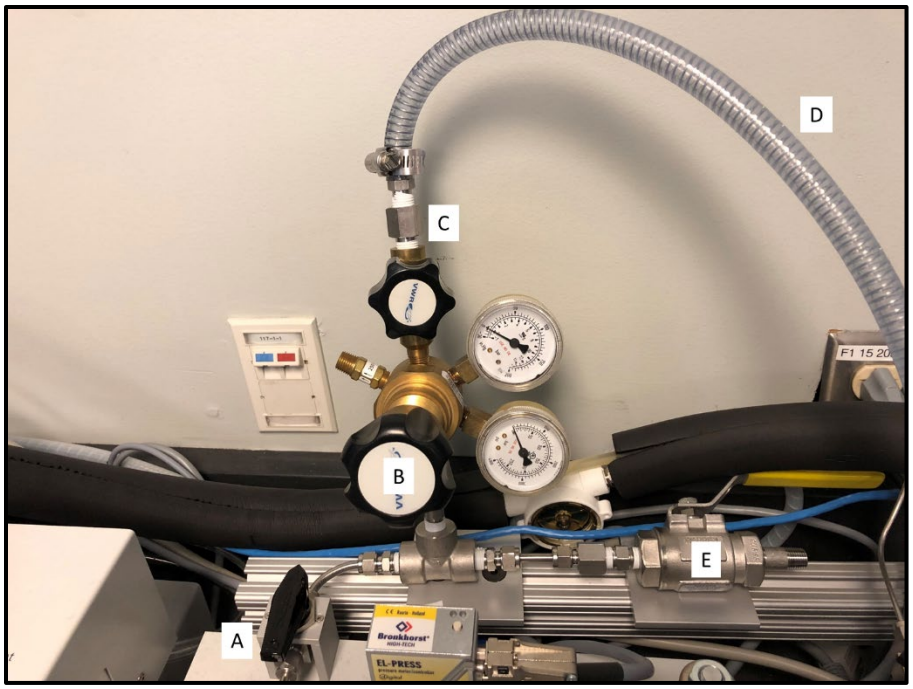

Figure C17: The QI DSC instrument setup. Parts included are A) outlet valve from the HPDSC cell, B) the QI regulator, C) the 10 µm diameter orifice, D) tubing to the vacuum pump, E) exhaust valve.

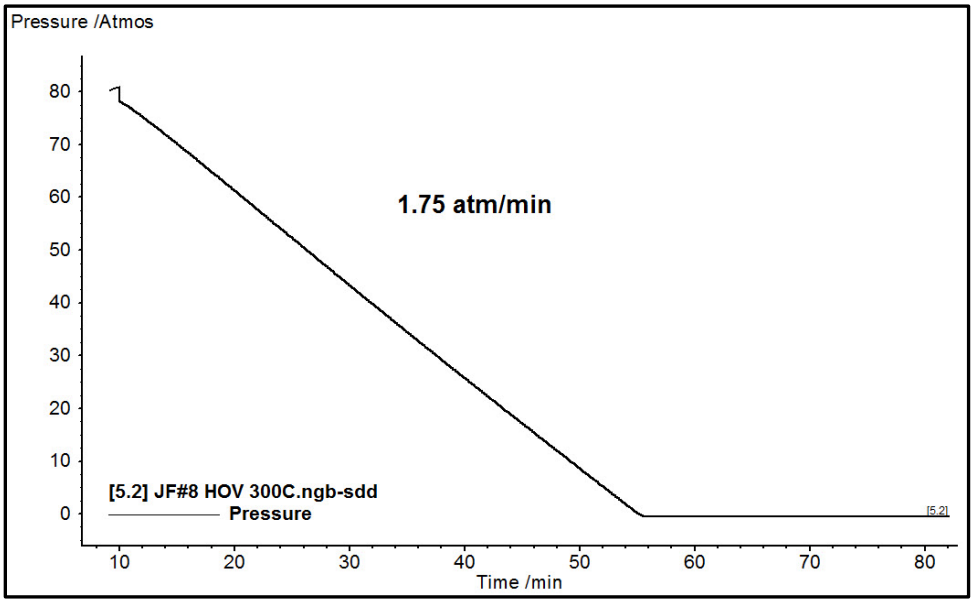

Figure C18: Typical pressure versus time for a HOV QI HPDSC experiment.